AN ABSTRACT OF THE THESIS OF

ANGUS JAMES MACKAY (Name) for the MASTER OF SCIENCE (Degree)

in GEOPHYSICS (Major) presented on November 1, 1968 (Date)

Title: CONTINUOUS SEISMIC PROFILING INVESTIGATION OF THE SOUTHERN OREGON CONTINENTAL SHELF BETWEEN CAPE BLANCO AND COOS BAY

Abstract approved: Redacted for Privacy
Donald F. Heinrichs

A structure map was constructed of the continental shelf between Cape Blanco and Coos Bay, Oregon, exclusively from an interpretation of approximately 700 km of continuous seismic profiles. At least ten discernible seismic units were mapped on the bases of acoustic appearance, lateral continuity, angular unconformities, and faults. The offshore units tentatively were correlated with onshore geology and are believed to range in age from the latest Jurassic to late Pleistocene. The sparker profiles reveal that the continental shelf off southern Oregon has experienced significant late Tertiary and Quaternary accretion due to deposition and tectonic uplift.

The oldest rock exposures, believed to be the latest Jurassic in age, crop out on the inner continental shelf on the topographic highs off Cape Blanco and Coquille Point. Erosional remnants of

probable Late Cretaceous turbidites and the middle Eocene sandstone beds also are exposed on the bathymetric high on the inner shelf southwest of Cape Arago. The initial emplacement of these three uplifted structural blocks is probably a result of late Eocene wrench faulting of the Port Orford shear zone and of the postulated shear zone at Coquille Point.

No other early Tertiary sediments apparently are exposed on this portion of the Oregon continental shelf, but they probably extend seaward at depth on the continental margin. Middle Tertiary strata are believed to be exposed on the outer shelf topographic high southwest of Cape Arago.

Sediments of Miocene to Pliocene age were deposited throughout much of the continental shelf that was surveyed. The greatest amount of deposition occurred in a north-south trending basin between Cape Blanco and Coquille Bank. Late to post-Pliocene tectonism uplifted and exposed the older underlying rocks on the inner shelf, which are probably of uppermost Jurassic to middle Tertiary age. These same stresses also deformed the Mio-Pliocene sediments into gently undulating structures on the inner shelf. The greatest deformation occurred on the outer shelf and formed Coquille Bank, a north-south trending, doubly plunging, asymmetrical anticline. The terraces or benches on the upper continental slope to the north and south of the Bank are structural features

resulting from the doubly plunging anticline.

Eustatic sea level lowerings during the Pleistocene truncated the shelf structures as deep as 130 m below present sea level. The detritus was deposited as a wedge of sediments, which forms an unconformable contact with the underlying strata on the outer shelf and upper slope between Coos Bay and Coquille Bank. In areas of deposition there is no distinct break between the shelf and the upper slope; the former merely merges into the latter in a continuous convex curve. In areas of nondeposition, the edge of the shelf is an erosional and structural feature.

A possible buried channel was detected northwest of the mouth of the Coquille River. This sediment filled channel is believed to be an erosional remnant of a former course of the Coquille River during a lower stand of sea level.

Continuous Seismic Profiling Investigation of the Southern Oregon Continental Shelf Between Cape Blanco and Coos Bay

by

Angus James Mackay

A THESIS

submitted to

Oregon State University

in partial fulfillment of
the requirements for the
degree of

Master of Science

June 1969

APPROVED:

Redacted for Privacy

Assistant Professor of Oceanography
in charge of major

Redacted for Privacy

Chairman of Department of Oceanography

Redacted for Privacy

Dean of Graduate School

Date thesis is presented November 1, 1968

Typed by Donna L. Olson for Angus James Mackay

ACKNOWLEDGEMENTS

I wish to express my sincerest gratitude to my major and minor professors, Dr. Donald F. Heinrichs and Dr. LaVerne D. Kulm, for offering so freely their time for conferences during the course of this investigation and for critically reviewing the manuscript. I would also like to especially thank Mr. William E. Bales for his irreplaceable assistance in operating the continuous seismic profiler. The author expresses his appreciation to Dr. Gerald A. Fowler for the identification of the benthic foraminiferans and for also reviewing the manuscript.

Many beneficial discussions were held with scientists not affiliated with Oregon State University whom I would also like to thank for their helpful guidance and advice. The author also expresses his gratitude to Roger H. Neudeck, for helpful information connected with his research studies. My appreciation is extended to J. Michael King for drafting assistance and to Gail Lowell for computer programming.

I am also indebted to the officers of the U. S. Bureau of Mines R/V CRIPPLE CREEK and to the Department staff members and students who acted as scientific observers and crew for the research vessel, for their important role in the data acquisition.

I also wish to express my gratitude to my parents for their

constant encouragement throughout the study and the many previous years of formal education.

This study is part of a detailed geological and geophysical "Study of the Continental Margin Off the State of Oregon" under contract No. 14-08-0001-10766 with the U. S. Geological Survey.

TABLE OF CONTENTS

	Page
INTRODUCTION	1
REGIONAL GEOLOGY AND PREVIOUS WORK	5
Coos Bay Synclinorium	5
Port Orford Shear Zone	6
Elevated Marine Terraces	7
Previous Work Offshore	8
Sedimentation and Stratigraphy	8
Gravity	9
Magnetics	11
BATHYMETRY	14
CONTINUOUS SEISMIC PROFILING	17
Instrumentation	19
Survey Procedure	22
Interpretation of Records	23
DISCUSSION OF RESULTS	28
Unit A	29
Port Orford Shear Zone	32
Surf Cut Terrace	33
Unit B	33
Unit C	47
Unit D	49
Unit E	51
Unit F	52
Unit G	57
Unit H	59
Unit I	60
Unit J	63
THE SHELF BREAK	66

Page

UNCONSOLIDATED SEDIMENT COVER 69

Resolution and Interpretation 69
Sediment Distribution 70

SUMMARY AND CONCLUSIONS 72

BIBLIOGRAPHY 87

APPENDIX I SPARKER TRACK LINE NAVIGATIONAL DATA 93

APPENDIX II APPARENT DIPS 104

APPENDIX III TRUE DIPS AND STRIKES 114

LIST OF FIGURES

Figure		Page
1.	Submarine physiography off Oregon.	2
2.	Track line map of the continuous seismic profiles.	3
3.	Free-air gravity anomaly map of the Oregon continental margin.	10
4.	Anomaly map of the total magnetic field off the coast of Oregon.	12
5.	Bathymetry of the continental shelf and upper slope between Coos Bay and Cape Blanco.	15
6.	Survey geometry of the continuous seismic profiler for normal incidence reflections.	18
7.	Block diagram of the electrical components of the sparker system.	18
8.	Velocity function curve.	25
9.	Sparker lines SP-22 and 23 showing a surf cut terrace in unit A.	34
10.	East-west profile SP-52D crossing the continental shelf from northwest of Blacklock Point to Coquille Bank.	36
11.	Gently undulating structures of unit B on a north-south profile from northwest of Blacklock Point to west of Coquille Point.	37
12.	East-west profiles across Coquille Bank.	43
13.	North-south profile SP-16 parallel to the axis of the Coquille Bank anticline.	44

Figure		Page
14.	North-south profile across units B, C, D, and E off Coquille Point.	48
15.	East-west traverse of the continental shelf southwest of Cape Arago across four distinct units, F, G, H, and J.	54
16.	Sediment wedge perched on the outer shelf and upper slope.	64
17.	Unconsolidated sediment map.	71a

LIST OF PLATES

Plate		
1.	Structure map of the continental shelf off southern Oregon.	In pocket

LIST OF TABLES

Table		
1.	Postulated correlations of seismic units with onshore geology.	73

CONTINUOUS SEISMIC PROFILING INVESTIGATION OF THE SOUTHERN OREGON CONTINENTAL SHELF BETWEEN CAPE BLANCO AND COOS BAY

INTRODUCTION

Submerged margins of the continents, the continental shelf and slope, have received a great deal of attention from geologists and geophysicists for both academic and economic interests. The geological development and history of the continental margin can be reconstructed by investigating its stratigraphy and structure. The stratigraphy can be studied from ocean bottom and sub-bottom rock samples; and the structure can be determined by geophysical techniques. Continuous seismic profiling is perhaps the best geophysical method for a detailed structural investigation.

During the summer of 1967, a continuous seismic profiling investigation, using a sparker seismic source, was conducted along 70 km of the southern Oregon coast between Coos Bay and Cape Blanco (Figure 1). Approximately 700 km of sparker track lines were recorded in the survey area, which extends from 42° 45' N to 43° 25' N latitudes and from approximately the 20 m depth contour to 125° W longitude (Figure 2). The major part of the sparker survey consisted of east-west seismic profiles beginning at water depths of approximately 20 m and extending across the continental shelf to a depth of about 400 m on the upper continental slope. The east-west

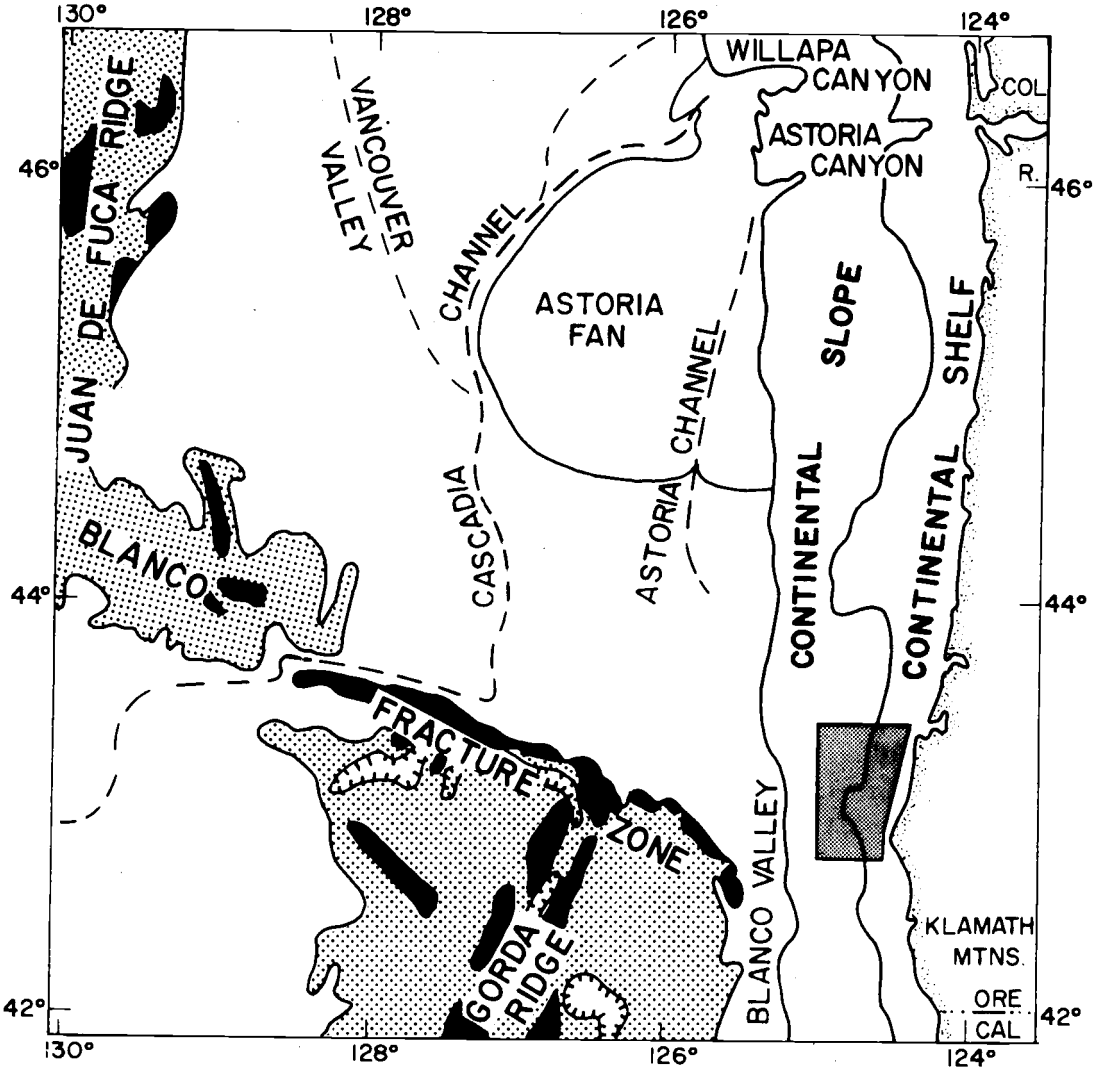

Figure 1. Submarine physiography off Oregon. Shaded region shows the location of the study area. Heavy stipple represents hilly areas; black depicts mountains.

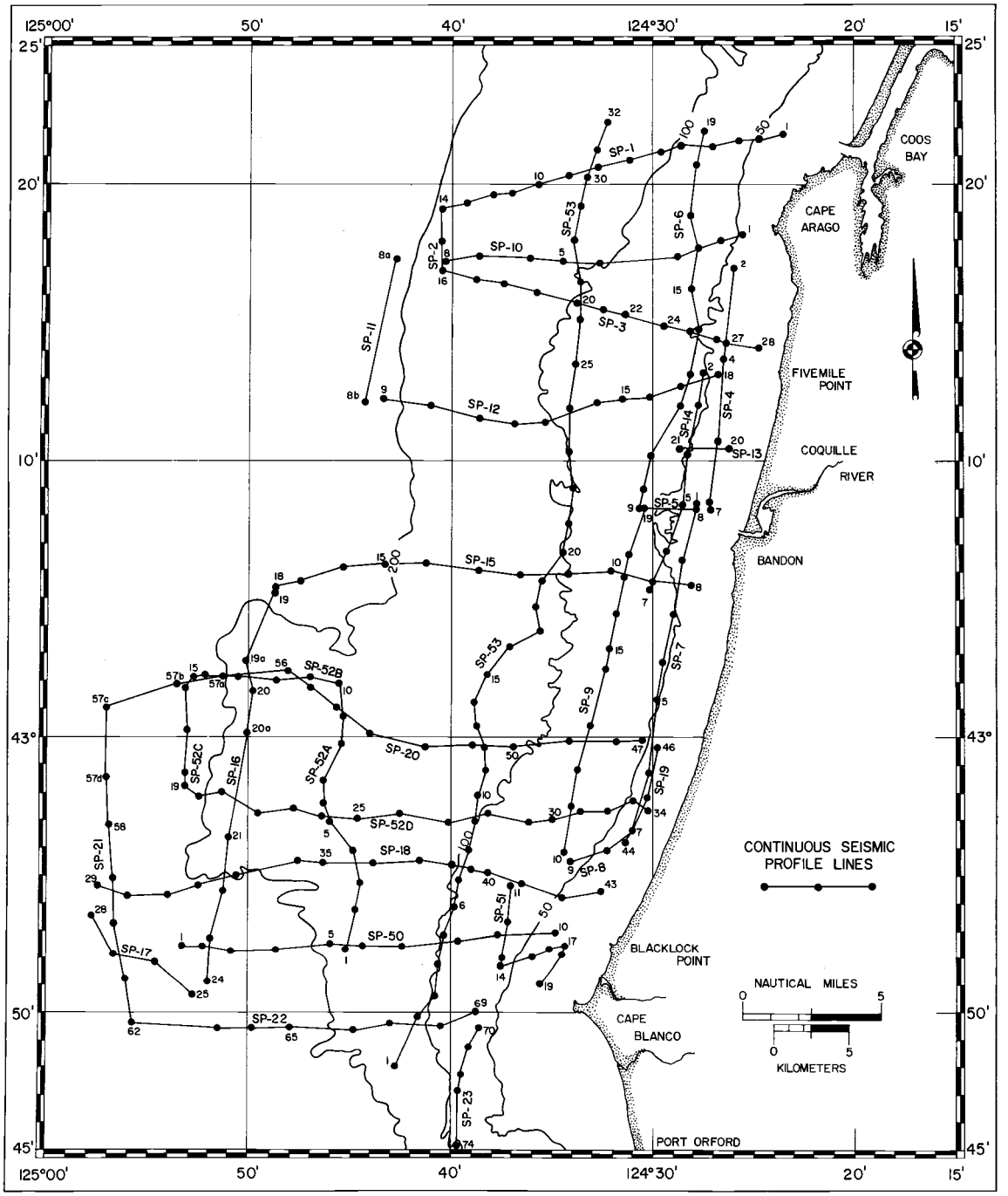

Figure 2. Track line map of continuous seismic profiles. Individual lines are designated by "SP- ". Numbers beside solid dots refer to navigation fixes. Contours in meters.

lines were spaced approximately 7 to 9 km apart and were joined together in a grid with north-south trending lines. Additional sparker profiles were run off the Coquille River and the Sixes River just north of Cape Blanco in search for possible buried stream cut channels on the continental shelf.

The structure of the continental shelf and upper continental slope was mapped from an interpretation of the sparker records. An attempt was made to correlate offshore geologic features and seismic events with the mapped onshore coastal geology. Inferences were made as to the ages of the offshore geologic units, to the periods of tectonism, and to the development of the continental margin in this area. The unconsolidated sediment distribution and thickness were also determined from the sparker records. The findings of this investigation are only preliminary, and more detailed geological and geophysical investigations can be conducted on the basis of the results of this study.

REGIONAL GEOLOGY AND PREVIOUS WORK

Along the coast of southern Oregon from Bandon to Cape Blanco the Tertiary sedimentary and volcanic rocks of the Coast Range are in juxtaposition with the older Mesozoic units of the Klamath Mountain province (Wells and Peck, 1961). In an attempt to reconstruct the Cenozoic history of the Pacific northwest, Snavely and Wagner (1963) suggested that the southern end of the Coast Range geosyncline overlies the older Klamath Mountain province. North trending shear zones along the southern Oregon coast extending from the Oregon-California state line to Cape Blanco are in obvious contrast with the typical northeast trending structural and metamorphic pattern of the Klamath-Siskiyou province (Dott, 1965). The structural pattern of shear zones along the coast appears to extend as far north as Bandon (Howard and Dott, 1961). Principal geological features important to this study are the Coos Bay synclinorium, the Port Orford shear zone, and the elevated coastal marine terraces.

Coos Bay Synclinorium

The geology of the Coos Bay synclinorium was first described by Diller in 1901 in his pioneer mapping of the Coos Bay quadrangle. Because of good exposures of the sedimentary section of the

synclinorium at Cape Arago, and economic interest in coal, and the heavy mineral placer deposits in the beaches and marine terraces, the Coos Bay quadrangle is one of the best studied areas along the Oregon coast. Investigators who have more recently studied the area include Allen and Baldwin (1944), Griggs (1945), Baldwin (1945, 1964, and 1966), Dott (1964, and 1966), and Ehlen (1967).

The north trending synclinorium is discordant with the more prevalent northeast folds of the southern and central Oregon Coast Range (Wells and Peck, 1961). The synclinal feature contains the sedimentary section characteristic of the southern Coast Range. The rocks range in age from the Late Cretaceous to early Eocene lower member of the Umpqua Formation through the Pliocene Empire Formation (Baldwin, 1965 and 1966).

Port Orford Shear Zone

Although Diller (1903) was the first investigator to map the Cape Blanco area in detail, the Port Orford shear zone was first described by Koch, Kaiser, and Dott (1961) at its sea cliff exposure at Port Orford, Oregon, 21 km southeast of the Cape. Dott (1962) also recognized a shear zone at Blacklock Point 5 km northeast of the Cape. According to Dott, the shear zone is coextensive with the previously named shear zone at Port Orford and is one of a series of such zones which lace the southwest Oregon and northern California

coasts.

The Port Orford shear zone trends north-northwest and appears to be as wide as 3 km (Dott, 1962). Dott (1962, p. 132) described the chief characteristics of the fault as "intense shearing, brecciation, overturning of strata, and great heterogeneity of contiguous rock types and ages". In the shear zone the exposed rock types are extremely varied. The units range from the Otter Point Formation (Koch, 1966) (originally mapped by Dott (1962) as the Dothan? Formation) of presumably latest Jurassic age to extensive Cenozoic deposits. Dott (1962) indicates that the shear zone was clearly active after the middle Eocene and again after the Miocene and was overlain by extensive Pleistocene marine terrace deposits.

In his studies of the Port Orford area, Koch (1966) reclassified and divided the Upper Jurassic and Lower Cretaceous units of the southern Oregon coast, originally mapped as Myrtle Group by Diller (1903), into the Otter Point, Humbug Mountain, and Rocky Point Formations. His revised interpretation has been incorporated by Baldwin (1966) and Phillips (1968) and will be used in this study.

Elevated Marine Terraces

Along the southern Oregon coast between Cape Arago and Cape Blanco, remnants of numerous marine terraces have been recognized as high as 460 m above sea level (Griggs, 1945). The elevated

terraces are a result of multiple eustatic sea level changes during the Pleistocene glaciation. The sea level changes were superimposed upon the late Pliocene to Pleistocene vertical uplift of the Oregon Coast Range. Marine mollusks from a shell layer in the Elk River beds at Cape Blanco, about 60 m in elevation, have been dated by Richards and Thurber (1966) with C^{14} and Th^{230}/U^{234} techniques and are at least 33,000 years old. The youngest, lowest, and most prominent terraces, the Whiskey Run and the Pioneer Terraces (Griggs, 1945) of very late to post-Pleistocene age (Baldwin, 1945), have been upwarped to elevations of 38 m at Cape Arago and 69 m at Cape Blanco. From these two headlands the marine terraces dip both to the north and the south to significantly lower elevations.

The elevated marine terraces indicate that the southern Oregon coast has undergone broad regional uplift since the late Pliocene or early Pleistocene through the Holocene. The late Pleistocene or Holocene uplift has been the greatest at Cape Arago and Cape Blanco.

Previous Work Offshore

Sedimentation and Stratigraphy

Maloney (1965 and 1967) studied the geology of the continental terrace off the central coast of Oregon, 50 km to the north of the

investigation area. He reported that siltstones, deposited at bathyal depths during the late Miocene and Pliocene, crop out on the banks of the central Oregon continental shelf. Benthic foraminifers in the siltstones indicated the shelf had been uplifted as much as 1 km by the late Pleistocene (Byrne, Fowler, and Maloney, 1966). Then the shelf was eroded by the migrating shoreline of the transgressions and regressions resulting from eustatic changes in sea level.

The continental shelf sediments from the Columbia River to Cape Blanco have been analyzed by Runge (1966). In obtaining his unconsolidated sediment samples he defined rock outcrops on the ocean bottom 13 km southwest of Cape Arago and on Coquille Bank, 28 km northwest of Cape Blanco. Boettcher (1967) also reported the rocky area southwest of Cape Arago.

Gravity

Surface-ship, gimbal-mounted gravimeter surveys have been conducted off the Oregon coast to abyssal depths by the Oregon State University Geophysics Research Group. The free-air gravity anomaly maps west of Oregon have been published by Dehlinger, Couch, and Gemperle (1967 and 1968). Along the southern Oregon coast, two pronounced large negative anomalies are noted on the continental shelf (Figure 3). One parallels the coast from approximately the Rogue River south to Cape Mendocino, and the other

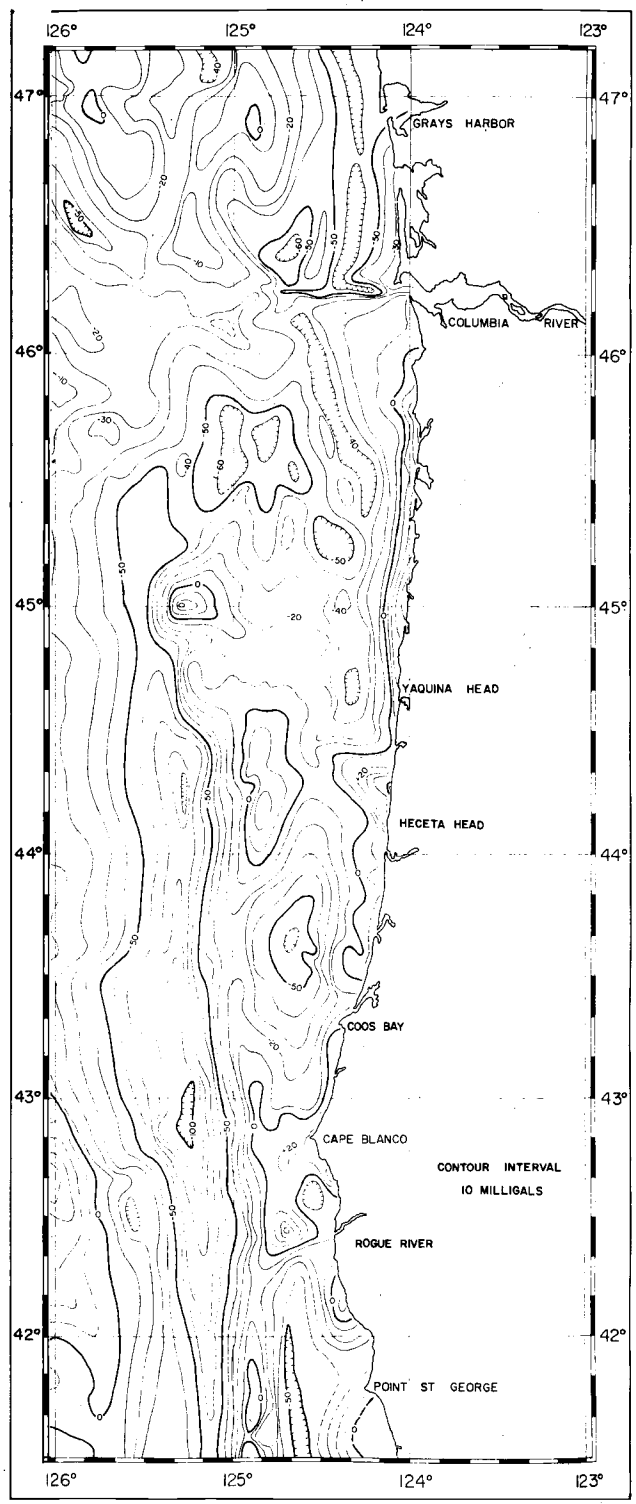

Figure 3. Free-air gravity anomaly map of the Oregon continental margin. Adapted from Dehlinger, Couch, and Gemperle (1969).

extends from Coos Bay north to Heceta Head. These anomalies have been interpreted (Dehlinger, Couch, and Gemperle, 1967 and 1968) as thick sections of low density rocks, indicating the presence of synclinal or downfaulted structures in the sedimentary layers.

A positive 20 mgal free-air gravity anomaly occurs on the continental shelf off Cape Blanco and extends south to Rogue River. The gravity high is probably caused by high density basement rocks cropping out on the continental shelf or by a shallow high density basement covered by a thin, low density sedimentary section.

Magnetics

A ship-towed magnetometer survey has been conducted off the Pacific Northwest coast by Emilia, Berg, and Bales (1966). The anomaly map of the total magnetic field off the Oregon coast (Emilia, Berg, and Bales, 1968a) displays an absence of large magnetic anomalies on the continental shelf from Coos Bay to the Oregon-California state line (Figure 4). There are apparently no extensive volcanic intrusives or flows along the southern Oregon shelf as compared to the seaward extensions of the coastal volcanics noted along the central and northern Oregon coast (Emilia, Berg, and Bales, 1968b). Thus, the previously discussed positive free-air anomaly off Cape Blanco is probably not caused by igneous intrusives or flows, but rather by the seaward extension of high density

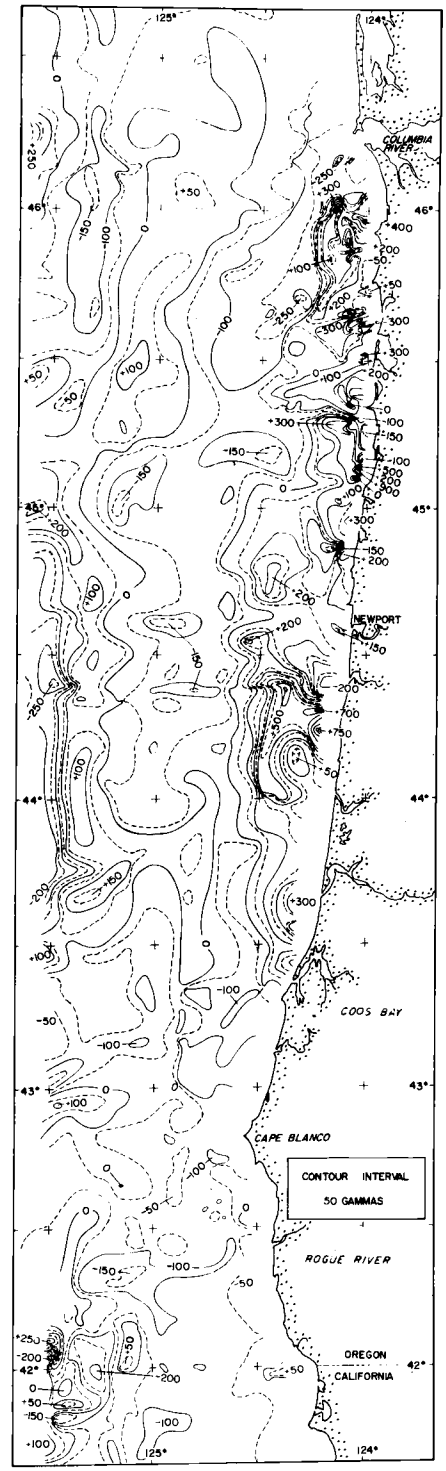

Figure 4. Anomaly map of the total magnetic field off the coast of Oregon. Adapted from Emilia, Berg, and Bales (1968a).

Mesozoic rocks observed onshore by Koch (1966).

Local, steep gradient magnetic anomalies have been noted off some of the rivers of southern Oregon (Kulm et al., 1968). These anomalies are believed to be caused by heavy mineral-bearing sands high in magnetite concentrations, located on or just below the sea floor.

BATHYMETRY

The bathymetry of the southern Oregon continental margin has been mapped in detail in fathoms by Byrne (1963) and in meters by the U. S. Coast and Geodetic Survey (1968). Byrne (1963) noted that the continental shelf off the southern Oregon coast is characteristically narrower, steeper, and deeper than the world average.

In the area of investigation the shelf break generally occurs at water depths of approximately 120 m to 180 m, and the shelf width varies from 15 km off Cape Blanco to 27 km at Coquille Bank northwest of the Cape. From echo sounding profiles across the continental margin, Byrne (1963) noted that the slope of the shelf in the study area ranges from 18' to 40'.

The bathymetry of the study area reveals several anomalous topographic features on the shelf and upper slope (Figure 5). The most prominent features are Coquille Bank, 28 km northwest of Cape Blanco, and the adjacent benches or terraces to the north and the south of the Bank on the upper continental slope. Southwest of Cape Arago in the area where Runge (1966) and Boettcher (1967) reported rock outcrops, the 60 m through 140 m contours are bowed westward towards the outer edge of the shelf. A similar westward convexing of the bottom contours is displayed off Fivemile Point and off Bandon in shallower depths. Southwest of Cape Blanco, two

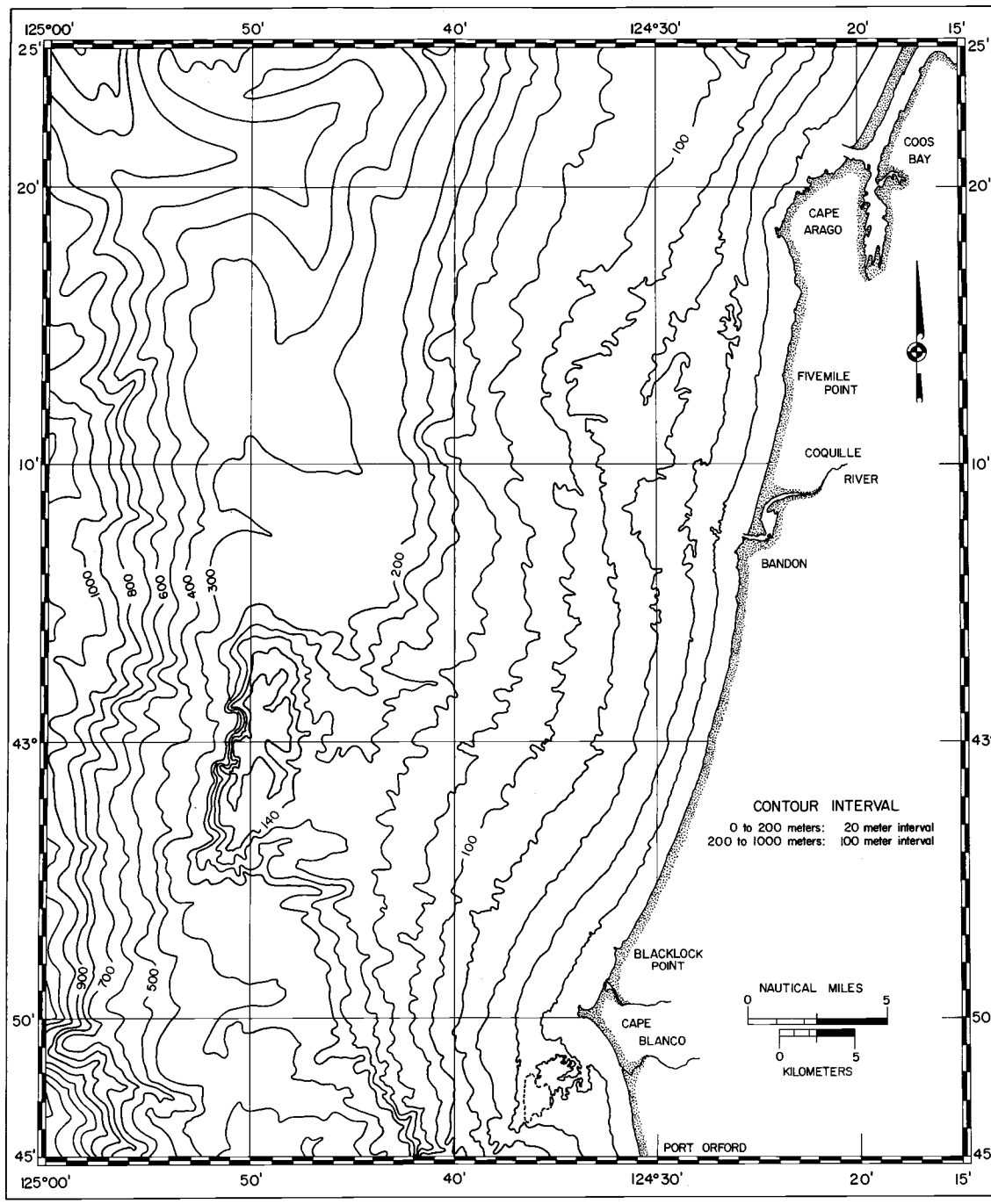

Figure 5. Bathymetry of the continental shelf and upper slope between Coos Bay and Cape Blanco. Adapted from U. S. Coast and Geodetic Survey bathymetry chart (U. S. C. and G. S., 1968).

prominent reefs, the Blanco and Orford Reefs, produce a threat to coastal navigation with sea stacks occurring as far as 7 km from the coast.

CONTINUOUS SEISMIC PROFILING

A continuous seismic profiler is essentially a reflection seismograph with provisions for continuous recording. Acoustic impulses are generated in the water at regular intervals, and the acoustic energy is propagated through the water column and into the underlying sediments (Figure 6). Part of the acoustic signal is reflected at the ocean bottom and from each geologic interface having the necessary contrast in acoustic impedance (the product of seismic velocity multiplied by density). Hydrophones, receiving transducers, convert the reflected acoustic signals into electrical signals, which are amplified, filtered, and recorded on a graphic recorder. Continuous seismic profiles are essentially time sections in which the ship's running time is recorded horizontally across the record and ocean-bottom and sub-bottom reflection times are recorded vertically down the record.

The graphic recorder is highly desirable in this type of geophysical mapping system, because it presents the seismic data as a ready-plotted geologic (time) section. It also provides the necessary vertical exaggeration for mapping gently dipping beds. The record quality and depth of seismic penetration varies with the output power of the sparker sound source, water depth, sea state, and geologic conditions of the ocean bottom and sub-bottom.

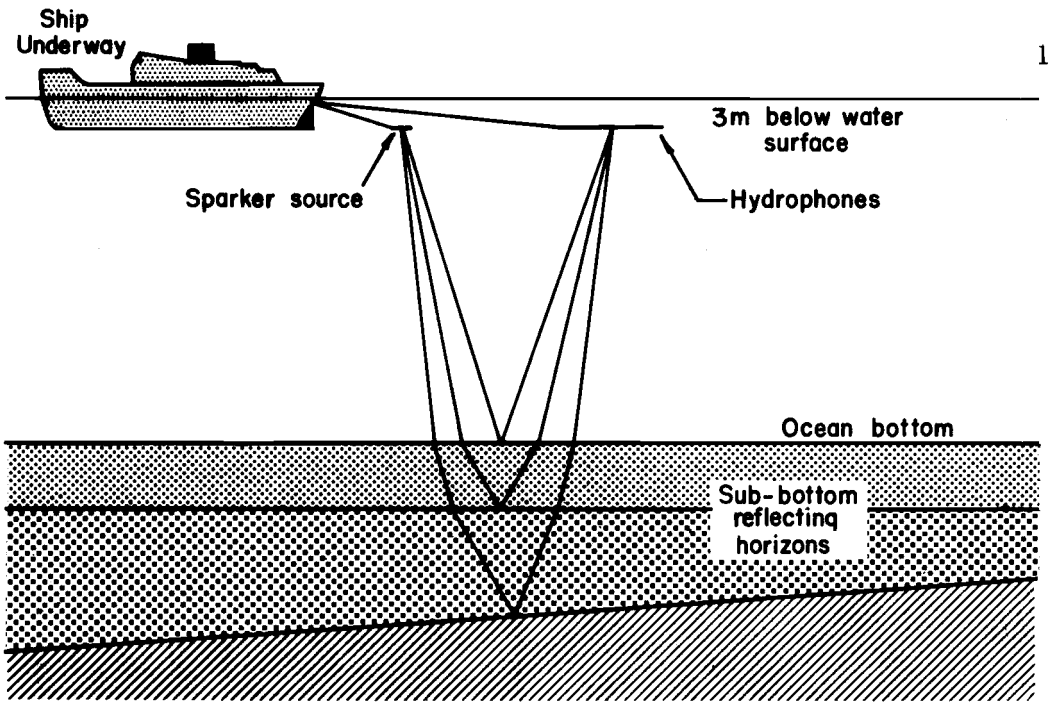

Figure 6. Survey geometry of the continuous seismic profiler for normal incidence relfections.

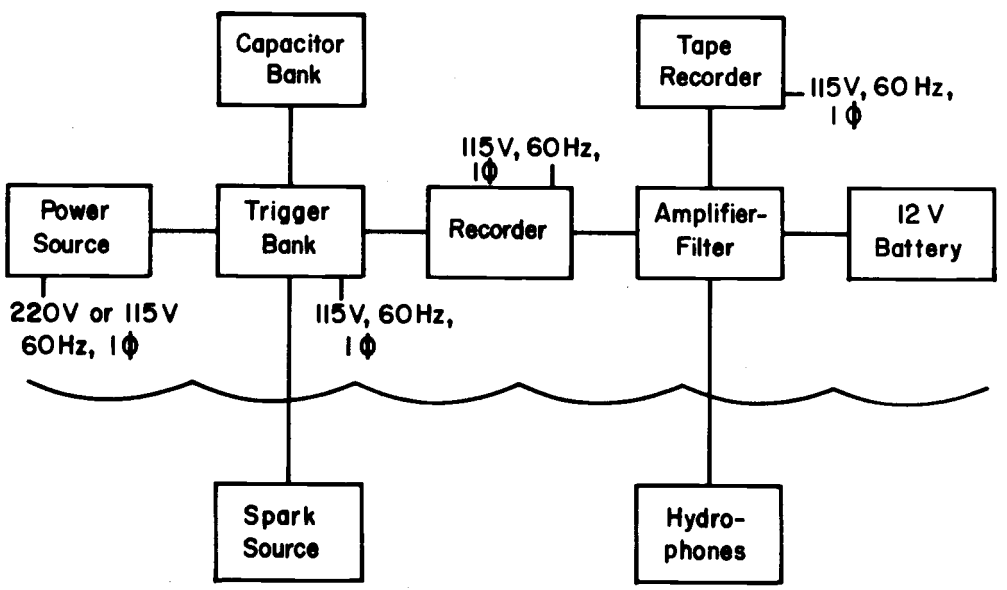

Figure 7. Block diagram of the electrical components of the sparker system.

Instrumentation

The continuous seismic profiler used in the survey consisted of E. G. & G. (Edgerton, Germeshausen, and Grier Corp.) capacitors, trigger, and spark electrodes coupled with an assortment of integrated units, recorder, amplifier-filter, and hydrophones (Figure 7).

The DC power supply, consisting of a transformer and a rectifier circuit, converted 220 v, 60 Hz, single phase, AC current from the ship's generator to 5000 v, DC current. The high voltage DC current charged two parallel, 2000 joule capacitor banks and an additional parallel, 1000 joule capacitor bank, contained in the trigger, to 5000 v.

The trigger bank controlled the capacitor discharge by an air-gap switch or spark thyratron. At regular intervals, the air-gap trigger switch received a high voltage AC pulse from the programmer in the graphic recorder. The pulse, similar to the voltage delivered to a spark plug in a gasoline engine, momentarily ionized the air, resulting in a spark between the high voltage electrodes of the switch. This completed the electrical circuit across the gap and allowed the 5000 v, DC current to pass from the capacitor banks to the electrodes trailing in the water.

The sparker sound source consists of three 0.6-cm diameter,

rubber insulated brass anodes equally spaced at 50 cm between tips within a large ground-return cage (Rusnak, 1967, p. C83). At regular intervals on command from the graphic recorder, the capacitors are discharged creating an explosive spark in the water, as the high voltage DC current dissipates in the sea water between the anodes and the cage. A bubble pulse is generated, and its intensity is related to the energy from the arcing system. The multiple-electrode spark source produces a cylindrical wave front perpendicular to the axis of the array. According to Hersey (1963), a single electrode discharge is only 0.5 to 10 percent efficient in converting electrical energy into acoustical energy; but higher efficiency is obtained with multiple electrodes. The power output of the system was varied from 500 to 5000 joules (watt-sec) by switching the storage capacity of the capacitor banks. The maximum energy output of this sparker system is at frequencies between 125 and 250 Hz (Huckabay, 1967).

Acoustical energy reflected from the ocean bottom and sub-bottom layers is converted into electrical signals by a towed neutrally buoyant, 30-meter long Geospace hydrophone streamer, containing 20 piezoelectric receiver elements at a fixed spacing of 1.2 m. From the receiver elements, which are wired in parallel, a single pair of shielded leads was connected to a Geospace 111 seismic amplifier-filter powered by a 12 v battery. The seismic data were recorded unfiltered on magnetic tape by an Ampex SP-300 tape

recorder and in a filtered condition on a graphic recorder. The filters were set for band-pass with the "Locut" at 63 Hz and the "Hicut" at 205 Hz. In order to reduce confusion in the record interpretation, the band-pass filter settings were generally left unchanged for the entire survey.

The amplified and filtered seismic signals were fed into an Ocean Sonics Graphic Depth Recorder, which graphically reproduces the signals on 18-inch wet Alden paper. The incoming signal voltages were half-wave rectified and printed as a variable density record.

The sweep rate or time of the recorder is controlled by the programmer, which also controls the firing rate of the sparker sound source. Depending on the water depth, the recorder was operated on the water depth scale of 0 to 366 m with a sweep time of 0.5 seconds or 0 to 732 m with a sweep time of 1.0 seconds. In order to record the complete time section from the water surface to the reflecting horizons below the ocean bottom, the firing rate must be equal to or greater than the sweep rate. The sparker profiles were generally recorded with a firing interval from two to four seconds. The sweep rate and the firing interval were adjusted with each profile for optimum record quality.

Survey Procedure

During seismic survey, ambient noise from both electrical and acoustical sources must be kept as low as possible. Mechanical acoustical noise from the ship and from ocean whitecaps, caused by high winds, are received by the hydrophone streamer and are fed into the system. In order to reduce acoustical noise, the sparker sound source and hydrophones were towed astern of the ship at slow speeds of 7 to 11 km/hr. Higher ship speeds increased the acoustical noise level and markedly reduced the quality of the records. The electrode cage was towed 9 m astern of the ship at a depth of 3 m. The hydrophone streamer was towed approximately 30 m behind the ship at a depth of 1.5 to 3 m. This procedure was used to clear the ship's wake, whose bubbles absorb sound, and to place the receiving elements farther from the acoustic noise of the ship.

In order to improve both the energy output of the sparker source and the signal received by the hydrophones, the source and hydrophone streamer towing depths are commonly adjusted to be approximately one-quarter wavelength of the lowest desired signal frequency (Hersey, 1963). According to Huckabay (1967), the optimum signal returning from reflecting geologic horizons would be at a frequency of approximately 100 Hz, so attempts were made to place the source and receiver at an optimum towing depth of 3 m.

The seismic data were recorded as continuously as possible. The most frequent interruptions were changes in the spark source power level, which was varied according to water depth and desired penetration. Continuous seismic profiles were shot in water depths from 20 to 400 m. In depths shallower than 20 m, the time interval between the bottom reflection and the first ocean bottom multiple was so short that little useful information was obtained. In depths greater than 400 m, exiguous information was obtained because of the absorption of acoustic energy in the water column and the scattering of energy on the steeper continental slope. The power of the sparker system was varied according to the water depth with a minimum power of 500 joules at 20 m to a maximum power of 5000 joules at depths greater than 100 m. The records were marked at 15 minute intervals to correspond with the simultaneous navigation fixes.

Navigation for the sparker track lines was primarily by radar and supplemented by Loran, water depth, and dead reckoning. The accuracy of the ship's positioning decreased from $\pm$ 0.5 km within 8 km of the coast to approximately $\pm$ 2 km at distances greater than 30 km from the shore.

Interpretation of Records

The ship's speed and heading between fixes was computed by plane sailing navigation (Bowditch, 1958) on a digital computer.

Some of the navigational errors in the survey were reduced by adjusting the fixes of the track lines according to water depth, ship's speed, intersections with other lines, and navigational accuracy. The adjusted navigation data is listed in Appendix I.

For easier interpretation and multiple reproduction the 18-inch wide sparker records were reduced to one-half scale by Rapid Blue Print Co., Los Angeles, California. Each of the reduced records was picked to accent the real primary events and to remove the multiples and then was interpreted for anticlinal and synclinal features, faults, unconformities and acoustic appearance.

Two sets of velocity data for the area of investigation, one from a reflection survey and the other from a refraction survey, were obtained from prominent oil companies, who wish to remain anonymous. A best fit curve to the two sets of velocity information was used as the time-depth curve throughout the entire area of study (Figure 8). The velocity function was determined by Miller's Procedure (Dix, 1962, p. 116) to be approximately $V = (1707 + 1.39z)$ m/sec, where z is the depth below the ocean bottom in meters.

Apparent dips were calculated on a digital computer for sample reflecting horizons, assuming straight ray-paths with normal incidence with the reflecting horizons. The equation for the dip computation (Dobrin, 1960, p. 137) is given by:

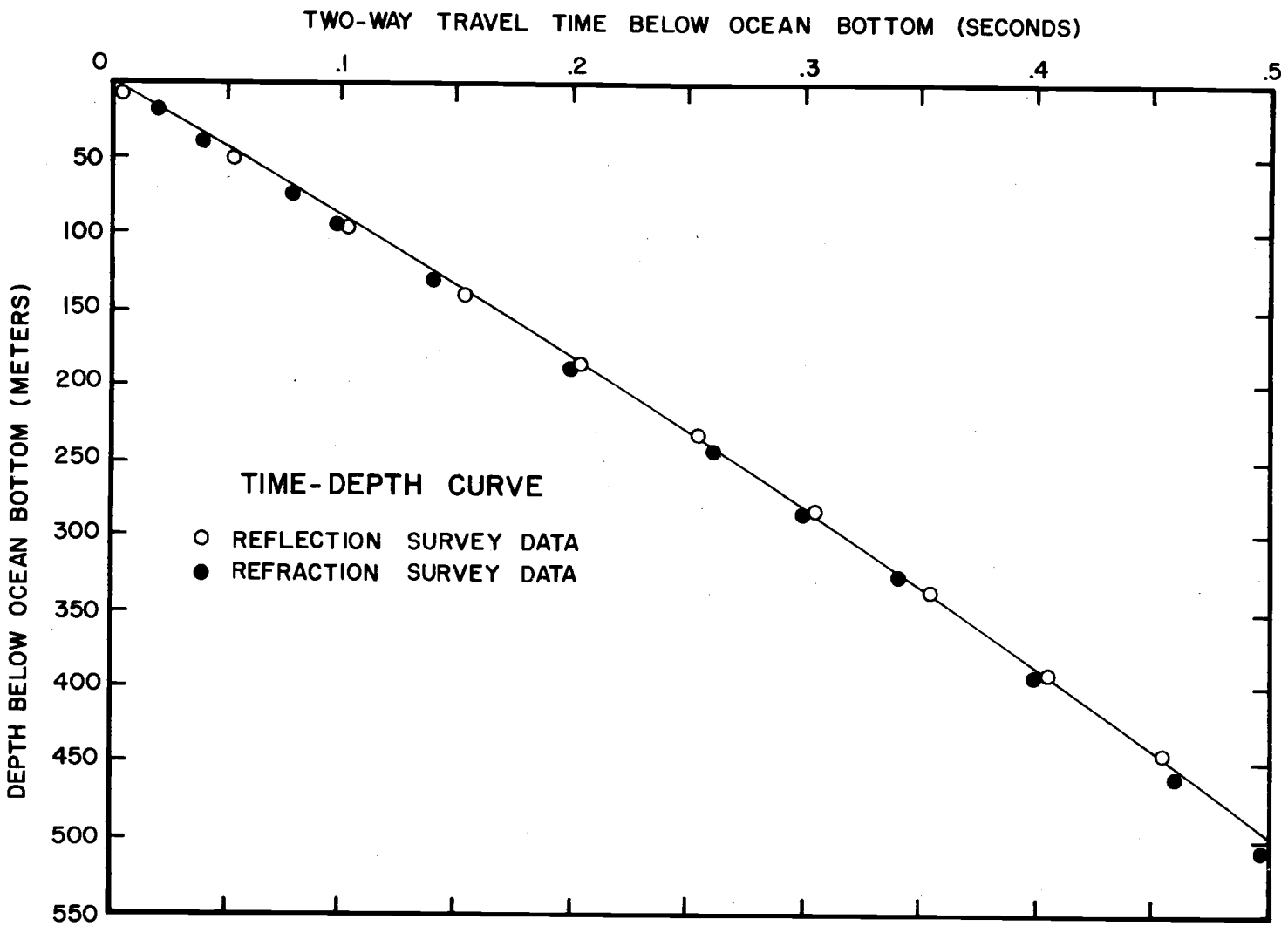

Figure 8. Velocity function curve.

$$\phi = \text{Sin}^{-1} \frac{\overline{V} \Delta T}{2X}$$

$\overline{V}$ is the average compressional velocity in both the water and rock mediums to the depth of the event being considered; ΔT is the difference in two-way time of the seismic reflection measured at two close points on the sea surface; and X is the distance the ship has traveled between the two points. This computation was simplified by reading the water depth from the sparker records below the two points on the surface, timing the events from the ocean bottom to the reflection, and converting the two-way travel time into depth by using the velocity curve shown in Figure 8. Since the sparker sections are two dimensional, unmigrated time sections, the dip computation becomes

$$\phi = \text{Tan}^{-1} \frac{X}{\Delta D} .$$

X is the distance between the points on the sea surface, and D is the difference in depth below sea level between two vertical projections of the points on the reflecting horizon. The results of the dip computations are given in Appendix II.

Several unavoidable errors enter into the calculations of the apparent dips. First, the computation is simplified by assuming

straight ray-paths and normal incidence and reflection with the seismic horizon, which eliminates normal moveout corrections. Actually, the ray-paths are refracted into curves by increasing velocity with depth, and the received reflections may not be of normal incidence. Since the majority of the dip computations were computed for reflections less than 400 m, a straight ray-path is a close approximation.

The other sources of unreliability in the apparent dips are caused by navigational and velocity function errors. Navigational inaccuracies, the major source of error, generate uncertainties in the distance a ship has travelled between two points. Velocity errors, caused by projecting the time-depth curve throughout the entire region of investigation will plot the seismic reflections at inaccurate depths below the ocean bottom. For shallow, flat-lying and moderately dipping seismic horizons, these errors are of little significance ($\pm 1^{o}$), but their effects are amplified for seismically steeply dipping (greater than 6^{o}) reflectors.

True dips and strikes were determined graphically by sterographic net from two apparent dips of a correlated event at the intersections of sparker profiles whenever possible (Donn and Shimer, 1958). The primary source of error in the dip and strike determinations were the uncertainties in the apparent dips, which have been previously discussed. The true dips and strikes are listed in Appendix III.

DISCUSSION OF RESULTS

A structural map of the continental shelf was compiled from the interpretation of the sparker records (Plate I). The map is based solely on the sparker record interpretations, which note angular unconformities, faults, and folds. The surface distribution of ten distinguishable seismic units[1] also is presented on the structural map. Some of the observed offshore units were correlated tentatively with mapped onshore formations and features, but without actual rock samples the inferences can be only very broad and general.

Since the majority of the continental margin is covered by a thin veneer of unconsolidated sediments, the sediment cover is removed from the sea floor in the construction of the map. The structural map thus displays the various mappable seismic units of the continental terrace and their associated structural features. Inferences then can be made about the geologic development and history of the continental margin by using the laws of superposition and original horizontality.

---

[1] The term "seismic unit" refers to a discernible and mappable part of the seismic records based on acoustic appearance, angular unconformities, lateral continuity, and faults. It should not be confused with the rock-stratigraphic unit, formation. A seismic unit may contain more than one rock unit.

In a sense, the sparker survey is similar to a land mapping project, in which the area is investigated along continuous lines in a pre-determined grid. The land survey would have the advantage of studying the lithologic and paleontologic properties of the rock outcrops, but the continuous seismic profiling survey has the advantage of viewing the third or vertical dimension from the sparker records, which are ready-plotted geologic (time) cross sections.

Plate I is a structural map of the continental shelf and upper slope of the area of investigation. Since the rock units and age determinations can only be broadly inferred, the observed seismic units and structural features can be more logically discussed on the basis of geographical distribution, beginning at the southeast, off Cape Blanco, rather than in the normal chronological order of oldest to youngest. In the Summary and Conclusions an attempt is made to discuss the observed geological events and seismic units in chronological order.

Unit A

Seaward of Cape Blanco, unit A crops out on the sea floor (Plate I). Poor to no seismic returns on the sparker records are characteristic of the seismic unit A. The few reflections recorded on the profiles indicate that the unit A is structurally very complex

with seismically steep dips[2] and numerous folds and faults. Only one anticline and an adjacent syncline could be correlated from one profile to another. The validity of this correlation and the structural orientation is somewhat questionable.

Seismic unit A is bounded on the north and the west by a continuous normal fault and on the northeast by what appears to be the seaward extension of the Port Orford shear zone. The unit extends to the south beyond the study area, and the southern limit is undefined. Sediments on the north and west side of the normal fault display upward deformation against the fault. Thus, the sedimentary units to the north and west of the fault are apparently younger than unit A.

The Blanco and Orford Reefs, previously noted as a region of irregular bathymetry (Figure 5), southwest of Cape Blanco lie within unit A. Some ocean bottom rock outcrops displayed on the sparker records and the Reefs indicate that seismic unit A is quite resistant to erosion.

The 20 mgal positive free-air anomaly (Dehlinger, Couch, and Gemperle, 1968) seaward of Cape Blanco also coincides with seismic

---

[2]Seismically steep dips occur when the rock units are inclined at approximately 7^{o} to 20^{o} from the horizontal. Dips greater than 20^{o} are not thought to be detectable with this profiling system, because of the short spread distance between the spark source and the hydrophones and the vertical exaggeration of the graphic recorder.

unit A. This suggests that unit A is probably composed of rocks of greater densities than the adjacent material to the north and west. Higher density rocks would account for the greater resistance to marine erosion, exhibited by the Blanco and Orford Reefs.

Unit A may very well be the Otter Point Formation described at Port Orford by Koch (1966) and mapped at Cape Blanco as the Dothan? Formation by Dott (1962). Koch (1966, p. 36) states that "the uppermost Jurassic Otter Point Formation includes bedded chert, numerous graded beds, and several zones of pillowed flows and pyroclastic rocks". The offshore strata may also be composed of the Rocky Point or Humbug Mountain Formations, which crop out east of the Port Orford shear zone (Koch, 1966). They also may contain erosional remnants of late Tertiary sediments that crop out on Cape Blanco (Dott, 1962). The Mesozoic rocks would probably have a significantly higher seismic velocity than the velocity function obtained in the neighboring Tertiary section (Figure 8). The dips in the unit may be as much as 50 percent greater than the attitudes computed from the lower velocity function. The correlation of unit A with the Otter Point Formation is suggested by structural complexity, lack of consistent reflecting horizons, greater erosional resistance, apparently greater density, propinquity to onshore exposures at Cape Blanco, and its geographic location west of the Port Orford shear zone.

Port Orford Shear Zone

A lack of any sub-bottom seismic reflections on the sparker profile SP-8 between fixes 8 and 9 and on the eastern end of SP-18 between fixes 42 and 43 (Figure 2 and Plate I) may be evidence of the northward extension of the Port Orford shear zone. Little or no seismic reflections would be expected in a zone that has been intensely brecciated and sheared. Thus, the Port Orford shear zone may extend across the shelf as far north as line SP-8, 6 km northwest of Blacklock Point.

North of SP-8 the shear zone is apparently covered by younger sedimentary rocks that have been deformed only gently. If the Port Orford shear zone is buried beneath these younger rocks, there has been no significant displacement along the shear zone since the deposition of the overlying sediments. Dott (1962) has indicated that the last movement along the shear zone occurred after the Miocene.

The structural relationship of the intersection of the shear zone and the previously discussed normal fault (associated with unit A) is not defined on the sparker records. However, the same sediments, which overlie the shear zone, are in fault contact with unit A. This infers that the normal fault is younger in age than the last movement of the shear zone (post-Miocene).

Surf Cut Terrace

Southwest of Cape Blanco on lines SP-22, 23, and 53, an apparent surf cut terrace in unit A is displayed on the seismic profiles (Figure 2 and Plate I). On profiles SP-22 and 23 (Figure 9) the eroded platform appears as a continuous, very prominent reflector and is at least 4 km wide and 9 km long. No seismic reflections are observed below this strong reflector. The toe of the platform is visible on SP-22 (Figure 9) and indicates that the terrace has been cut to a depth of 140 m. The terrace apparently extends eastward of line SP-23, for the back edge or notch of the abrasion platform is not observable on the sparker records. Unconsolidated marine deposits have buried the terrace on SP-22 and 53 and on the northern half of SP-23. The surf cut terrace is exposed on the southern half of SP-23 at a depth of approximately 90 m (Figure 9). The toe of the abrasion platform is evidence of a sea level lowering of 130 m. The width of the terrace of several kilometers attests that the platform was abraded by a transgressing sea and may have been cut by the Holocene transgression, which began some 18,000 years ago.

Unit B

Off Cape Blanco west of unit A to Coquille Bank and north to Bandon, seismic unit B is exposed on the continental shelf. Its

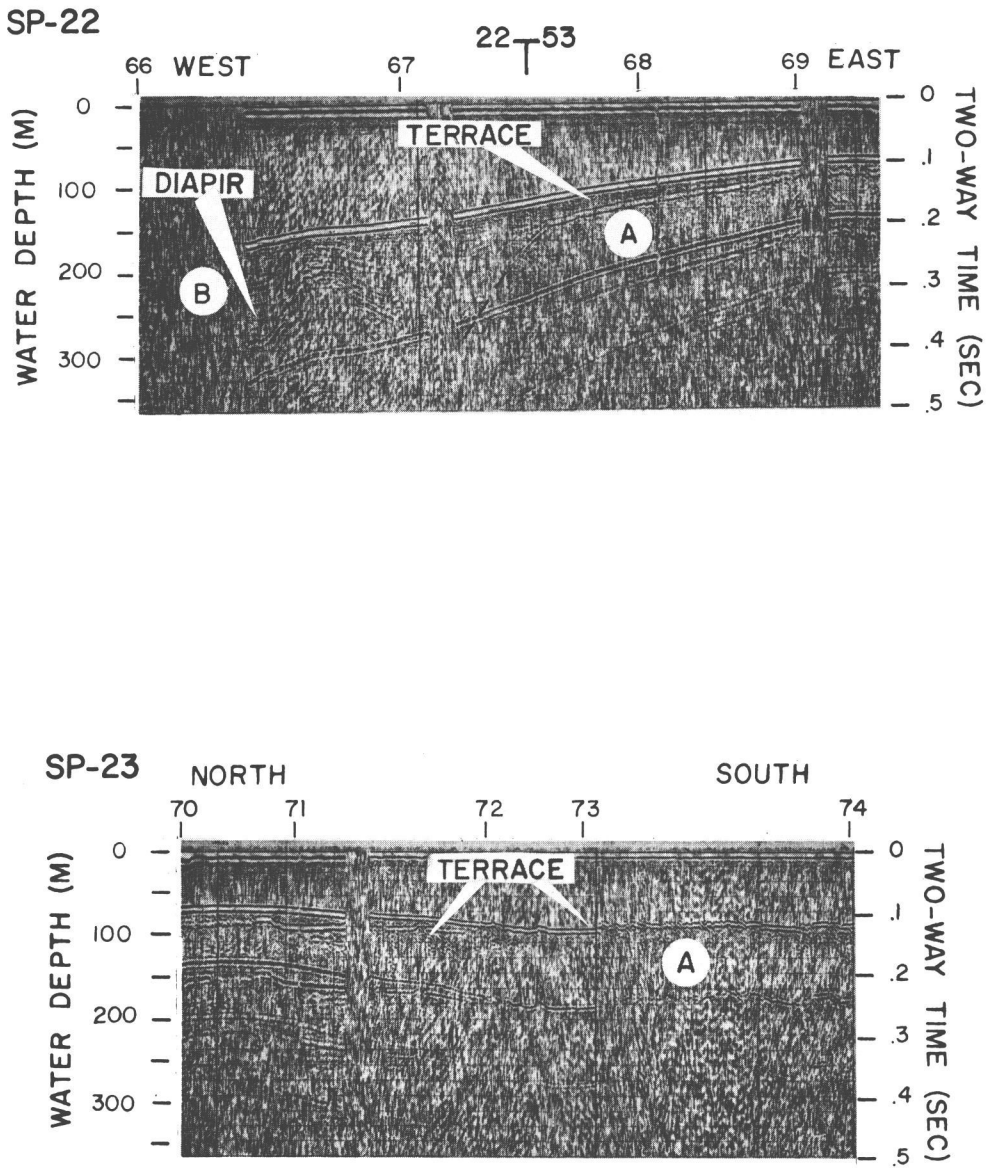

Figure 9. Sparker lines SP-22 and 23 showing a surf cut terrace in unit A. The terrace appears as a continuous, prominent reflector. A local diapir is seen on the west end of SP-22. "T" designates ties or intersections with other seismic profiles, and the smaller numbers refer to navigation fixes positioned in Figure 2. Vertical exaggeration 10X.

sedimentary section yields good sparker records with deep penetration (0.5 sec two-way time) and laterally continuous reflections. Several angular unconformities are exhibited on the sparker profiles, showing at least seven distinct periods of deposition, deformation, erosion (or non-deposition), and subsequent deposition (Plate I and Figures 10 and 11). The surface exposures of the seven depositional periods or small sedimentary basins within B are displayed on Plate I.

The rather low angle unconformities delimit the seismic sub-units[3] of unit B and are more readily visible on the inner portion of the shelf (Figure 11). On the outer portion of the shelf and on Coquille Bank, the sub-units are separated by what appear to be disconformities, which are recognized by acoustic appearance and laterally continuous reflections (Figure 10). The angular discordances between sub-units II, III, IV, and VI are quite small and are visible in the inner shelf and are associated with minor folds (Figure 10).

In the northeastern portion of unit B, north of 43° N. latitude, the angular unconformity between sub-unit I and the underlying

---

[3]Seismic sub-units refer to detectable subdivisions within a seismic unit, based on angular unconformities and acoustic appearance of the sparker records. Seismic unit B is comprised of at least seven seismic sub-units, I through VII.

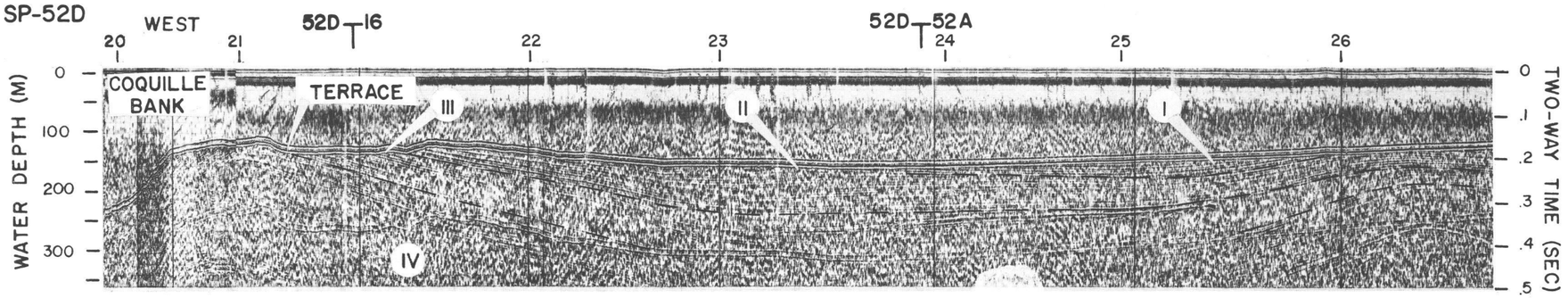

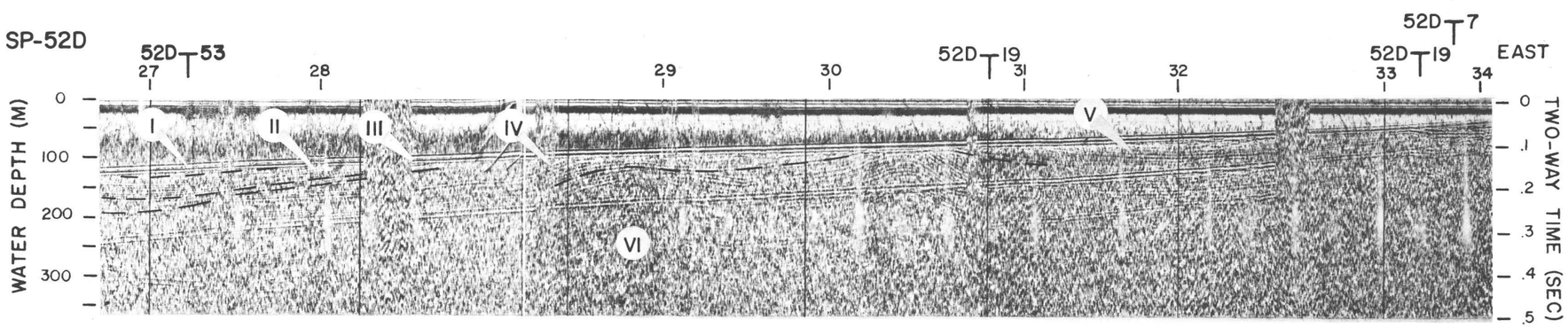

Figure 10. East-west profile SP-52D crossing the continental shelf from northwest of Blacklock Point to Coquille Bank. Within seismic unit B the record shows six seismic sub-units (I through VI) distinguished by angular unconformities. The unconformities have been dashed for clarity. The west end of the profile crosses the Coquille Bank anticline. Vertical exaggeration 6X.

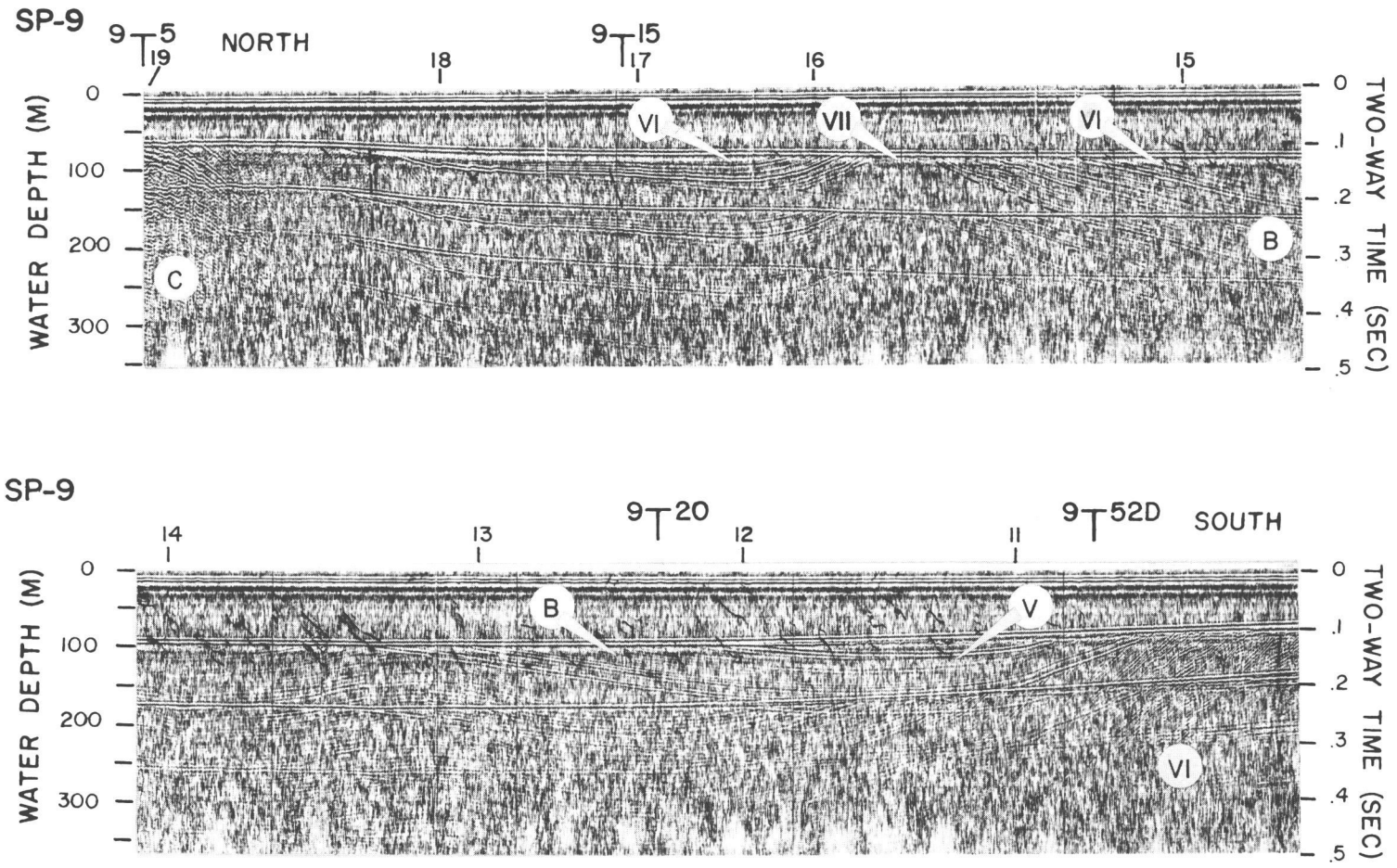

Figure 11. Gently undulating structures of unit B on a north-south profile from northwest of Blacklock Point to west of Coquille Point. Four sub-units (IV, V, VI, and VII) are distinguishable by the prominent angular unconformities. Vertical exaggeration 8X.

sedimentary section is much more prominent, because the underlying strata have been tilted to steeper dips. In this region sub-units II, III, and IV have experienced significant erosion; and sub-unit I overlies in succession each of these older sub-units. On SP-52D (Figure 10) sub-unit I is quite thin, but to the north and to the south of this traverse it thickens significantly. The angular unconformity at the base of sub-unit I probably represents the greatest hiatus of all the unconformities noted.

Sub-unit V also forms a distinct angular unconformity on the inner shelf with the underlying sub-unit VI (Figures 10 and 11). On SP-52D (Figure 10) V appears to be correlative across an anticline with IV, but V also could be interconnected with I, II, or III. The east-west profile SP-20 at approximately 43^{o} N. latitude indicates that V may be interrelated across the anticline with sub-units I or IV. Because its relationship with the other sub-units is not clear, V is given a separate designation. However, V is best tentatively correlated with I, because both I and V form quite discernible angular unconformities with the underlying sedimentary strata.

The oldest sub-unit, VII, crops out on the eroded axis of an anticline (Figure 11). One poor seismic reflection within V suggests an angular unconformity between VII and the overlying sub-unit VI.

There appears to be a westward shift and constriction of the younger sub-units (Plate I and Figure 10). This probably is due

both to deposition and to erosion on the inner shelf. Several structural features are correlated between adjacent profiles, and the gentle folds generally strike in a north-south direction. In many instances the seismic reflections demonstrate that the seismic sub-units of unit B thicken in the basin lows and thin over the structural highs (Figure 10). This suggests that in some cases there has been simultaneous deposition and deformation. Northwest of Blacklock Point sub-unit V has been warped into a small structural basin (Figures 10 and 11).

Unit B is believed to consist of Miocene and Pliocene sediments deposited in a north-south trending synclinorium. Miocene sediments have been dredged from Coos Bay by the U. S. Army Corps of Engineers. The abundant Miocene fossils in the dredge tailings were described by Moore (1963). Baldwin (1966) implied that in the axis of the South Slough Syncline the Tunnel Point Formation is unconformably overlain by a thick section of Miocene beds, which in turn are unconformably overlain by the Empire Formation of Pliocene age. Koch (1966) tentatively has identified Miocene sediments 2.5 km southeast of Port Orford. Miocene sediments, which are unconformably overlain by the Empire Formation, have been reported by Durham (1953) on the south side of Cape Blanco. The Empire Formation is in turn unconformably overlain by the Port Orford Formation (Baldwin, 1945) of probably middle to late Pliocene age.

The Empire Formation is reported to crop out at the mouth of China Creek 5 km south of Bandon (Baldwin, 1966). Miocene-Pliocene boulders have been observed along the beach from China Creek to 6 km north of Blacklock Point (Phillips, 1968) and abundant loose Pliocene fossiliferous boulders have been found on the beach of the sand spit just north of Bandon (Baldwin, 1964). The boulders apparently have been washed ashore from surf zone exposures or eroded from hidden beach and sea cliff sources. A preliminary examination (Fowler, 1968) of the foraminifers in a rock sample taken from a pipe dredge haul 8 km west of Fivemile Point in unit E which is probably correlative with unit B (see the section on unit E for complete discussion), indicates a Pliocene age and a paleo-bathymetry of outer sub-littoral to upper-bathyl (Plate I).

The Miocene and Pliocene rock outcrops in the vicinity of Coos Bay, Bandon, Cape Blanco, and Port Orford localities have been described by Baldwin (1964), Durham (1953), and Koch (1966) as massive poorly consolidated sandstone of relatively uniform lithology with distinct angular unconformities between each of the late Tertiary formations. Numerous prominent unconformities are observed offshore in unit B. Good seismic reflection records, which are characteristic of the unit B, can be expected from massive sandstone beds of uniform lithology. The sediments of B also overlie the possible seaward extension of the Port Orford shear zone. The lack

of significant deformation in B also indicates that the sediments are late Tertiary because the last movement of the shear zone is postulated to be post-Miocene (Dott, 1962). Thus, the correlation of the sedimentary unit B with the onshore Miocene and Pliocene formations is suggested by numerous angular unconformities, good seismic records with laterally consistent reflecting horizons, proximity to onshore rock outcrops and beach awash boulders, and stratigraphic position of the sedimentary sub-units overlying the possible seaward extension of the Port Orford shear zone.

Off Cape Blanco, the sub-units of B are upturned by the normal faulting of unit B against A, which is believed to be the Otter Point Formation of latest Jurassic age. Seismic reflections reveal that the sub-units of B thin towards unit A as if it was formerly a structural high at the time of the deposition of the younger sediments. Unit A has subsequently undergone further uplift by normal faulting. Based on the correlation of B with the onshore Miocene and Pliocene formations, the normal faulting is late to post-Pliocene. Both the B and A seismic units were truncated during the Pleistocene. The differential uplift of Cape Blanco may be related to the offshore uplift of unit A.

The sparker records reveal that Coquille Bank, situated 28 km northwest of Cape Blanco, is a north-south trending, doubly

plunging, asymmetrical anticline (Figures 10, 12, and 13). This shoal is approximately 4.5 km wide and 14 km long.

The sub-units of unit B are best exposed on the east limb and on the north and south noses of the bank (Figures 10, 12 and 13). The flanks of the shoal are an excellent place for sampling much of the sedimentary section of unit B with a series of bottom rock samplers or shallow core holes; however, no samples as yet have been obtained by the Department of Oceanography. The sedimentary section exposed on the east limb of the shoal can be traced eastward on the seismic profiles to the inner shelf outcrops of the sub-units of B, which are believed to be of Miocene to Pliocene age. On the east flank of the anticline, the sub-units II, III and IV of unit B (Figures 10 and 12) crop out and dip 3 to 5 degrees eastward. Laterally continuous seismic reflections are obtained from II and IV, and the prominent irregular outcrops at the ocean bottom suggest that the sub-units are resistant to marine erosion and are well consolidated. However, sub-unit III displays relatively few continuous acoustic reflections; and, in many cases, there is a noticeable lack of seismic returns from it. Surficial exposures of sub-unit III are not irregular like those of II and IV, but are smooth, and are covered, in some instances, by unconsolidated sediments. On profiles 52D, 20, 52A, and 16 (Figures 10, 12 and 13) the outcrops

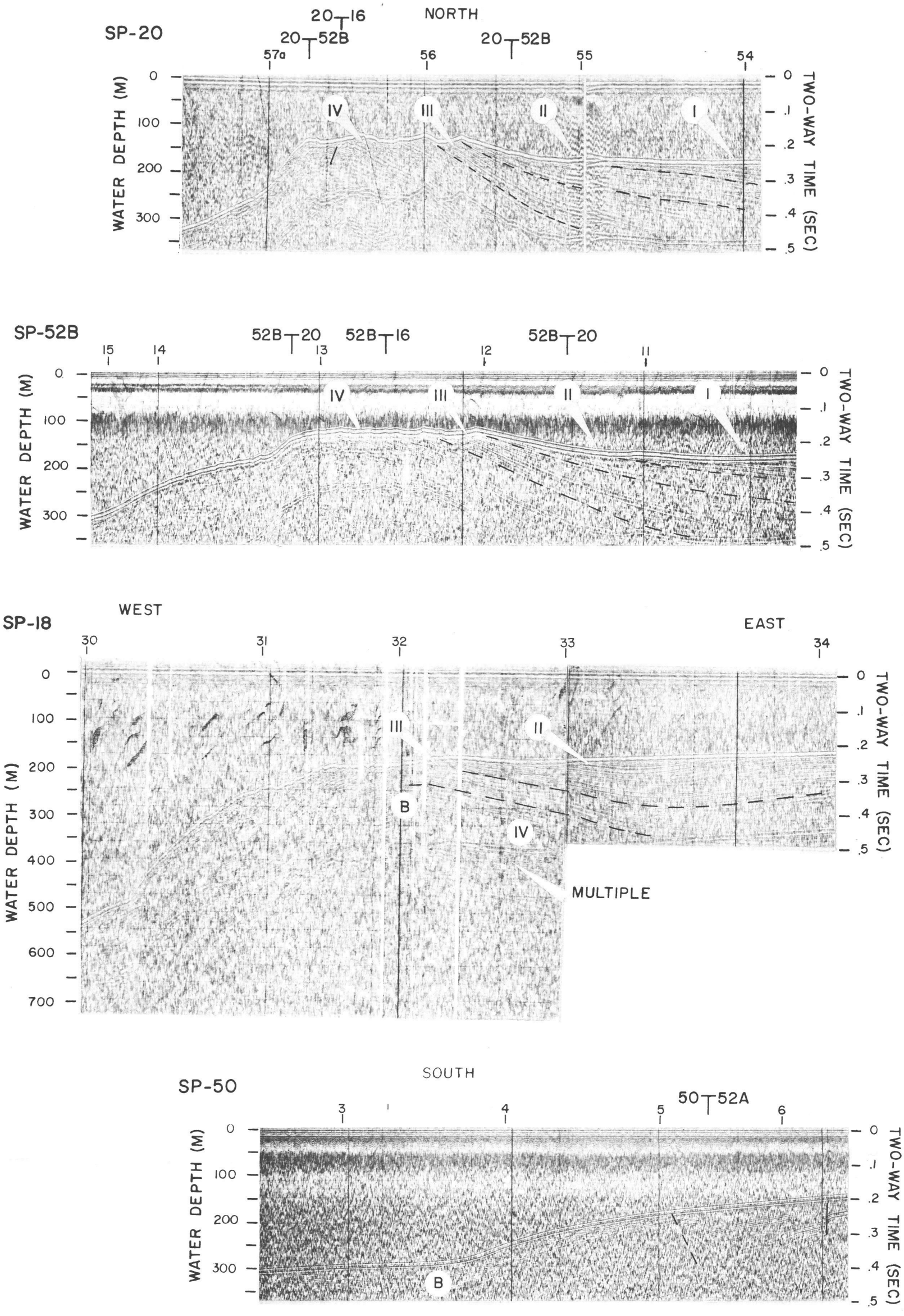

Figure 12. East-west profiles across Coquille Bank. A north-south trending, asymmetrical anticline is exhibited on the profiles. Vertical exaggeration 8X.

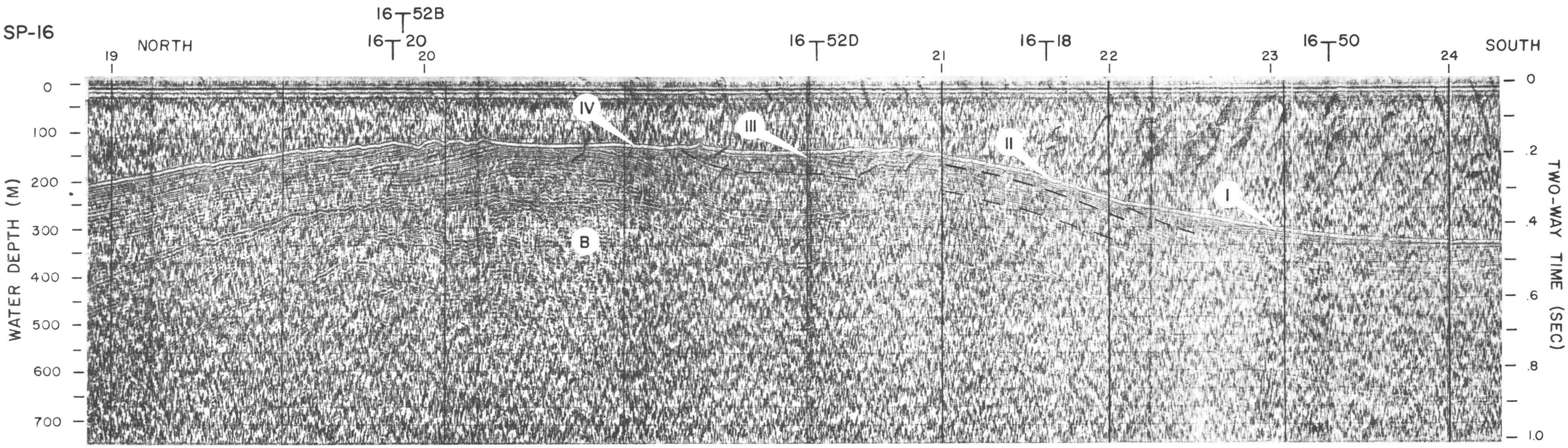

Figure 13. North-south profile SP-16 parallel to the axis of the Coquille Bank anticline. The doubly plunging aspect of the structure is revealed on the record. The unconformities of the seismic sub-units are dashed for clarity. Vertical exaggeration 10X.

of III form noticeable lows in the bathymetry. Sub-unit III is apparently less resistant to erosion than the more competent beds of II and IV and is probably of different lithology or less consolidated than its adjacent strata.

The steep and relatively straight western side of Coquille Bank expressed in the bathymetry suggests faulting on the west limb of the anticline (Figure 5). The thick sedimentary section of sub-units II and III that crop out on the east limb of the structure (Figures 10 and 12) are apparently missing on the western flank of this asymmetrical anticline. The absence of the sedimentary section of II and III further implies faulting on the west limb of the structure, although no fault zone can be distinguished from the poor seismic records of the seaward side of the shoal.

Adjacent to the Coquille Bank anticline are two broad, north and south plunging synclines, which parallel the shoal. The axial plane of the synclines dip to the west, while the axial plane of the anticline slopes towards the east. The terraces or benches noted in the bathymetry (Figure 5) to the north and south of Coquille Bank are apparently structural features, resulting from the north and south plunging anticline-syncline complex (Figure 12 [SP-50] and 13). Both of the terraces slope away from Coquille Bank, either to the north or to the south (Figure 5).

The north-south trending structures in unit B, particularly

the asymmetrical faulted anticline of Coquille Bank, suggest that the late to post-Pliocene deforming stresses were essentially compressional forces from the west. Maloney (1965) has postulated that the benches, hills, and scarps of the continental slope off central Oregon are the result of step block faults. These low angle faults differ from the common type of normal faults in that both the hanging wall and foot wall have moved upward. The foot wall has moved farther than the hanging wall, making the net displacement like that of a normal fault. This type of slope structure implies that the deforming stresses were also compressional and upward from the west. The postulated fault on the west flank of Coquille Bank may be the same type of fault as described by Maloney.

The most outstanding characteristic of Coquille Bank is its flat truncated top at a depth of about 120 to 130 m (Figures 10, 12 and 13). This depth is in close agreement with the maximum eustatic lowering of the sea level at 120 m (Curray, 1961) at the beginning of the Holocene transgression. The truncated top of Coquille Bank is evidently an erosional remnant of a surf cut terrace. The shoal may have undergone subaerial erosion during sea level lowerings of greater than 130 m; however, the last significant erosion of the Bank was the planation of its top. The present depth of the terrace suggests the Bank may have been truncated during the late-Wisconsin glaciation. If the crest of the anticline was eroded during the

late-Wisconsin, present water depth indicates there has been no appreciable uplift of Coquille Bank during the Holocene.

Unit C

West of Bandon unit C forms prominent rock outcrops on the sea floor. Sparker profiles traversing the unit disclose that it is structurally very complex with seismically steep dips and numerous folds and faults (Figures 11 and 14). The poor seismic returns and structural complexity of this area are similar to those observed in unit A off Cape Blanco. The rock outcrops of unit C are visibly resistant to marine erosion and produce a topographic high on the inner shelf (Figures 5 and 14).

Unit C is believed to be a northern extension of the Otter Point Formation described by Koch (1966). Baldwin (1966) has noted the outcrops of this formation at Coquille Point. Although C is tentatively correlated with unit A, C is given a separate designation, because of the geographic separation of the two exposures. The correlation of the seismic unit C with the Otter Point Formation is inferred by its structural complexity, poor seismic records, greater erosional resistance, and contiguity with onshore outcrops. The unit may also contain Late Cretaceous, rhythmically bedded, turbidites, which crop out at the mouth of Crooked Creek 4 km south of Bandon (Baldwin, 1966).

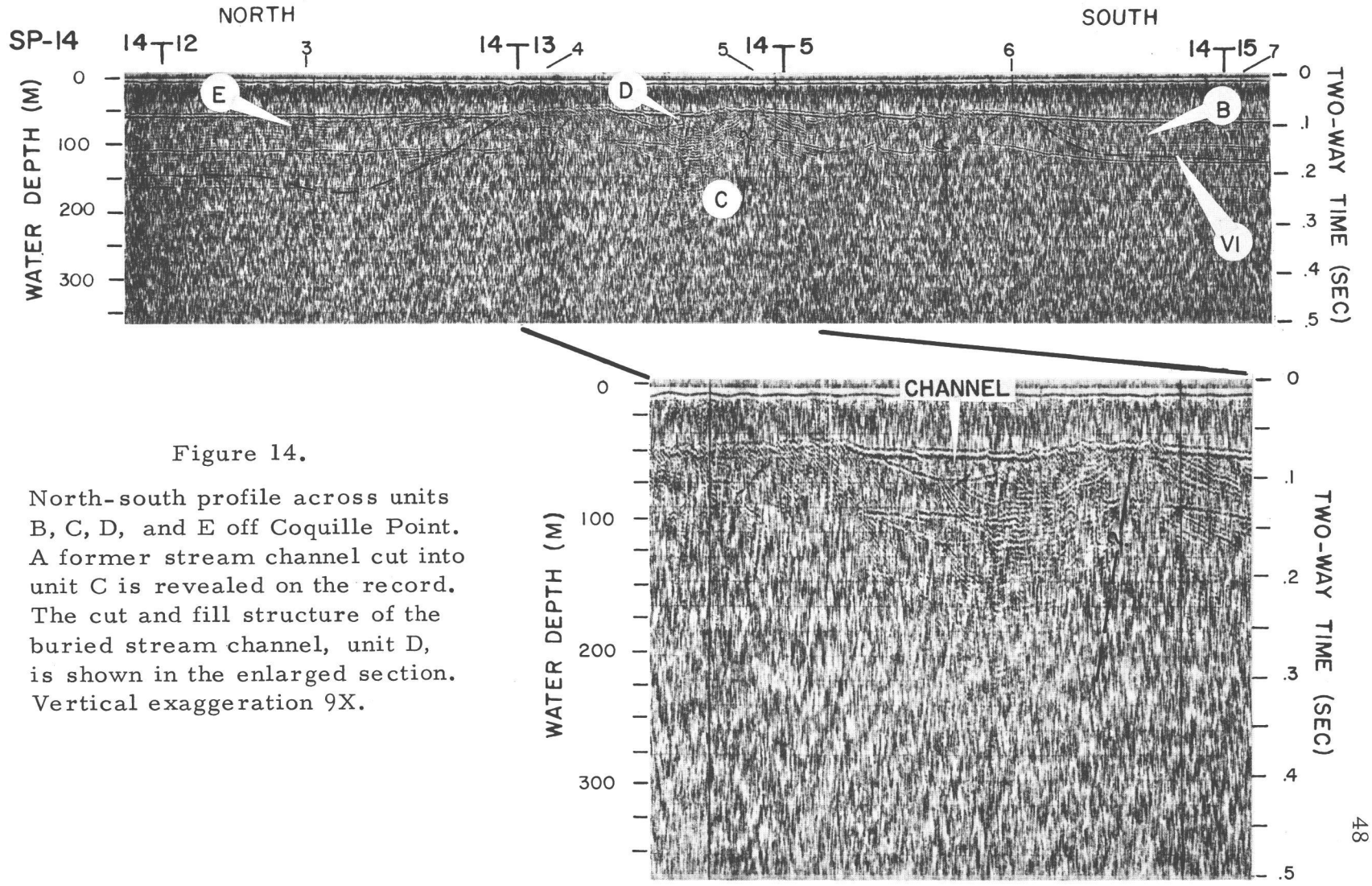

Figure 14.

North-south profile across units B, C, D, and E off Coquille Point. A former stream channel cut into unit C is revealed on the record. The cut and fill structure of the buried stream channel, unit D, is shown in the enlarged section. Vertical exaggeration 9X.

Younger sediments of units B and E appear to unconformably overlie unit C from both the north and the south (Figures 11 and 14). The younger sediments of B thin towards C as if the area west of Bandon was a structural high during the deposition of the late Tertiary sediments of B and E. Late to post-Pliocene uplift has tilted the overlying sediments upward a few degrees. Both units have been truncated subsequently by erosion during the Pleistocene.

Dott (1966) postulates a shear zone through Bandon. Only weak evidence of faulting is seen on the very southern end of line SP-4, but the structural complexity and poor sparker records of unit C may be indicative of a shear zone. The lack of deformation of the overlapping sediments of units B and E of Miocene to Pliocene age indicates that there has been little significant movement in the postulated fault zone since the deposition of the younger sediments.

Unit D

Five and a half kilometers northwest of Coquille Point, a buried stream channel, which was cut in unit C, is displayed on the sparker lines SP-13 and SP-14 (Figure 14). The buried channel, unit D, trends northwest in about 50 m of water. The bottom of the channel forms a distinct angular unconformity with the steep southwest dipping reflections of unit C, which may be the Otter Point Formation. The maximum thickness of the channel fill is

approximately 25 m, and the rough ocean bottom displayed on both the sparker and fathometer records indicates the presence of consolidated rock exposures in the buried channel.

Baldwin (1945, 1964, and 1966) named and described the Coquille Formation of late Pleistocene age as a former filled channel of the Coquille River. The formation is exposed between Whiskey Run and Cut Creek, north of the river's present mouth. Baldwin (1966, p. 200) described the formation as containing "semiconsolidated conglomerate, sandstone, and mudstone with numerous stumps and logs, all of which were deposted in a bay during a stage of alluviation similar to that taking place today". At the mouth of Whiskey Run the formation unconformably overlies the pre-Tertiary graywackes of Fivemile Point.

Unit D is believed to be a remnant of a former course of the Coquille River during a lower sea level stand and possibly correlates with the Coquille Formation 6 km to the northeast. The offshore buried channel would be of late Pleistocene age and may have been formed during the last lowering of sea level. The correlation of unit D with the Coquille Formation is suggested by the cut and fill structure on the sparker records, apparent consolidation, and propinquity with the Coquille Formation and the present river mouth.

Unit E

Unit B south of Bandon has been previously described in the discussion of the southern portion of the study area. Between Fivemile Point and Bandon a similar sedimentary section, seismic unit E, crops out on the sea floor (Figure 14 and Plate I). The unit produces good seismic profiles with relatively continuous reflections. The ocean bottom reflection on the sparker and fathometer records and a dredge haul on the western boundary of E verify that the sediments are consolidated.

Unit E has been structurally deformed into a broad synclinal basin whose axis plunges to the south-southeast towards Bandon (Plate I). The base of the syncline is clearly visible in the northern and western portions of the basin and forms a distinct angular unconformity with the older, underlying sedimentary rocks, which dip apparently to the south. The sediments in the synclinal basin are believed to be of Miocene to Pliocene age and appear to be correlative with the extensive sedimentary section to the south of Bandon (unit B). Unit E is given a separate designation because B and E are divided by the structural and topographic high of unit C (Plate I). Foraminifers, analyzed from a dredge sample on the western boundary of this unit off Fivemile Point, have been tentatively identified by Fowler (1968) as Pliocene in age. These sediments were

apparently deposited in outer sub-littoral to upper-bathyl depths. Fossiliferous Pliocene boulders have been reported to have washed ashore on the sand spit just north of Bandon from a source in the surf zone (Baldwin, 1964). Similar seismic records with prominent and continuous reflecting horizons, a dredge haul sample, and proximity with beach awashed boulders are the bases for the suggested correlation of unit E with unit B south of Bandon and with onshore Miocene and Pliocene formations.

Sediments of E overlie C to the south and the older units G and H to the north. Sparker profile SP-12 reveals that the Mio-Pliocene sediments of E are faulted against F on the northwest. No east-west profiles cross the southwestern portion of unit E, so the southern extent of the fault between E and F is undetermined. Because of this lack of information, units E and F are postulated to be in questionable sediment contact on the southwest (Plate I). The syncline associated with E was probably formed as a result of the late to post-Pliocene uplift of the older surrounding seismic units C, F, G, and H.

Unit F

Unit F's appearance on the continuous seismic profiles is quite different from the surrounding strata. Many strong reflections appear on the seismic profiles, but the reflections are very

irregular and are soon laterally interrupted by the numerous faults that lace the unit (Figure 15). Structurally the unit consists of gently undulating small folds superimposed on an east-west trending major anticline. Bottom photographs of the rock outcrops on the southern flank of the anticline show evidence of bedding trending from approximately N 50 E to due east-west (Neudeck, 1968). The Pan American Oil Corporation OCS-P-0112 well (43° 14' 45.7" N. latitude and 124° 35' 34.5" W. longitude) was drilled on this anticline. The numerous faults and folds displayed on the records could not be correlated between adjacent sparker profiles, so the orientation of the structural features is merely speculative.

The sparker and fathometer records display irregular outcrops throughout unit F's exposure on the continental shelf (Figure 15). The unit evidently was resistant to Pleistocene marine erosion because it forms a distinct, large topographic high southwest of Cape Arago (Figure 5).

A discernible change in dip and acoustic appearance of the strata on sparker record SP-53 suggest faulting between F and B on the south and F and I on the north (Plate I). The east-west orientation of the fault traces and the upward displacement of unit F are conjectural, because each fault is crossed by only the one profile. Seismic unit F is unconformably overlain on the west by a wedge of sediments, unit J, on the outer edge of the shelf (Figure 15).

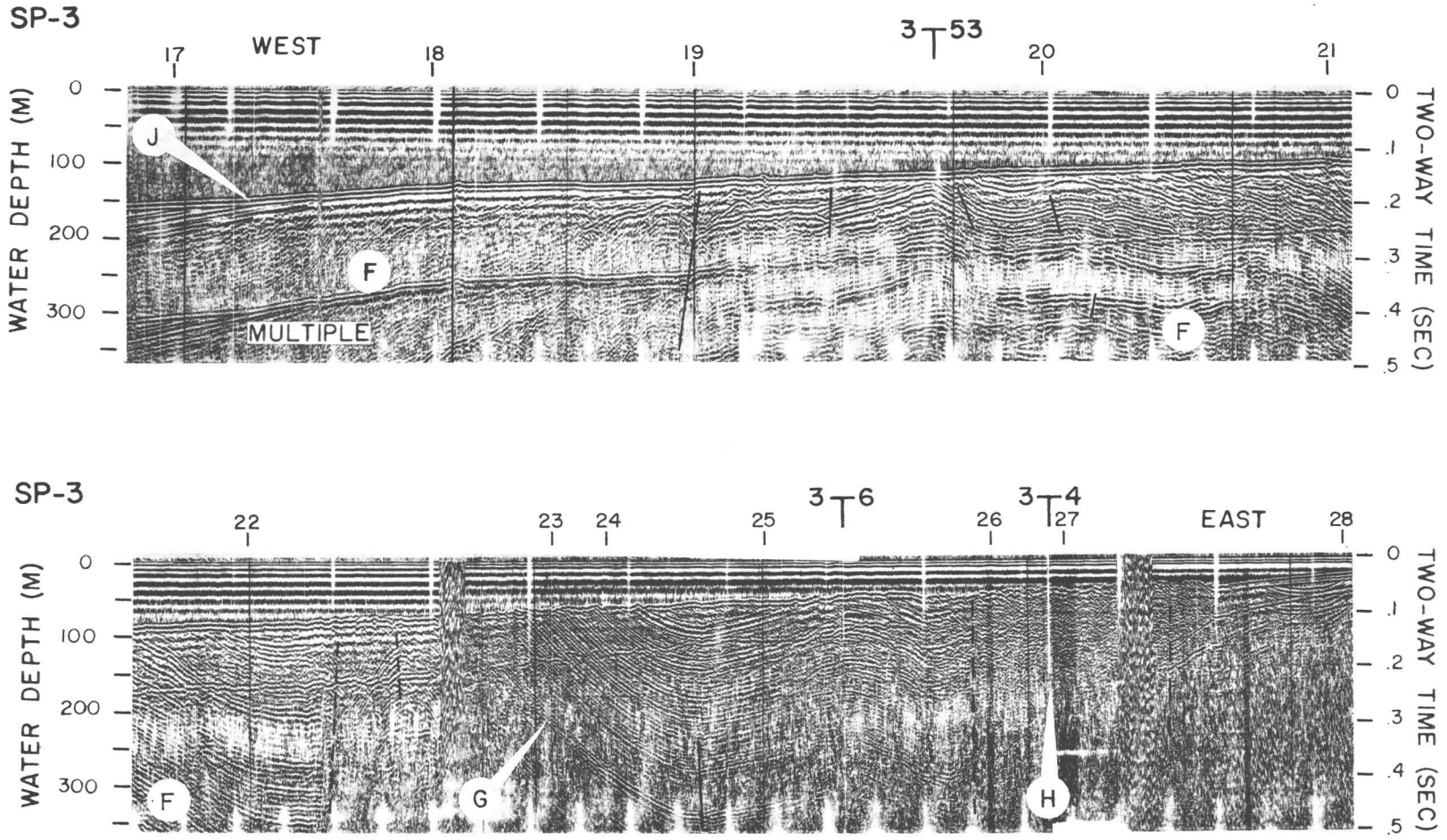

Figure 15. East-west traverse of the continental shelf southwest of Cape Arago across four distinct units, F, G, H, and J. Continuous or dashed lines accent the recognizable faults. Vertical exaggeration 6X.

The east-west trending fault traces of F are postulated to terminate against north-south oriented faults (Plate I). The fault trace, forming the northeast boundary of F, is positioned by three sparker traverses (Figure 15). However, the fault on the southeastern boundary was crossed only once. No east-west sparker profiles cross the boundary between F and units C and E. A questionable sedimentary contact is speculated between F and C and between F and the southwestern limit of E. It is possible that the eastern boundary of F may be one continuous north-south fault trace. The north-south striking faults could be part of the wrench fault system, common to the southwestern Oregon coast (Koch, 1966), or of a normal fault system, which are frequent in the southern Oregon Coast Range (Baldwin, 1965 and Phillips, 1968). The sense of movement could not be determined from the sparker records; but bathymetry, stratigraphic relationship of F and B, and faulting of F against younger strata, units B and E, suggest at least some vertical component of the net slip.

Erosional remnants of the strata of B unconformably overlie F in the southern portion of the older seismic unit. The younger sediments of unit B are preserved in graben-like features. The north-south dimensions of the younger sediments are defined on line SP-53; but the longitudinal dimensions and orientations of the grabens are only inferred, for no east-west seismic profiles cross

the structural features.

At least the southern portion of unit F was covered by overlying sediments of B, which are believed to be Miocene to Pliocene in age. During the Pliocene, the deposition of B and E may have extended across the southern half of unit F and possibly across unit C. Unit F has experienced subsequent late to post-Pliocene uplift and minor faulting, and the majority of the overlying younger sediments have been removed by the migrating shoreline of the Pleistocene transgressions and regressions.

Unit F's location on the outer continental shelf makes any correlation with an onshore coastal outcropping formation very difficult. The stratigraphic relationship of the erosional remnants of B overlying F indicates that unit F is probably early Pliocene or older. Its greater structural complexity and erosional resistance further suggest that F is older than seismic units B and E. Unit F is probably of middle Tertiary age, Oligocene to Miocene. The Coos Bay embayment or synclinorium received littoral and inner sub-littoral marine deposits from the late Eocene through the Pliocene (Snavely and Wagner, 1963). Significant marine deposition probably occurred contemporaneously on the continental shelf. Most of the lower and middle Tertiary rocks on the continental shelf and upper continental slope probably are covered by Pliocene deposits. However, this portion of the outer shelf apparently has experienced

late Cenozoic uplift, exposing the postulated middle Tertiary sedimentary rocks. Regardless of what the actual correlation may be, unit F is a distinct mappable seismic unit and is different from any of those previously discussed.

Unit G

Faulted against unit F is a north-south trending, southward plunging syncline. This syncline and an adjacent minor anticline comprise unit G (Plate I). The unit produces good seismic records with deep penetration and strong continuous reflections (Figure 15). The good reflections suggest that the sedimentary rocks consist of massive laterally continuous, competent beds. The sedimentary beds crop out at a depth of about 40 to 70 m in the southern portion of the seismic unit, and form the outer part of the topographic high northwest of Fivemile Point (Figure 5). In some instances, the strong reflectors continue through the ocean bottom reflection of the bubble pulse and imply that the bedding surfaces are exposed on the sea floor (Figure 15).

The syncline is faulted against unit F on the west and unit H on the east (Plate I). A questionable angular unconformity, visible on SP-6, suggests that unit G is in sedimentary contact with I on the north. The sediments of E overlie the southern limits of the synclinal structure of H. In both cases the overlying sediments have

been tilted upward by late to post-Pliocene uplift of unit G. Pleistocene erosion has removed all but the bordering sediments of the less resistant strata of E and I and has exposed the more resistant deposits of G.

It is very difficult to correlate the sediments of unit G with an onshore formation. The stratigraphic relationship of G with units E and I discloses that G is older than these contiguous deposits. Seismic unit G is presumed to consist of the middle Eocene Tyee Formation. The Tyee Formation is composed of massive, rhythmically bedded micaceous sandstones grading upward into siltstones (Baldwin, 1964). Prior to the deposition of the upper Eocene Coaledo Formation, erosion removed the Tyee Formation from a large portion of the Coos Bay quadrangle (Allen and Baldwin, 1944). However, the Sacchi Beach member of the Tyee Formation is exposed at Sacchi Beach 5 km north of Fivemile Point. The underlying massive phase of the Tyee is presumably down dropped against older pre-Tertiary strata that crop out at Fivemile Point (Baldwin, 1966). The offshore syncline is apparently a similar down dropped block or graben, which escaped the erosion after the deposition of the Tyee Formation.

Unit G is correlated tentatively with the Tyee Formation by the acoustical appearance of its reflections, erosional resistance, the north-south trending synclinal structure, and the proximity with

onshore outcrops. However, it may also be the Coaledo Formation (deltaic shallow-water sandstones, siltstones, and shales) or rhythmically bedded turbidites of Late Cretaceous age. Outcrops of the Coaledo Formation form the coastal promontory, Cape Arago, to the northeast of unit G. Late Cretaceous turbidites crop out at Fivemile Point. The validity of the geologic correlation of unit G cannot be established without actual samples of the rock; but it seems certain that unit G is a separate seismic unit from any of those previously discussed.

Unit H

Unit H is in fault contact with the east limb of the south plunging syncline of unit G. Very poor to no seismic reflections were obtained on the sparker profiles across unit H (Figure 15). The poor records suggest that the rocks have been intensely folded and faulted. Resistant ocean bottom outcrops form a high on both the sparker records and on the bathymetry 5 km northwest of Fivemile Point (Figures 5 and 15).

Unit H may be correlative with northwest trending sandstones and siltstones that crop out along the sea cliffs at Fivemile Point between the mouths of Whiskey Run and Twomile Creek just south of Sacchi Beach. Evidence of cross bedding in the rhythmically bedded turbidites at the Point indicate that the steeply dipping

sedimentary rocks are overturned to the east (Ehlen, 1969). These strata are similar to the turbidites that crop out at Crooked Creek south of Bandon and north of Blacklock Point (Baldwin, 1966). Late Cretaceous fossils, referred to by Dott (1962), in the graywacke north of Blacklock Point suggest that the exposures at Crooked Creek and Fivemile Point are of a similar age. The more resistant sandstone beds are nearly vertical at Fivemile Point. Sea stacks, extending as far as a half kilometer offshore off the Point, may be the seaward extension of the resistant graywacke. Steeply dipping beds and their associated outcrops would tend to scatter and defract the sound energy, resulting in poor seismic returns. The correlation of unit H with the turbidites at Fivemile Point is questionable; however, the relationship is suggested by the poor seismic records, erosional resistance, and contiguous onshore outcrops at the Point.

Unit H is overlain on the south by the younger sediments of unit E. A sediment contact also is postulated on the north between H and the younger unit I. The overlying sediments have been subsequently tilted upward with the late to post-Pliocene uplift of units F, G, and H. Differential weathering has left H as a bathymetric high (Figure 5).

Unit I

Good sparker records across unit I depict moderately undulating

sedimentary strata. The gently folded structures trend in a northerly direction, but their exact orientation could not be determined. Only a few rock outcrops are apparent on the sea floor, which indicates that this consolidated unit is less resistant to erosion than its adjacent sedimentary deposits to the south. Unit I coincides with the southern end of a free-air gravity anomaly trough or low (Figure 3), which has been interpreted as synclinal or downfaulted structure in the sedimentary layers (Dehlinger, Couch, and Gemperle, 1967). The negative free-air gravity anomaly extends from Coos Bay to Heceta Head as an elongated trough or low and is evidence of a thick section of low-density sedimentary layers on the central and outer continental shelf.

As previously noted in the discussion of unit F, a distinct change in dip and acoustic appearance on sparker profile SP-53 infer a questionable east-west striking fault off Cape Arago between units I and F. Poor evidence of an angular unconformity between I and underlying G on line SP-6 suggests a sediment contact between the two units off Cape Arago (Plate I). A similar contact is suggested with unit H. On the west unit I is unconformably overlain by unit J at approximately the shelf break (150 m). The northern expanse of I is undetermined, but it probably coincides with the majority of the negative free-air gravity trough on the central and outer shelf from Coos Bay to Heceta Head.

The sedimentary rocks of unit I are believed to be also of Miocene to Pliocene age. The seismic unit produces prominent continuous reflections, similar to those returned from units B and E. The north-south trending, gently undulating folds of I are similar to the structures of B on the inner portion of the shelf. Unit I and E have the same stratigraphic relationship with units G and H; units B, E, and I are faulted against unit F. A preliminary interpretation of a recent sparker profile across the continental shelf at approximately 43^{o} 25' N. latitude reveals a distinct angular unconformity between I and the underlying strata on the inner and central continental shelf (Kulm, 1968). The angular discordance of the strata is similar to those observed on the inner continental shelf at the base of unit E and between the sub-units of B. In addition, Miocene and Pliocene sediments were deposited in the nearby Coos Bay synclinorium (Baldwin, 1966).

On the basis of acoustic appearance, structural and stratigraphic relationships with adjacent seismic units, and proximity with onshore outcrops, the sedimentary rocks of unit I are inferred to be of Miocene to Pliocene age and probably are correlative with the sediments of B and E. Each of the correlative units are separated by older rocks and are given separate designations.

Post depositional stresses have folded unit I into gently undulating, north-south striking structures. The late to post-Pliocene

deformation is probably associated with the uplift of its contiguous units, F, G, and H. Pleistocene erosion has smoothed the bathymetry of the continental shelf in the outcrop area of unit I (Figure 5).

Unit J

A wedge of sediments, unit J, unconformably overlies units F, I, and possibly B along the edge of the continental shelf for at least 28 km from Coos Bay to Bandon (Plate I). Good seismic returns with strong, prominent, laterally continuous reflections were obtained from these strata (Figures 15 and 16). The stratigraphic relationship of unit J and unit B at the southern end of the wedge of sediments is not defined on the seismic records, but it is inferred that the sediments of J also overlie those of B and are, therefore, younger.

The wedge of sediments begins at the edge of the continental shelf at a water depth of 130 to 150 m and thickens westward on the upper continental slope (Figures 15 and 16). The sparker survey lines do not extend seaward far enough to determine the lower limit of the sediment wedge, but the strata is seen on SP-11 at a water depth of 330 m. Unit J probably extends down onto the terrace or bench on the upper continental slope north of Coquille Bank (Figure 5).

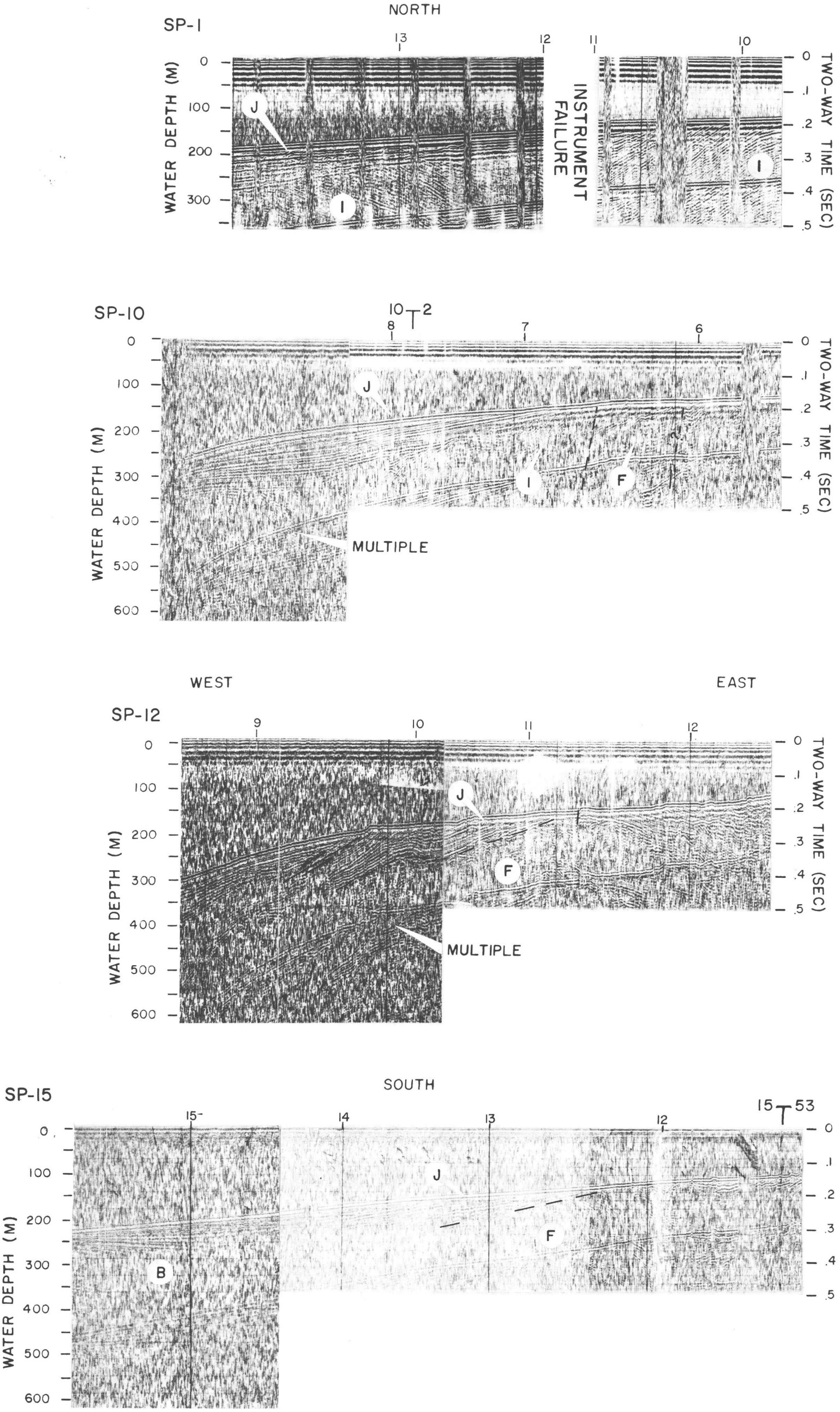

Figure 16. Sediment wedge perched on the outer shelf and upper slope. The base of the sediments of unit J forms an angular unconformity with the underlying strata. Vertical exaggeration 8X.

The wedge of sediments has undergone little deformation; however, on line SP-12 (Figure 15) some slumping has occurred. In deep water on SP-11, the sediments thin over the gently undulating structural highs and thicken in the troughs, which suggests that deposition and deformation have been contemporaneous.

The most outstanding feature of unit J is its contact with the older underlying units B, F, and I at a water depth of 130 to 150 m (Plate I). The wedge of sediments is possible evidence of a lower stand or stands of sea level of at least 130 m during the Pleistocene. The continental shelf experienced marine and subaerial erosion during the several Pleistocene sea level lowerings, and the detritus was deposited seaward on what is now the upper continental slope. The Coos and Coquille Rivers may have carried significant loads of sediments to the sea and contributed markedly to the outbuilding of the wedge. The truncated structural features and eroded seismic units are clearly visible on the sparker records and are evidence of extensive Pleistocene erosion of the continental shelf (Figures 15 and 16). Unit J is interpreted to consist of late Pliocene to Pleistocene sediments deposited during a single, or a series of, sea level regressions and transgressions.

THE SHELF BREAK

The continental shelf is believed to be an erosional and depositional feature due to numerous transgressions and regressions of the sea, particularly those resulting from Pleistocene glaciation (Shepard, 1963). The last major regression during the Wisconsin glaciation lowered sea level approximately 120 m (Curray, 1961). The world average depth of the shelf break of 132 m suggests that the shelf edge is an erosional feature (Shepard, 1963). However, in some areas geophysical and geological evidence indicate that the shelf and shelf break are also of constructional and structural origin (Dietz, 1964; Guilcher, 1963; and Uchupi and Emery, 1967). Continuous seismic profiles off the southern Oregon coast illustrate that the continental shelf break is an erosional, structural, and depositional feature, all within a short distance of 70 km.

The wedge of sediments, unit J, perched unconformably on top of the outer shelf and upper slope strata indicate significant Pleistocene deposition took place on the edge of the continental shelf from Cape Arago to Coquille Bank (Figures 15 and 16). The shelf has undergone extensive erosion during the lower stands of sea level. As a result detritus was apparently deposited in the inner sublittoral zone, which is now the uppermost part of the continental slope. This suggests that the lowest stand of the late Pleistocene shoreline was

130 m below the present sea level. This agrees quite closely with the world average depth of 132 m for the shelf break.

Thus, along 28 km of the continental margin between Cape Arago and Coquille Bank the shelf break is both an erosional and depositional feature. During these lower still stands, the upper continental slope experienced significant outbuilding, while the shelf was extensively eroded. No true distinction exists between the outer edge of the shelf and the upper slope; the former merely merges into the latter in a continuous convex curve (Figure 16).

The crest of the Coquille Bank anticline, as previously described, apparently was truncated at a depth of about 120 to 130 m by surf cutting during Pleistocene sea level lowerings. The major portion of the sedimentary section of the west limb of the anticline has been removed by faulting (Figures 5, 10 and 12). The surf cut platform and the fault escarpment form a distinct shelf break at approximately 130 m. Thus, on Coquille Bank the shelf break is of erosional and structural origin.

South of Coquille bank, the shelf break is both a depositional and structural feature. Off Cape Blanco on line SP-22 (Figure 9), the shelf edge is structurally controlled by what appears to be a diapir instrusion. The diapir probably is a serpentinite intrusive, similar to those found onshore in the Klamath Mountain province. On line SP-50 just north of the Cape sub-bottom reflections are

conformable with the ocean bottom on the outer shelf and upper slope (Figure 16).

The continental shelf break in the study area is of multiple origin. The majority of the shelf and upper slope has experienced late to post-Pliocene tectonism. The oscillating shoreline of the Pleistocene eustatic sea level changes eroded the late Tertiary to early Pleistocene structures on the shelf and have deposited the detritus on the outer shelf and upper slope. Thus, the shelf break is an erosional, structural, and depositional feature.

UNCONSOLIDATED SEDIMENT COVER

The unconsolidated sediment was mapped from both the sparker and echo sounding data. Both sets of data were recorded simultaneously over the 700 km of track line. Additional information was obtained from underwater photographs (Neudeck, 1968) and bottom samples taken by Runge (1966) and Boettcher (1967).

Resolution and Interpretation

The ocean bottom reflection of the bubble pulse masks approximately the first 12 to 18 milliseconds (two-way travel time) of the sub-bottom seismic information and limits the resolution of the sediment thickness to approximately 9 to 15 m. Detectible sediment cover greater than 15 m was timed and converted into depths below the ocean bottom from the time-depth curve (Figure 8). Rocky areas were delineated by irregular traces of the sea floor on the fathograms and by bottom photographs and samples.

Areas portraying a smooth ocean bottom on the fathometer were interpreted to be regions covered by unconsolidated sediments. If the bottom of the unconsolidated sedimentary layer could be interpreted on the sparker profiles, it was timed and converted into depths. In areas where the unconsolidated sediments were not visible on the seismic profiles, the overlying cover was assumed to be less

than the resolution of the sparker system, 9 to 15 m, but at least a few meters thick.

The sediment distribution and thickness were mapped as five zones: rocky areas, 0 to 15 m, 15 to 20 m, 20 to 25 m, and greater than 25 m thick (Figure 17). This type of presentation was selected because of the uncertainties in determining sediment thicknesses less than 15 m due to the ocean bottom reflection of the bubble pulse.

Sediment Distribution

On the continental shelf between Cape Arago and Cape Blanco, there is a distinct lack of unconsolidated sediment cover. Most of the area is covered by only a thin veneer of sediments less than 15 m thick. There are only a few small pockets of unconsolidated sediments off Coos Bay where the sparker records reveal a sediment thickness greater than 15 meters.

A large area of sediment cover, greater than 15 m thick was detected on the east side of Coquille Bank. Recent deposition is apparently the greatest landward of the Bank. The Bank is probably a controlling factor in the greater accumulation of sediments on this portion of the shelf.

A larger and thicker accumulation of sediment was detected west of Cape Blanco. Sediment thicknesses are greater than 25 m and cover what is interpreted to be a surf cut terrace (Figure 9).

On line SP-23 the sediments appear to be piled on top of the terrace in the northern half of the line, while the terrace crops out on the ocean bottom on the southern half of the line. Whether this thicker accumulation of unconsolidated sediments owes its origin to a former beach, to wave and current action on the Blanco and Orford Reefs, or to the proximity to former channels of the Sixes and Elk Rivers during lower stands of sea level must be only conjectural until the stratigraphy of the sedimentary veneer is studied.

Large exposures of rocks crop out southwest of Cape Arago, off Bandon, on Coquille Bank, and off Cape Blanco. There is a distinct interrelationship between the rock outcrop pattern, the seismic units, and the bathymetry (Plate I, Figures 5 and 17).

The rocky area off Cape Arago and Bandon consists of units C, F, G, H, and, in a few instances, E. The outcrops form the previously noted topographic highs and a distinct irregularity in the bathymetry contours (Figure 5). The sub-units of B are best exposed on the rocky flanks and axis of the Coquille Bank anticline (Figures 10, 12, and 13). In the other areas units B and I are covered by unconsolidated sediments, which produce a relatively smooth bottom. Unit A is exposed in a few outcrops off Cape Blanco, and the Orford and Blanco Reefs are believed to be a part of the same unit A. The rock outcrops on the continental shelf in the study area are a result of existing structure, tectonism, and differential weathering.

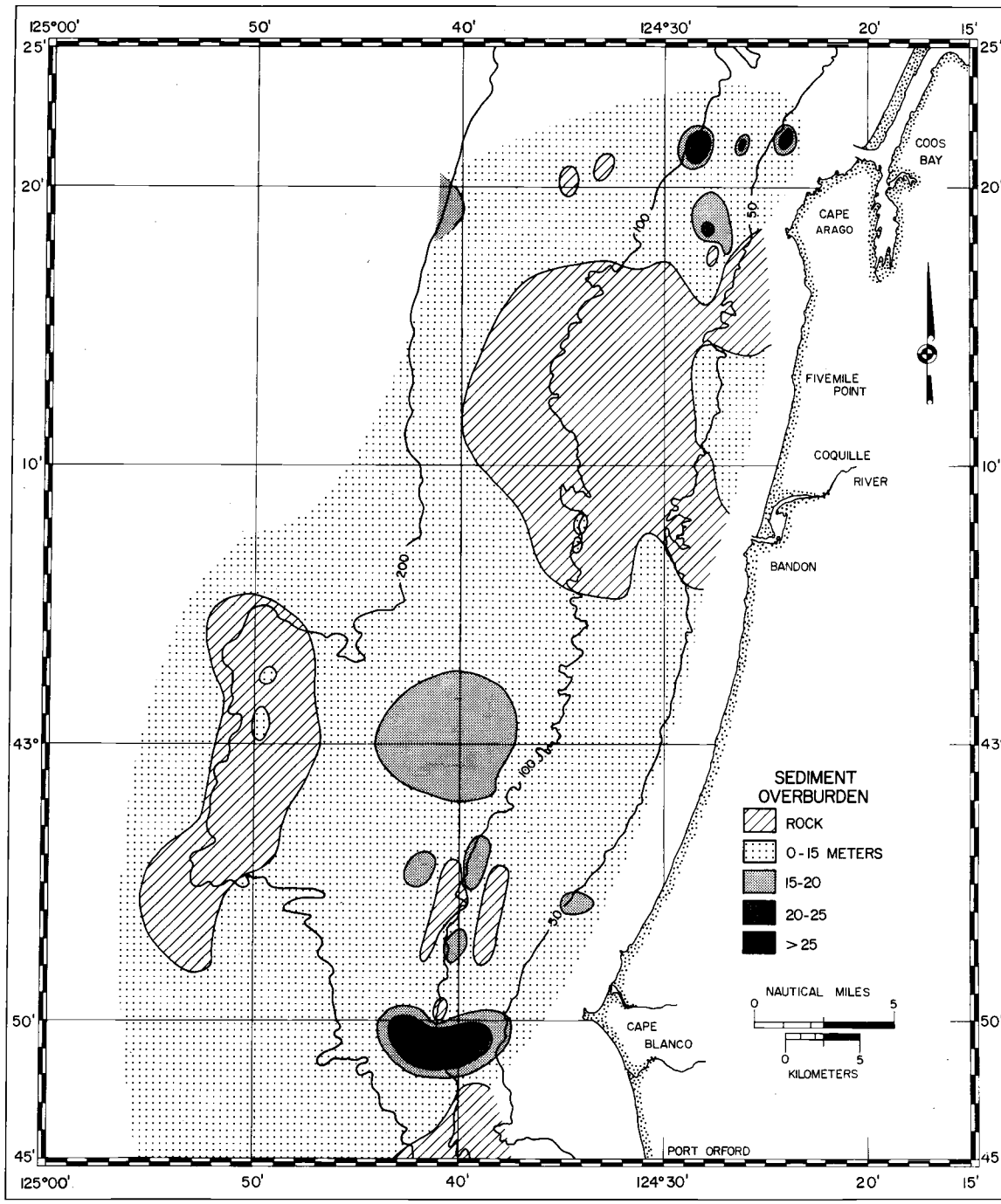

Figure 17. Unconsolidated sediment map. Note the large areas of rock outcrops on Coquille Bank and southwest of Cape Arago. Contours in meters.

SUMMARY AND CONCLUSIONS

A continuous seismic profiling investigation was conducted over approximately 700 km of track lines on the southern Oregon continental shelf and upper slope between Coos Bay and Cape Blanco (Figure 2). A structural map of the continental shelf was compiled solely from the interpretation of these sparker records. Since the majority of the continental margin is covered by a thin veneer of Quaternary unconsolidated sediments, the sediment cover was removed from the sea floor in the fabrication of the map. At least ten discernible seismic units were identified on the continental shelf. The rock outcrop patterns of these units are shown on the structure map (Plate I). The interpretation of the sparker records is supported by bathymetry, gravity and magnetic data, and rock outcrop patterns (Figures 3, 4, 5, and 17).

Several onshore geologic formations and structures are believed to extend offshore onto the continental shelf. The offshore seismic units were correlated tentatively with onshore coastal formations or periods of speculated marine deposition. In summarizing the geological history of the investigated area, the correlations of the seismic units and their proposed relative ages are assumed to be those listed in Table 1. The validity of the interpretation is untested until rock samples are obtained for both stratigraphic and

Table 1. Postulated correlations of seismic units with onshore geology.

Seismic Unit	Postulated Age of Seismic Units	Possible Correlative Formation(s)
D	Late Pleistocene	Coquille Formation
J	Late Pliocene to Pleistocene	--
B, E, I	Miocene to Pliocene	Port Orford Formation Empire Formation Miocene beds at Cape Blanco and Coos Bay
F	Oligocene to Miocene	--
G	Middle Eocene	Tyee Formation
H	Late Cretaceous	Rhythmically bedded turbidites at Fivemile Point
A, C	Uppermost Jurassic	Otter Point Formation

paleontologic studies. As yet no published stratigraphic studies are available for this portion of the shelf. However, adjacent onshore stratigraphic studies by other investigators (Allen and Baldwin, 1944; Baldwin, 1945, 1963; Dott, 1961, 1964 and 1965; Snavely and Wagner, 1963; Koch, 1966; and Phillips, 1968) can be projected broadly offshore to aid in the discussion of the geological history of the continental shelf between Coos Bay and Cape Blanco.

The oldest rocks exposed on the continental shelf are believed to be the uppermost Jurassic Otter Point Formation (Table 1). Large hiatuses in the late Mesozoic and early Cenozoic are inferred from the interpretation of the sparker records (Table 1). A better understanding of the geological development of the shelf can be obtained by briefly sketching the adjacent onshore region's early geologic history, based on the findings of other investigators.

The study area is located on the continental margin of the westernmost edge of the Cordilleran mobile belt in southern Oregon. The Cordilleran belt has been generally eugeosynclinal throughout most of the Paleozoic to late Cenozoic time (Dott, 1965). In his model of block tectonics of the earth, Morgan (1968, p. 1971) postulates that "the Coast Ranges of Oregon and Washington are probably the fill of an uplifted trench, and the Cascades are probably the volcanic counterpart of this now extinct system". The dominance of continental-type andesites throughout the Cordilleran Geosyncline

infers the presence of essentially continental crust throughout its known history. However, because of the large ultramafic bodies in the Klamath Mountain province, Dott (1965) suggests that the crust may be transitional between typically continental and typically oceanic types.

The diastrophism displayed in the arcuate structural and metamorphic pattern of the Klamath Mountains resulted from the Nevadan orogeny of late Jurassic age (Dott, 1965). The westwardly convex Klamath structural arc became the foundation for orogenic accretion which continued into the early Tertiary.

During the latest Jurassic, a sea transgressed the lower elevations of the Klamath province (Koch, 1966). The mainly fine-grained detritus of the Otter Point Formation was deposited by turbidity currents and landslides at bathyal depths off southwestern Oregon. At the end of the Jurassic, the southwestern Oregon coast experienced a diastrophic episode, which corresponded to the northern California terminal Jurassic "Diablan" orogeny (Koch, 1966). This orogeny culminated the late Mesozoic eugeosynclinal conditions of the coastal regions of the Klamath province and initiated the wrench faulting, characteristic of the northern California and southern Oregon coasts (Dott, 1966).

In the early Cretaceous, a shallow sea transgressed the coastal margins of the Klamath Mountains. Tectonism at or near

the end of the early Cretaceous locally halted the coastal turbidite deposition and uplifted selected areas along the coast. None of the early Cretaceous deposits are believed to crop out on the shelf in the study area.

North of the Klamath Mountain province, western Oregon and Washington was the site of a eugeosyncline that occupied the present site of the Olympic Mountains, the Coast Ranges, the Puget-Willamette lowland, and the western Cascades (Snavely and Wagner, 1963). The structural deformation and deposition in the southern end of the geosyncline probably was controlled by the elevated Klamath Mountain province.

During the Late Cretaceous, the sea transgressed over the northern end western flanks of the Klamath terrane. Sediments of the lower member of the Umpqua Formation (Late Cretaceous through early Eocene) were deposited by turbidity currents in a subsiding eugeosynclinal basin north of the Klamath terrane (Phillips, 1968). Scattered eroded remnants of the once extensive Late Cretaceous turbidites, deposited along the western edge of the Klamath area, are found at the following onshore localities: Fivemile Point; Crooked Creek, south of Bandon; Blacklock Point; and Cape Sebastian, 38 km north of the Oregon-California state line. The rhythmically bedded turbidites also are believed to crop out on the continental shelf in the region represented by unit H immediately

seaward of Fivemile Point (Plate I).

Marine deposition of the lower Umpqua Formation at the southern end of the geosynclinal basin continued through the early Eocene (Baldwin, 1965). During the early Eocene extensive basaltic pillow lavas erupted onto the sea floor of the subsiding eugeosyncline (Snavely and Wagner, 1963). At the end of the early Eocene, the lower Umpqua Formation was uplifted and was severely faulted and folded along northeast trending axes (Baldwin, 1964).

The sea reoccupied the southern Coast Range geosynclinal basin, and the middle and upper members of the Umpqua were deposited in a shallow marine environment (Baldwin, 1965). Although none of the members of the Umpqua Formation are believed to crop out on the continental shelf between Coos Bay and Cape Blanco, they probably extend seaward at depth onto the shelf beneath the middle and late Tertiary deposits. The massive, thickly bedded, coarse-grained sandstone of the middle Eocene Tyee Formation unconformably overlies the members of the Umpqua Formation and suggests major uplift of the Klamath source area. The Tyee Formation in the Coos Bay quadrangle represents deposition in littoral to inner sublittoral environments (Allen and Baldwin, 1944). The southern portion of the Oregon Coast Range geosyncline was filled essentially by the shallow marine and turbidity deposits of the Tyee Formation by close of the middle Eocene (Snavely and Wagner, 1963).

At the beginning of the late Eocene, areas of the southern Coast Range were locally uplifted. The middle Eocene strata were folded, faulted, and preserved in fault troughs (Baldwin, 1964; Phillips, 1966). Koch (1966) and Howard and Dott (1961) have described block faulted structures associated with the north trending wrench faults of the southwestern Oregon coast. Such a wrench fault tectonic pattern was propounded by Moody and Hill (1956). Similar models for Tertiary structures of southern California were proposed by Corey (1962) to explain the horst and graben surface expression often associated with wrench fault tectonics. A horst and graben structure involving the Otter Point and lower Umpqua Formations was mapped 14 km southeast of Bandon by Phillips (1968). Phillips also described several shear zones within the uppermost Jurassic Otter Point Formation. Dott (1962) has proposed a shear zone, the Port Orford shear zone, through Cape Blanco that was clearly active from the late Eocene to the post-Miocene. He also has postulated a shear zone through the Otter Point Formation at Coquille Point (Dott, 1966). The block faulting, described onshore by Phillips (1968) and observed offshore of Cape Arago, Bandon, and Cape Blanco in this investigation, may be a result of late Eocene wrench faulting (Plate I).

Thus, the emplacement of seismic units A and C, which tentatively are correlated with the uppermost Jurassic Otter Point

Formation, on the inner continental shelf off Cape Blanco and Coquille Point may be the result of middle Tertiary wrench fault tectonics. Seismic units G and H, which are believed to be the Tyee Formation and the Late Cretaceous turbidites, respectively, off Fivemile Point probably are similarly emplaced by the late Eocene lateral block faulting (Plate I). During this period of tectonism, extensive erosion removed much of the early Eocene section south of Coos Bay; and erosional remnants of the Tyee Formation preserved locally in down faulted blocks both onshore at Sacchi Beach and 7 km offshore as unit G.

The tectonism at the beginning of the late Eocene divided the Coast Range geosyncline into several individual basins and significantly reduced the area of marine deposition (Snavely and Wagner, 1963). The Coos Bay embayment or synclinorium was one of these local basins and received littoral and inner sublittoral marine deposits from the late Eocene through the Miocene. Offshore, the continental shelf was probably characterized by significant middle Tertiary marine deposition. Unit F is believed to consist of sediments of Oligocene to Miocene age. Similar strata probably extends over much of the continental shelf but is presently overlain by the Pliocene deposits.

At the end of the Miocene the southern Coast Range was uplifted, and the Coos Bay embayment was warped into a north-south

trending synclinorium (Allen and Baldwin, 1944; and Snavely and Wagner, 1963). During this period of tectonism, the offshore strata of unit F also was folded and faulted, perhaps by renewed movement of the wrench fault system (Figure 14). The older seismic units A, C, G, and H probably experienced further deformation and uplift.

During the Pliocene, detritus from erosion of the uplifted southern Coast Range continued to be deposited in the Coos Bay embayment and on the adjacent continental shelf. The late Tertiary sediments appear to have covered unit A off Cape Blanco and the southern half of unit F, the middle Tertiary strata. In fact, the correlative late Tertiary units B, E, and I probably were continuous throughout most of the study area and also covered the structural highs formed by C, G, and H off Bandon and Fivemile Point (Plate I and Figure 14).

Sparker records of seismic unit B reveal that the greatest Mio-Pliocene deposition occurred in a north-south trending basin between Cape Blanco and Coquille Bank (Figure 10). Within unit B, seven seismic sub-units, discernible by angular unconformities and acoustic appearance, infer at least seven periods of deposition, gentle deformation, erosion or non-deposition and subsequent deposition (Plate I and Figures 10 and 11). Thickening and thinning of the sub-units over gently undulating anticline and synclinal structures suggest simultaneous deposition and deformation. The north-south

trending Mio-Pliocene folds imply east-west compressional deforming stresses throughout the deposition of the sediments. The angular unconformity which separates sub-unit I and the underlying strata probably represents the greatest erosional break, and it may be the most important of all the unconformities noted on the sparker records. Northwest of Blacklock Point, sub-unit I unconformably overlies in succession each of the older sub-units II, III, IV, and V (Plate I).

Strata, which are acoustically similar to unit B, are exposed northwest of Bandon and west of Cape Arago, units E and I respectively. No angular unconformities or sub-units were noted within these two units; however, a distinct angular discordance with the underlying strata of questionable age occurs at the base of E and I.

The late Tertiary sediments of unit B apparently cover the seaward extension of the postulated Port Orford shear zone north of Cape Blanco. The lack of deformation of the overlying unit B infers there has been no significant movement of the fault since the deposition of these younger sediments.

Late to post-Pliocene stresses, associated with the renewed uplift of the Coast Range, vertically displaced the older strata of A, C, F, G, and H off Cape Blanco, Bandon, and Cape Arago and folded the late Tertiary strata of units B, E, and I along north-south striking axes (Plate I). The Coos Bay synclinorium also experienced

recurrent post-Pliocene folding along its north-south trending axes (Baldwin, 1966). Off Cape Blanco, the uplift of unit A has upwarped the adjacent sub-units of unit B. The sedimentary beds of B and E have been upturned similarly by the uplift of C and F off Coquille Point (Figure 14). The uplift of the older surrounding units, C, F, G, and H, has warped unit E into a south plunging syncline. The late Tertiary strata of unit I also have been tilted upward by the late to post-Pliocene vertical displacement of its contiguous units F, G, and H.

The inner continental shelf folds of unit B characteristically have lower dips than the outer shelf structures (Figure 10). The greatest deformation of the Mio-Pliocene strata of unit B occurred on the outer shelf in the formation of Coquille Bank, a north-south trending, doubly plunging, asymmetrical anticline (Figures 10, 12 and 13). The structural development of the shoal may have been contemporaneous with the uplift of the older units, A, C, F, G, and H. The seaward limb of the anticline has been faulted down to the west and an adjacent syncline parallels the anticlinal axis on the east (Figure 10). The terraces or benches, expressed in the bathymetry on the upper continental slope, are structural features resulting from the north and south plunging anticline-syncline complex (Figures 5, 12, and 13).

The north-south trending, late Tertiary structure of the Coos

Bay embayment implies deformation from east-west compressional stresses. The similarly oriented continental shelf structures of seismic units B and I, especially the Coquille Bank anticline, also suggest east-west compression. The step block faults postulated by Maloney (1965) on the central Oregon continental slope further suggest deforming stresses from the west. A possible source for the compressional stresses on the continental shelf may be located farther offshore in the seismically active Juan de Fuca and Gorda Ridges (Figure 1), which are believed to be the northern extension of the East Pacific Rise (Menard, 1960).

Several geophysical models have been proposed to explain the continuous, north-south trending magnetic anomalies associated with the East Pacific Rise. Dietz (1961) postulates sea floor spreading from the Rise; Wilson (1965) suggests transform faulting along the Blanco Fracture Zone; and Morgan (1968) proposes tectonic blocks, which are rifting along the Rise. Any of these postulated models would produce eastward movement of the oceanic crust on the continental side of the Rise. Extensive compressional stresses would occur at the oceanic-continental crust interface as the oceanic crust dips beneath the thicker and less dense continental crust. The remarkable north-south linearity of the base of the continental slope off Oregon probably is a result of the seaward limit of the continental-type crust and of the compressional stresses on the continental

margin. The irregular topography of the Oregon continental slope presumably are structural features, folds and step block faults, resulting from compression from the west (Byrne, 1966).

Elevated marine terraces onshore indicate that the entire coast between Cape Arago and Cape Blanco has undergone broad regional uplift which began in the late Pliocene and contined throughout the Quaternary. The uplift is greatest at Cape Arago and Cape Blanco and may be associated with the late to post-Pliocene uplift of the older seismic units seaward of the two Capes.

The continental shelf experienced extensive marine and subaerial erosion during the numerous late Pliocene and Pleistocene transgressions and regressions of the sea. The late Tertiary strata of units B, E, and I were eroded from the top of the presently exposed older, uplifted units of A, C, F, G, and H.

All of the seismic units experienced further erosion; the detritus was deposited as a wedge of sediments, unit J, on the outer continental shelf and upper continental slope (Figures 15 and 16). The wedge of sediments is discernible along the outer edge of the shelf for at least 28 km from Coos Bay to Bandon (Plate I). The wedge of sediments, which is believed to be of late Pliocene to Pleistocene age, begins at the edge of the continental shelf at a water depth of 130 to 150 m. It unconformably overlies the older units B, F, and I and thickens westward on the upper continental

slope. The contact of the sedimentary wedge with the older underlying units is possible evidence of eustatic sea level lowerings of at least 130 m.

Additional evidence of a lower sea level stand is the truncated top of the Coquille Bank anticline (Figures 10, 12 and 13). The depth of the terrace at 120 to 130 m indicates the Bank may have been cut at the beginning of the Holocene transgression.

The submerged surf cut terrace southwest of Cape Blanco in unit A is further evidence of a lower stand of sea level (Figure 9). The seaward limit of the terrace occurs at a depth of 140 m.

A possible buried channel was detected northwest of the mouth of the Coquille River (Figure 14). The sediment filled channel, unit D, is believed to be an erosional remnant of a former course of the Coquille River during a lower stand of sea level. The unit is correlated with the onshore Coquille Formation of late Pleistocene age.

The continental shelf break in the study area is of multiple origin. The majority of the shelf and upper slope has experienced late to post-Pliocene tectonism. The oscillating Pleistocene shoreline has truncated the shelf structures to a depth of 130 m and has deposited the detritus, in some areas, on the outer shelf and upper slope. In areas of deposition, there is no sharp break between the shelf and the upper slope; the former merely merges into the latter in a continuous convex curve (Figure 16). In areas of non-deposition,

the edge of the shelf is erosionally and structurally controlled (Figure 12). Thus, the shelf break is an erosional, depositional, and tectonic feature and may have been developed by a combination of any of the three geological processes.

There is an apparent lack of unconsolidated Pleistocene and Holocene sediment cover on the continental shelf between Cape Arago and Cape Blanco. Most of the shelf is covered by a thin veneer of sediments less than 15 m thick; however, several small isolated pockets of thicker sediment cover were detected on the sparker profiles (Figure 17).

Large exposures on rock crop out southwest of Cape Arago, off Bandon, on Coquille Bank, and off Cape Blanco. There is a distinct interrelationship between the rock outcrop pattern, the seismic units, and the bathymetry (Plate I, Figures 5 and 17). The rock outcrops on the continental shelf are a result of existing structure, tectonism, and differential weathering.

BIBLIOGRAPHY

Allen, John E. and Ewart M. Baldwin. 1944. Geology and coal resources of the Coos Bay quadrangle, Oregon. Portland. 153p. (Oregon. Dept. of Geology and Mineral Industries. Bulletin 27)

Baldwin, Ewart M. 1945. Some revisions of the late Cenozoic stratigraphy of the southern Oregon coast. Journal of Geology 53: 35-46.

_____ 1963. Lower and middle Eocene formations of southwestern Oregon. In: (Abstract) Abstracts for 1963: Abstracts of papers submitted for six meetings with which the Society was associated. New York. p. 188. (Geological Society of America. Special Paper 76)

_____ 1964. Geology of Oregon. 2d ed. Eugene, distributed by the University of Oregon Cooperative Bookstore. 165p.

_____ 1965. Geology of the south end of the Oregon coast range Tertiary basin. Northwest Science 39: 93-103.

_____ 1966. Some revisions of the geology of the Coos Bay area, Oregon. Ore Bin 28: 189-203.

Boettcher, Richard S. 1967. Foraminiferal trends of the central Oregon shelf. Master's thesis. Corvallis, Oregon State University. 134 numb. leaves.

Bowditch, Nathaniel. 1958. American Practical Navigator. Washington, D. C., U. S. Government Printing Office. 1524p.

Byrne, John V. 1963. Geomorphology of the Oregon continental terrace south of Coos Bay. Ore Bin 25: 149-157.

_____ 1966. Effect of the East Pacific Rise on the geomorphology of the continental margin off Oregon. (Abstract) In: Program of the 1966 Annual Meetings of the Geological Society of America, San Francisco. p. 33-34.

Byrne, John V., Gerald A. Fowler and Neil J. Maloney. 1966. Uplift of the continental margin and possible continental accretion off Oregon. Science 154: 1654-1656.

Corey, W. H. 1962. Effects of lateral faulting on oil exploration. American Association on Petroleum Geologists, Bulletin 46: 2199-2212.

Curray, Joseph R. 1961. Late Quaternary sea level: a discussion. Geological Society of America, Bulletin 72: 1707-1712.

Dehlinger, Peter, R. W. Couch and Michael Gemperle. 1967. Gravity and structure of the eastern part of the Mendocino escarpment. Journal of Geophysical Research 72: 1233-1247.

_____ 1968. Continental and oceanic structure from the Oregon coast westward across the Juan de Fuca Ridge. Canadian Journal of Earth Sciences 5: 1079-1090.

_____ 1969. Oceanic Structures: Northern California to British Columbia. In: The Sea, ed. by J. C. Maxwell. Vol. 4. New York, Interscience. (In press)

Dietz, Robert S. 1961. Continental and ocean basin evolution by spreading of the sea floor. Nature 190: 854-857.

_____ 1964. Origin of continental slopes. American Scientist 52: 50-69.

Diller, J. S. 1901. Description of the Coos Bay quadrangle. Washington, D. C. 5p. (U. S. Geological Survey. Geologic Atlas of the United States. Folio 73)

_____ 1903. Description of the Port Orford quadrangle. Washington, D. C. 6p. (U. S. Geological Survey. Geologic Atlas of the United States. Folio 89)

Dix, C. Hewitt. 1962. Seismic prospecting for oil. New York, Harper. 414p.

Dobrin, Milton B. 1960. Introduction to geophysical prospecting. New York, McGraw-Hill. 446p.

Donn, William L. and John A. Shimer. 1958. Graphic methods in structural geology. New York, Appleton-Century-Crofts. 180p.

Dott, R. H., Jr. 1961. Permo-Triassic diastrophism in the Cordilleran region. American Journal of Science 259: 561-582.

_____ 1962. Geology of the Cape Blanco area, southwest Oregon. Ore Bin 24: 121-133.

_____ 1964. Ancient deltaic sedimentation in eugeosynclinal belts. In: Developments in sedimentology, ed. by L. M. J. U. van Stratten. Vol. 1. Amsterdam, Elsevier. p. 105-113.

_____ 1965. Mesozoic-Cenozoic tectonic history of the southwestern Oregon coast in relation to Cordilleran orogenesis. Journal of Geophysical Research 70: 4687-4707.

_____ 1966. Eocene deltaic sedimentation at Coos Bay, Oregon. Journal of Geology 74: 373-420.

Durham, J. W. 1953. Miocene at Cape Blanco, Oregon. (Abstract) Geological Society of America, Bulletin 64: 1504-1505.

Ehlen, Judi. 1967. Geology of state parks near Cape Arago, Coos County, Oregon. Ore Bin 29: 61-82.

_____ 1969. Geology of a coastal strip near Bandon, Coos County, Oregon. Master's thesis. Eugene, University of Oregon. (In progress)

Emilia, D. A., J. W. Berg, Jr. and W. E. Bales. 1966. A magnetic survey off the Pacific Northwest coast. Ore Bin 28: 205-210.

_____ 1968a. Magnetic anomalies off the northwest coast of the United States. Geological Society of America, Bulletin 79: 1053-1062.

_____ 1968b. Oceanic extensions of coastal volcanics: northwestern Oregon. Ore Bin 30: 21-31.

Fowler, Gerald A. 1968. Unpublished research in Cenozoic continental margin stratigraphy. Corvallis, Oregon State University, Department of Oceanography.

Griggs, A. B. 1945. Chromite-bearing sands of the southern part of the coast of Oregon. Washington, D. C. p. 113-150. (U. S. Geological Survey. Bulletin 945-E)

Guilcher, A. 1963. Continental shelf and slope (continental margin). In: The Sea, ed. by M. N. Hill. Vol. 3. New York, Interscience. p. 281-311.

Hersey, J. B. 1963. Continuous reflection profiling. In: The Sea, ed. by M. N. Hill. Vol. 3. New York, Interscience. p. 47-72.

Howard, J. K. and R. H. Dott, Jr. 1961. Geology of Cape Sebastian state park and its regional relationships. Ore Bin 23: 75-81.

Huckabay, W. B. 1967. Geophysical consultant, Scientific Services Laboratory. Personal communication. Dallas, Texas.

Koch, John G. 1966. Late Mesozoic stratigraphy and tectonic history, Port Orford-Gold Beach area, southwestern Oregon coast. American Association of Petroleum Geologists, Bulletin 50: 25-71.

Koch, J. G., W. R. Kaiser and R. H. Dott, Jr. 1961. Geology of the Humbug Mountain state park area. Ore Bin 23: 23-30.

Kulm, L. D. 1968. Unpublished research in continuous seismic profiling of the central Oregon continental shelf. Corvallis, Oregon State University, Department of Oceanography.

Kulm, L. D. et al. 1968. Evidence for possible placer accumulations on the southern Oregon continental shelf. Ore Bin 30: 81-104.

Maloney, Neil Joseph. 1965. Geology of the continental terrace off the central coast of Oregon. Ph.D. thesis. Corvallis, Oregon State University. 233 numb. leaves.

_____ 1967. Geomorphology of the continental margin off central Oregon, U. S. A. Boletin del Instituto Oceanographic de la Universidad de Oriente 6: 116-146.

Menard, H. W. 1960. The east Pacific rise. Science 132: 1737-1746.

Moody, J. D. and M. J. Hill. 1956. Wrench-fault tectonics. Geological Society of America, Bulletin 67: 1207-1246.

Moore, E. J. 1963. Miocene marine mollusks from the Astoria Formation in Oregon. Washington, D. C. 100p. (U. S. Geological Survey Professional Paper 419)

Morgan, W. Jason. 1968. Rises, trenches, great faults, and crustal blocks. Journal of Geophysical Research 73: 1959-1982.

Neudeck, Roger H. 1968. Unpublished research in ocean bottom photography. Corvallis, Oregon State University, Department of Oceanography.

Phillips, R. Lawrence. 1968. Structure and stratigraphy of the northern quarter of the Langlois quadrangle, Oregon. Master's thesis. Eugene, University of Oregon. 91 numb. leaves.

Richards, Horace G. and David L. Thurber. 1966. Pleistocene age determinations from California and Oregon. Science 152: 1091-1092.

Runge, E. J., Jr. 1966. Continental shelf sediments, Columbia River to Cape Blanco, Oregon. Ph.D. thesis. Corvallis, Oregon State University. 143 numb. leaves.

Rusnak, Gene A. 1967. High-efficiency subbottom profiling. Washington, D. C. p. C81-C91. (U. S. Geological Survey Professional Paper 575-C)

Shepard, Francis P. 1963. Submarine geology. 2d ed. New York, Harper and Row. 557p.

Snavely, Park D., Jr. and Holly C. Wagner. 1963. Tertiary geologic history of Oregon and Washington. Olympia. 25p. (Washington. Division of Mines and Geology. Investigation 22)

Uchupi, Elazar and K. O. Emergy. 1967. Structure of continental margin off Atlantic coast of United States. American Association of Petroleum Geologists, Bulletin 51: 223-234.

United States. Coast and Geodetic Survey. 1968. Umpqua River to Cape Ferrelo. Washington, D. C. 1 sheet. (C. and G. S. 1308N-17)

Wells, F. G. and D. L. Peck. 1961. Geologic map of Oregon west of the 121st meridian. Washington, D. C. 1 sheet. (U. S. Geological Survey. Miscellaneous Investigations Map I-325)

Whitcomb, James Hall. 1965. Marine geophysical studies offshore--Newport, Oregon. Master's thesis. Corvallis, Oregon State University. 51 numb. leaves.

Wilson, J. T. 1965. Transform faults, oceanic ridges, and magnetic anomalies southwest of Vancouver Island. Science 150: 482-485.

APPENDICES

APPENDIX I

SPARKER TRACK LINE NAVIGATIONAL DATA

Sparker Line No.[a]	Fix No.	Time	Latitude (North)	Longitude (West)	Course (Degrees)	Speed (m/min)	Speed (km/hr)
1	1	6-22-1019	43° 21.8'	124° 23.6'			
					257°	128	7.7
1	2	6-22-1032	43° 21.6'	124° 24.8'			
					270°	104	6.2
1	3	6-22-1045	43° 21.6'	124° 25.8'			
					258°	138	8.3
1	4	6-22-1058	43° 21.4'	124° 27.1'			
					270°	111	6.7
1	5	6-22-1115	43° 21.4'	124° 28.5'			
					257°	118	7.1
1	6	6-22-1129	43° 21.2'	124° 29.7'			
					255°	131	7.9
1	7	6-22-1145	43° 20.9'	124° 31.2'			
					255°	131	7.9
1	8	6-22-1201	43° 20.6'	124° 32.7'			
					255°	123	7.4
1	9	6-22-1218	43° 20.3'	124° 34.2'			
					255°	123	7.4
1	10	6-22-1235	43° 20.0'	124° 35.7'			
					252°	123	7.4
1	11	6-22-1250	43° 19.7'	124° 37.0'			
					262°	124	7.4
1	12	6-22-1301	43° 19.6'	124° 38.0'			
					252°	131	7.9
1	13	6-22-1315	43° 19.3'	124° 39.3'			
					257°	98	5.9
1	14	6-22-1332	43° 19.1'	124° 40.5'			
					180°	157	9.4
2	15	6-22-1345	43° 18.0'	124° 40.5'			
					180°	136	8.2
2	16	6-22-1400	43° 16.9'	124° 40.5'			
					104°	169	10.1
3	17	6-22-1414	43° 16.6'	124° 38.8'			
					101°	128	7.7
3	18	6-22-1429	43° 16.4'	124° 37.4'			
					104°	139	8.4
3	19	6-22-1445	43° 16.1'	124° 35.8'			
					105°	140	8.4
3	20	6-22-1505	43° 15.7'	124° 33.8'			
					102°	119	7.2
3	21	6-22-1520	43° 15.5'	124° 32.5'			
					104°	153	9.2
3	22	6-22-1530	43° 15.3'	124° 31.4'			
					106°	133	8.0

Sparker Line No.	Fix No.	Time	Latitude (North)	Longitude (West)	Course (Degrees)	Speed (m/min)	Speed (km/hr)
3	24	6-22-1550	43° 14.9'	124° 29.5'			
					102°	179	10.8
3	25	6-22-1600	43° 14.7'	124° 28.2'			
					108°	142	8.5
3	26	6-22-1613	43° 14.4'	124° 26.9'			
					105°	175	10.5
3	27	6-22-1617	43° 14.3'	124° 26.4'			
					100°	137	8.2
3	28	6-22-1633	43° 14.1'	124° 24.8'			
4	2	6-26-1212	43° 17.0'	124° 26.0'			
					186°	246	14.8
4	4	6-26-1237	43° 13.7'	124° 26.5'			
					184°	232	13.9
4	5	6-26-1301	43° 10.7'	124° 26.8'			
					188°	196	11.7
4	6	6-26-1322	43° 8.5'	124° 27.2'			
					160°	197	11.8
4	7	6-26-1324	43° 8.3'	124° 27.1'			
5	8	6-26-1329	43° 8.3'	124° 27.9'			
					270°	210	12.6
5	9	6-26-1347	43° 8.3'	124° 30.7'			
					12°	102	6.1
6	10	6-26-1400	43° 9.0'	124° 30.5'			
					14°	153	9.2
6	11	6-26-1415	43° 10.2'	124° 30.1'			
					30°	202	12.1
6	12	6-26-1434	43° 12.0'	124° 28.7'			
					18°	215	12.9
6	13	6-26-1444	43° 13.1'	124° 28.2'			
					10°	200	12.0
6	14	6-26-1500	43° 14.8'	124° 27.8'			
					351°	175	10.5
6	15	6-26-1515	43° 16.2'	124° 28.1'			
					8°	201	12.0
6	16	6-26-1529	43° 17.7'	124° 27.8'			
					346°	191	11.4
6	17	6-26-1541	43° 18.9'	124° 28.2'			
					7°	177	10.6
6	18	6-26-1600	43° 20.7'	124° 27.9'			
					14°	191	11.4
6	19	6-26-1612	43° 21.9'	124° 27.5'			
7	1	6-27-1115	43° 8.4'	124° 27.8'			
					196°	227	13.6
7	2	6-27-1132	43° 6.4'	124° 28.6'			
					188°	208	12.5

Sparker Line No.	Fix No.	Time	Latitude (North)	Longitude (West)	Course (Degrees)	Speed (m/min)	Speed (km/hr)
7	3	6-27-1150	43° 4.4'	124° 29.0'			
					192°	215	12.9
7	4	6-27-1205	43° 2.7'	124° 29.5'			
					189°	219	13.1
7	5	6-27-1217	43° 1.3'	124° 29.8'			
					186°	211	12.6
7	6	6-27-1240	42° 58.7'	124° 30.2'			
					196°	202	12.1
7	7	6-27-1300	42° 56.6'	124° 31.0'			
					234°	219	13.1
8	8	6-27-1310	42° 55.9'	124° 32.3'			
					253°	213	12.8
8	9	6-27-1322	42° 55.5'	124° 34.1'			
9	10	6-27-1330	42° 55.8'	124° 34.4'			
					10°	188	11.3
9	11	6-27-1347	42° 57.5'	124° 34.0'			
					10°	163	9.8
9	12	6-27-1402	42° 58.8'	124° 33.7'			
					15°	192	11.5
9	13	6-27-1418	43° .4'	124° 33.1'			
					14°	212	12.7
9	14	6-27-1436	43° 2.4'	124° 32.4'			
					10°	188	11.3
9	15	6-27-1444	43° 3.2'	124° 32.2'			
					14°	208	12.5
9	16	6-27-1455	43° 4.4'	124° 31.8'			
					12°	139	8.4
9	17	6-27-1514	43° 5.8'	124° 31.4'			
					10°	126	7.5
9	18	6-27-1526	43° 6.6'	124° 31.2'			
					17°	206	12.3
9	19	6-27-1542	43° 8.3'	124° 30.5'			
10	1	6-28- 853	43° 18.2'	124° 25.6'			
					256°	255	15.3
10	2	6-28- 859	43° 18.0'	124° 26.7'			
					249°	226	13.6
10	3	6-28- 913	43° 17.4'	124° 28.9'			
					266°	205	12.3
10	4	6-28- 938	43° 17.2'	124° 32.7'			
					270°	221	13.2
10	5	6-28- 949	43° 17.2'	124° 34.5'			
					275°	241	14.4
10	6	6-28- 958	43° 17.3'	124° 36.1'			
					273°	219	13.2
10	7	6-28-1014	43° 17.4'	124° 38.7'			
					261°	166	10.0

Sparker Line No.	Fix No.	Time	Latitude (North)	Longitude (West)	Course (Degrees)	Speed (m/min)	Speed (km/hr)
10	8	6-28-1028	43° 17.2'	124° 40.4'			
11	8a		43° 17.3'	124° 42.8'			
11	8b		43° 12.1'	124° 44.3'			
12	9	6-28-1203	43° 12.2'	124° 43.4'			
					97°	233	14.0
12	10	6-28-1217	43° 12.0'	124° 41.0'			
					106°	281	16.9
12	11	6-28-1229	43° 11.5'	124° 38.6'			
					99°	145	8.7
12	12	6-28-1245	43° 11.3'	124° 36.9'			
					85°	128	7.7
12	13	6-28-1302	43° 11.4'	124° 35.3'			
					69°	181	10.8
12	14	6-28-1322	43° 12.1'	124° 32.8'			
					84°	177	10.6
12	15	6-28-1332	43° 12.2'	124° 31.5'			
					84°	136	8.1
12	16	6-28-1345	43° 12.3'	124° 30.2'			
					70°	154	9.2
12	17	6-28-1359	43° 12.7'	124° 28.7'			
					74°	205	12.3
12	18	6-28-1412	43° 13.1'	124° 26.8'			
13	20	6-28-1528	43° 10.4'	124° 26.3'			
					270°	191	11.4
13	21	6-28-1545	43° 10.4'	124° 28.7'			
14	2	7- 6-1047	43° 13.2'	124° 27.6'			
					187°	187	11.2
14	3	7- 6-1059	43° 12.0'	124° 27.8'			
					194°	214	12.9
14	4	7- 6-1115	43° 10.2'	124° 28.4'			
					185°	239	14.3
14	5	7- 6-1129	43° 8.4'	124° 28.6'			
					199°	208	12.5
14	6	7- 6-1145	43° 6.7'	124° 29.4'			
					203°	187	11.2
14	7	7- 6-1200	43° 5.3'	124° 30.2'			
15	8	7- 6-1245	43° 5.5'	124° 28.1'			
					274°	184	11.0
15	9	7- 6-1259	43° 5.6'	124° 30.0'			
					285°	183	11.0
15	10	7- 6-1315	43° 6.0'	124° 32.1'			
					266°	190	11.4

Sparker Line No.	Fix No.	Time	Latitude (North)	Longitude (West)	Course (Degrees)	Speed (m/min)	Speed (km/hr)
15	11	7-6-1330	43° 5.9'	124° 34.2'			
					267°	217	13.0
15	12	7-6-1345	43° 5.8'	124° 36.6'			
					277°	191	11.5
15	13	7-6-1400	43° 6.0'	124° 38.7'			
					279°	228	13.7
15	14	7-6-1415	43° 6.3'	124° 41.2'			
					266°	190	11.4
15	15	7-6-1430	43° 6.2'	124° 43.3'			
					266°	190	11.4
15	16	7-6-1445	43° 6.1'	124° 45.4'			
					252°	199	12.0
15	17	7-6-1500	43° 5.6'	124° 47.5'			
					258°	225	13.5
15	18	7-6-1508	43° 5.4'	124° 48.8'			
16	19	7-6-1515	43° 5.2'	124° 48.8'			
16	19a		43° 2.7'	124° 50.1'			
16	20	7-6-1543	43° 1.6'	124° 49.8'			
16	20a		43° 0.2'	124° 49.9'			
16	21	7-6-1630	42° 56.3'	124° 51.0'			
					187°	236	14.2
16	22	7-6-1645	42° 54.4'	124° 51.3'			
					194°	232	13.9
16	23	7-6-1659	42° 52.7'	124° 51.9'			
					183°	185	11.1
16	24	7-6-1715	42° 51.1'	124° 52.0'			
17	25	7-6-1729	42° 50.6'	124° 52.8'			
					312°	207	12.4
17	26	7-6-1745	42° 51.8'	124° 54.6'			
					281°	194	11.6
17	27	7-6-1800	42° 52.1'	124° 56.7'			
					330°	200	12.0
17	28	7-6-1815	42° 53.5'	124° 57.8'			
18	29	7-6-1830	42° 54.6'	124° 57.5'			
					110°	144	8.7
18	30	7-6-1845	42° 54.2'	124° 56.0'			
					86°	181	10.9
18	31	7-6-1900	42° 54.3'	124° 54.0'			
					75°	151	9.0
18	32	7-6-1914	42° 54.6'	124° 52.5'			
					75°	176	10.5

Sparker Line No.	Fix No.	Time	Latitude (North)	Longitude (West)	Course (Degrees)	Speed (m/min)	Speed (km/hr)
18	33	7-6-1930	42° 55.0'	124° 50.5'			
					77°	176	10.5
18	34	7-6-1953	42° 55.5'	124° 47.6'			
					96°	234	14.0
18	35	7-6-2000	42° 55.4'	124° 46.4'			
					90°	235	14.1
18	36	7-6-2015	42° 55.4'	124° 43.8'			
					87°	208	12.5
18	37	7-6-2030	42° 55.5'	124° 41.5'			
					95°	231	13.9
18	38	7-6-2040	42° 55.4'	124° 39.8'			
					109°	229	13.8
18	39	7-6-2045	42° 55.2'	124° 39.0'			
					100°	220	13.2
18	40	7-6-2050	42° 55.1'	124° 38.2'			
					108°	242	14.5
18	41	7-6-2100	42° 54.7'	124° 36.5'			
					109°	191	11.5
18	42	7-6-2115	42° 54.2'	124° 34.5'			
					82°	174	10.4
18	43	7-6-2130	42° 54.4'	124° 32.6'			
19	44	7-6-2213	42° 56.2'	124° 31.4'			
					25°	232	13.9
19	45	7-6-2228	42° 57.9'	124° 30.3'			
					12°	201	12.1
19	46	7-6-2244	42° 59.6'	124° 29.8'			
20	47	7-6-2251	42° 59.9'	124° 30.5'			
					264°	212	12.7
20	48	7-6-2300	42° 59.8'	124° 31.9'			
					270°	195	11.7
20	49	7-6-2316	42° 59.8'	124° 34.2'			
					264°	216	13.0
20	50	7-6-2333	42° 59.6'	124° 36.9'			
					274°	238	14.3
20	51	7-6-2345	42° 59.7'	124° 39.0'			
					267°	240	14.4
20	52	7-6-2358	42° 59.6'	124° 41.3'			
					284°	222	13.3
20	53	7-7-0015	43° .1'	124° 44.0'			
					306°	190	11.4
20	54	7-7-0030	43° 1.0'	124° 45.7'			
					306°	146	8.7
20	55	7-7-0045	43° 1.7'	124° 47.0'			
					307°	124	7.4
20	56	7-7-0100	43° 2.3'	124° 48.1'			

Sparker Line No.	Fix No.	Time	Latitude (North)	Longitude (West)	Course (Degrees)	Speed (m/min)	Speed (km/hr)
20	57a		43° 2.1'	124° 51.3'			
20	57b		43° 1.8'	124° 53.7'			
20	57c		43° 1.0'	124° 57.1'			
21	57d		42° 58.5'	124° 57.1'			
21	58	7-7-0233	42° 56.8'	124° 57.0'	176°	272	16.3
21	59	7-7-0246	42° 54.9'	124° 56.8'	178°	225	13.5
21	60	7-7-0300	42° 53.2'	124° 56.7'	168°	200	12.0
21	61	7-7-0319	42° 51.2'	124° 56.1'	172°	230	13.8
21	62	7-7-0332	42° 49.6'	124° 55.8'	94°	183	11.0
22	63	7-7-0404	42° 49.4'	124° 51.5'	90°	210	12.6
22	64	7-7-0415	42° 49.4'	124° 49.8'	90°	222	13.3
22	65	7-7-0426	42° 49.4'	124° 48.0'	92°	229	13.7
22	66	7-7-0445	42° 49.3'	124° 44.8'	77°	193	11.6
22	67	7-7-0458	42° 49.6'	124° 43.0'	93°	262	15.7
22	68	7-7-0511	42° 49.5'	124° 40.5'	68°	276	16.6
22	69	7-7-0520	42° 50.0'	124° 38.8'	173°	280	16.8
23	70	7-7-0524	42° 49.4'	124° 38.7'	208°	244	14.6
23	71	7-7-0530	42° 48.7'	124° 39.2'	192°	190	11.4
23	72	7-7-0540	42° 47.7'	124° 39.5'	194°	229	13.7
23	73	7-7-0545	42° 47.1'	124° 39.7'	180°	265	15.9
23	74	7-7-0559	42° 45.1'	124° 39.7'			
50	1	8-3-0350	42° 52.4'	124° 53.3'	90°	136	8.1
50	2	8-3-0400	42° 52.4'	124° 52.3'	100°	138	8.3
50	3	8-3-0415	42° 52.2'	124° 50.8'	86°	190	11.4

Sparker Line No.	Fix No.	Time	Latitude (North)	Longitude (West)	Course (Degrees)	Speed (m/min)	Speed (km/hr)
50	4	8-3-0430	42° 52.3'	124° 48.7'			
					84°	246	14.7
50	5	8-3-0445	42° 52.5'	124° 46.0'			
					95°	198	11.9
50	6	8-3-0456	42° 52.4'	124° 44.4'			
					90°	170	10.2
50	7	8-3-0512	42° 52.4'	124° 42.4'			
					84°	205	12.3
50	8	8-3-0530	42° 52.6'	124° 39.7'			
					82°	211	12.6
50	9	8-3-0543	42° 52.8'	124° 37.7'			
					87°	232	13.9
50	10	8-3-0600	42° 52.9'	124° 34.8'			
51	11	8-3-0617	42° 54.6'	124° 37.0'			
					186°	186	11.2
51	12	8-3-0630	42° 53.3'	124° 37.2'			
					190°	163	9.8
51	13	8-3-0645	42° 52.0'	124° 37.5'			
					180°	148	8.9
51	14	8-3-0650	42° 51.6'	124° 37.5'			
					70°	135	8.1
51	15	8-3-0706	42° 52.0'	124° 36.0'			
					66°	134	8.1
51	16	8-3-0716	42° 52.3'	124° 35.1'			
					79°	108	6.5
51	17	8-3-0725	42° 52.4'	124° 34.4'			
					194°	114	6.9
51	18	8-3-0730	42° 52.1'	124° 34.5'			
					216°	158	9.5
51	19	8-3-0746	42° 51.0'	124° 35.6'			
52A	1	8-4-0230	42° 52.3'	124° 45.2'			
					15°	179	10.7
52A	2	8-4-0245	42° 53.7'	124° 44.7'			
					8°	125	7.5
52A	3	8-4-0300	42° 54.7'	124° 44.5'			
					345°	132	7.9
52A	4	8-4-0316	42° 55.8'	124° 44.9'			
					324°	133	8.0
52A	5	8-4-0335	42° 56.9'	124° 46.0'			
					343°	113	6.8
52A	6	8-4-0347	42° 57.6'	124° 46.3'			
					0°	123	7.4
52A	7	8-4-0359	42° 58.4'	124° 46.3'			
					24°	155	9.3
52A	8	8-4-0416	42° 59.7'	124° 45.5'			
					4°	143	8.6

Sparker Line No.	Fix No.	Time	Latitude (North)	Longitude (West)	Course (Degrees)	Speed (m/min)	Speed (km/hr)
52A	9	8-4-0429	43° .7'	124° 45.4'	0°	139	8.3
52A	10	8-4-0445	43° 1.9'	124° 45.4'	280°	147	8.8
52B	11	8-4-0500	43° 2.1'	124° 47.0'	265°	154	9.2
52B	12	8-4-0515	43° 2.0'	124° 48.7'	274°	163	9.8
52B	13	8-4-0530	43° 2.1'	124° 50.5'	275°	154	9.2
52B	14	8-4-0545	43° 2.2'	124° 52.2'	257°	167	10.0
52B	15	8-4-0550	43° 2.1'	124° 52.8'	216°	92	5.5
52C	16	8-4-0600	43° 1.7'	124° 53.2'	177°	185	11.1
52C	17	8-4-0615	43° .2'	124° 53.1'	183°	185	11.1
52C	18	8-4-0630	42° 58.7'	124° 53.2'	180°	185	11.1
52C	19	8-4-0635	42° 58.2'	124° 53.2'	128°	150	9.0
52D	20	8-4-0643	42° 57.8'	124° 52.5'	77°	139	8.3
52D	21	8-4-0655	42° 58.0'	124° 51.3'	123°	130	7.8
52D	22	8-4-0716	42° 57.2'	124° 49.6'	81°	167	10.0
52D	23	8-4-0730	42° 57.4'	124° 47.9'	105°	132	7.9
52D	24	8-4-0746	42° 57.1'	124° 46.4'	95°	178	10.7
52D	25	8-4-0759	42° 57.0'	124° 44.7'	83°	188	11.3
52D	26	8-4-0815	42° 57.2'	124° 42.5'	100°	220	13.2
52D	27	8-4-0830	42° 56.9'	124° 40.1'	78°	213	12.8
52D	28	8-4-0843	42° 57.2'	124° 38.1'	102°	115	6.9
52D	29	8-4-0907	42° 56.9'	124° 36.1'	83°	116	6.9
52D	30	8-4-0920	42° 57.0'	124° 35.0'	74°	152	9.1
52D	31	8-4-0933	42° 57.3'	124° 33.6'	90°	147	8.8
52D	32	8-4-0945	42° 57.3'	124° 32.3'	67°	127	7.6

Sparker Line No.	Fix No.	Time	Latitude (North)	Longitude (West)	Course (Degrees)	Speed (m/min)	(km/hr)
52D	33	8-4-1000	42° 57.7'	124° 31.0'			
					124°	188	11.3
52D	34	8-4-1007	42° 57.3'	124° 30.2'			
53	1	8-5-0225	42° 48.0'	124° 42.7'			
					24°	183	11.0
53	2	8-5-0245	42° 49.8'	124° 41.6'			
					40°	128	7.7
53	3	8-5-0300	42° 50.6'	124° 40.7'			
					4°	136	8.2
53	4	8-5-0315	42° 51.7'	124° 40.6'			
					11°	139	8.3
53	5	8-5-0330	42° 52.8'	124° 40.3'			
					16°	129	7.7
53	6	8-5-0345	42° 53.8'	124° 39.9'			
					8°	125	7.5
53	7	8-5-0400	42° 54.8'	124° 39.7'			
					22°	146	8.8
53	8	8-5-0415	42° 55.9'	124° 39.1'			
					12°	126	7.6
53	9	8-5-0430	42° 56.9'	124° 38.8'			
					4°	124	7.4
53	10	8-5-0445	42° 57.9'	124° 38.7'			
					18°	117	7.0
53	11	8-5-0500	42° 58.8'	124° 38.3'			
					355°	99	6.0
53	12	8-5-0515	42° 59.6'	124° 38.4'			
					340°	88	5.3
53	13	8-5-0533	43° .4'	124° 38.8'			
					355°	99	6.0
53	14	8-5-0548	43° 1.2'	124° 38.9'			
					27°	149	8.9
53	15	8-5-0602	43° 2.2'	124° 38.2'			
					39°	158	9.5
53	16	8-5-0617	43° 3.2'	124° 37.1'			
					61°	165	9.9
53	17	8-5-0631	43° 3.8'	124° 35.6'			
					351°	113	6.8
53	18	8-5-0646	43° 4.7'	124° 35.8'			
					14°	123	7.4
53	19	8-5-0700	43° 5.6'	124° 35.5'			
					36°	153	9.2
53	20	8-5-0715	43° 6.6'	124° 34.5'			
					11°	139	8.3
53	21	8-5-0730	43° 7.7'	124° 34.2'			
					6°	186	11.2
53	22	8-5-0743	43° 9.0'	124° 34.0'			
					354°	143	8.6

Sparker Line No.	Fix No.	Time	Latitude (North)	Longitude (West)	Course (Degrees)	Speed (m/min)	Speed (km/hr)
53	23	8-5-0800	43° 10.3'	124° 34.2'			
					0°	198	11.9
53	24	8-5-0815	43° 11.9'	124° 34.2'			
					8°	199	12.0
53	25	8-5-0830	43° 13.5'	124° 33.9'			
					5°	198	11.9
53	26	8-5-0845	43° 15.1'	124° 33.7'			
					3°	173	10.4
53	27	8-5-0900	43° 16.5'	124° 33.6'			
					349°	177	10.6
53	28	8-5-0916	43° 18.0'	124° 34.0'			
					14°	163	9.8
53	29	8-5-0930	43° 19.2'	124° 33.6'			
					11°	130	7.8
53	30	8-5-0946	43° 20.3'	124° 33.3'			
					22°	120	7.2
53	31	8-5-1001	43° 21.2'	124° 32.8'			
					20°	131	7.9
53	32	8-5-1016	43° 22.2'	124° 32.3'			

APPENDIX II

APPARENT DIPS

Sparker Line No.	Between Fixes		Average Time	Latitude (North)	Longitude (West)	Ave. Depth Below Ocean Bottom (Meters)	Ave. Depth Below Sea Level (Meters)	Heading (Degrees)	Dip Angle (Degrees)
1	1	2	1024.5	43°21.7'	124°24.1'	43	86	257°	1°
1	2	3	1033.0	43°21.6'	124°24.9'	45	98	270°	1°
1	3	4	1053.5	43°21.5'	124°26.6'	68	149	258°	9°
1	4	5	1102.0	43°21.4'	124°27.4'	52	140	270°	6°
1	5	6	1119.0	43°21.3'	124°28.8'	81	177	257°	3°
1	6	7	1133.5	43°21.1'	124°30.1'	35	136	75°	4°
1	6	7	1133.5	43°21.1'	124°30.1'	161	263	75°	4°
1	7	8	1156.5	43°20.7'	124°32.3'	83	193	255°	6°
1	8	9	1207.0	43°20.5'	124°33.2'	36	151	255°	2°
1	10	11	1238.5	43°19.9'	124°36.0'	42	177	252°	9°
1	10	11	1245.8	43°19.8'	124°36.6'	97	235	252°	9°
1	12	13	1313.0	43°19.3'	124°39.1'	151	315	72°	4°
1	13	14	1323.0	43°19.2'	124°39.9'	48	225	257°	2°
1	13	14	1325.5	43°19.2'	124°40.0'	181	361	77°	8°
2	14	15	1339.8	43°18.4'	124°40.5'	150	332	180°	10°
2	14	15	1342.0	43°18.3'	124°40.5'	44	222	0°	1°
2	14	15	1342.0	43°18.3'	124°40.5'	102	280	0°	2°
2	14	15	1344.3	43°18.1'	124°40.5'	427	597	180°	2°
2	15	16	1352.5	43°17.4'	124°40.5'	73	238	0°	2°
2	15	16	1353.3	43°17.4'	124°40.5'	38	201	0°	1°
2	15	16	1354.5	43°17.3'	124°40.5'	188	350	180°	5°
2	16	17	1404.0	43°16.8'	124°40.0'	164	317	0°	5°
3	17	18	1416.5	43°16.6'	124°38.6'	23	169	281°	2°
3	17	18	1428.5	43°16.4'	124°37.4'	218	342	281°	6°
3	18	19	1441.5	43°16.2'	124°36.1'	49	170	284°	3°
3	19	20	1456.0	43°15.9'	124°34.7'	32	136	285°	3°
3	19	20	1449.5	43°16.0'	124°35.3'	55	165	285°	1°
3	20	21	1509.0	43°15.6'	124°33.5'	238	330	102°	2°
3	20	21	1512.0	43°15.6'	124°33.2'	53	143	102°	3°
3	21	22	1525.5	43°15.4'	124°31.9'	307	389	104°	9°
3	21	22	1527.0	43°15.4'	124°31.7'	86	167	104°	6°
3	22	24	1531.5	43°15.3'	124°31.3'	142	222	106°	2°
3	22	24	1546.5	43°15.0'	124°29.8'	82	145	106°	14°
3	24	25	1552.0	43°14.9'	124°29.2'	63	124	102°	6°
3	24	25	1552.0	43°14.9'	124°29.2'	183	243	102°	7°
3	24	25	1558.5	43°14.7'	124°28.4'	31	86	282°	1°
3	24	25	1558.5	43°14.7'	124°28.4'	283	338	282°	3°
3	25	26	1608.0	43°14.5'	124°27.2'	291	338	108°	7°
3	27	28	1626.0	43°14.2'	124°25.5'	100	132	280°	6°
4	2	4	1219.3	43°16.0'	124°26.1'	54	93	186°	7°
4	2	4	1235.5	43°13.9'	124°26.5'	42	82	186°	3°

Sparker Line No.	Between Fixes		Average Time	Latitude (North)	Longitude (West)	Ave. Depth Below Ocean Bottom (Meters)	Ave. Depth Below Sea Level (Meters)	Heading (Degrees)	Dip Angle (Degrees)
4	4	5	1240.0	43°13.3'	124°26.5'	29	71	184°	1°
4	4	5	1242.5	43°13.0'	124°26.6'	121	163	184°	1°
4	4	5	1246.0	43°12.6'	124°26.6'	102	144	184°	3°
4	4	5	1251.0	43°11.9'	124°26.7'	256	297	184°	7°
4	4	5	1253.0	43°11.7'	124°26.7'	79	119	184°	0°
4	4	5	1258.3	43°11.0'	124°26.8'	258	295	184°	2°
4	4	5	1300.8	43°10.7'	124°26.8'	63	99	4°	1°
4	4	5	1300.8	43°10.7'	124°26.8'	229	265	4°	3°
4	5	6	1311.3	43° 9.6'	124°27.0'	167	199	8°	9°
4	5	6	1318.5	43° 8.9'	124°27.1'	88	113	8°	5°
5	8	9	1337.5	43° 8.3'	124°29.2'	28	79	270°	3°
5	8	9	1341.8	43° 8.3'	124°29.9'	108	161	90°	8°
5	8	9	1341.5	43° 8.3'	124°29.8'	41	95	90°	8°
5	8	9	1346.3	43° 8.3'	124°30.6'	46	100	270°	9°
6	9	10	1355.3	43° 8.7'	124°30.6'	39	93	192°	5°
6	10	11	1405.0	43° 9.4'	124°30.4'	31	86	14°	5°
6	10	11	1408.5	43° 9.7'	124°30.3'	99	156	14°	3°
6	10	11	1411.8	43° 9.9'	124°30.2'	57	116	14°	10°
6	11	12	1416.0	43°10.3'	124°30.0'	102	162	210°	4°
6	11	12	1417.5	43°10.4'	124°29.9'	26	85	30°	0°
6	11	12	1426.0	43°11.2'	124°29.3'	40	96	30°	2°
6	11	12	1426.0	43°11.2'	124°29.3'	69	125	30°	2°
6	11	12	1423.5	43°11.0'	124°29.5'	93	148	210°	1°
6	12	13	1440.0	43°12.7'	124°28.4'	32	88	18°	0°
6	12	13	1440.0	43°12.7'	124°28.4'	112	168	198°	1°
6	12	13	1440.0	43°12.7'	124°28.4'	282	338	198°	3°
6	12	13	1440.0	43°12.7'	124°28.4'	66	123	18°	0°
6	13	14	1447.5	43°13.5'	124°28.1'	38	94	190°	1°
6	13	14	1447.5	43°13.5'	124°28.1'	87	143	190°	1°
6	13	14	1447.5	43°13.5'	124°28.1'	188	243	190°	4°
6	14	15	1501.0	43°14.9'	124°27.8'	109	160	171°	10°
6	14	15	1511.5	43°15.9'	124°28.0'	35	95	351°	4°
6	15	16	1523.3	43°17.1'	124°27.9'	61	129	8°	3°
6	15	16	1523.5	43°17.1'	124°27.9'	183	251	188°	4°
6	16	17	1539.0	43°18.7'	124°28.1'	52	126	346°	2°
6	16	17	1539.0	43°18.7'	124°28.1'	132	205	346°	2°
6	17	18	1549.0	43°19.7'	124°28.1'	50	130	187°	1°
6	17	18	1549.0	43°19.7'	124°28.1'	138	217	187°	1°
6	18	19	1602.5	43°20.9'	124°27.8'	40	126	14°	1°
6	18	19	1602.5	43°20.9'	124°27.8'	84	170	14°	1°
6	18	19	1608.5	43°21.5'	124°27.6'	27	116	194°	2°
6	18	19	1608.5	43°21.5'	124°27.6'	66	155	194°	2°
7	2	3	1137.8	43° 5.8'	124°28.7'	58	101	188°	10°
7	2	3	1139.8	43° 5.5'	124°28.8'	27	71	188°	2°
7	2	3	1139.8	43° 5.5'	124°28.8'	41	85	188°	2°
7	3	4	1155.5	43° 3.8'	124°29.2'	20	69	192°	0°

Sparker Line No.	Between Fixes		Average Time	Latitude (North)	Longitude (West)	Ave. Depth Below Ocean Bottom (Meters)	Ave. Depth Below Sea Level (Meters)	Heading (Degrees)	Dip Angle (Degrees)
7	3	4	1155.5	43° 3.8'	124°29.2'	98	147	192°	1°
7	4	5	1211.0	43° 2.0'	124°29.6'	88	134	189°	0°
7	5	6	1229.5	42°59.9'	124°30.0'	128	170	186°	1°
7	6	7	1252.5	42°57.4'	124°30.7'	30	64	16°	0°
7	6	7	1254.3	42°57.2'	124°30.8'	56	90	16°	0°
7	6	7	1257.5	42°56.9'	124°30.9'	160	192	16°	4°
9	10	11	1334.3	42°56.2'	124°34.3'	42	105	10°	9°
9	10	11	1341.5	42°56.9'	124°34.1'	63	130	10°	8°
9	10	11	1343.0	42°57.1'	124°34.1'	40	109	10°	3°
9	10	11	1343.5	42°57.1'	124°34.1'	30	100	10°	3°
9	11	12	1356.5	42°58.3'	124°33.8'	27	105	190°	0°
9	11	12	1356.5	42°58.3'	124°33.8'	82	160	190°	0°
9	11	12	1356.5	42°58.3'	124°33.8'	169	246	10°	4°
9	12	13	1405.5	42°59.1'	124°33.6'	119	199	15°	1°
9	12	13	1407.5	42°59.4'	124°33.5'	55	137	195°	1°
9	12	13	1407.5	42°59.4'	124°33.5'	77	158	195°	1°
9	12	13	1416.8	43° .3'	124°33.1'	64	147	195°	2°
9	13	14	1420.5	43° .7'	124°33.0'	27	109	194°	1°
9	13	14	1425.0	43° 1.2'	124°32.8'	79	161	14°	1°
9	14	15	1438.3	43° 2.6'	124°32.3'	84	167	190°	2°
9	14	15	1438.3	43° 2.6'	124°32.3'	268	349	190°	9°
9	15	16	1447.0	43° 3.5'	124°32.1'	47	126	194°	2°
9	15	16	1454.5	43° 4.3'	124°31.8'	50	129	194°	3°
9	15	16	1504.0	43° 5.4'	124°31.5'	31	106	14°	3°
9	15	16	1504.0	43° 5.4'	124°31.5'	42	117	14°	3°
9	17	18	1515.0	43° 5.9'	124°31.4'	28	100	190°	1°
9	17	18	1515.0	43° 5.9'	124°31.4'	38	111	190°	1°
9	18	19	1526.5	43° 6.7'	124°31.2'	55	120	197°	9°
9	18	19	1527.5	43° 6.8'	124°31.1'	22	86	197°	2°
9	18	19	1540.3	43° 8.1'	124°30.6'	43	100	197°	4°
10	2	3	905.3	43°17.7'	124°27.7'	56	119	249°	6°
10	2	3	905.0	43°17.7'	124°27.6'	18	81	249°	0°
10	3	4	915.3	43°17.4'	124°29.2'	97	173	86°	7°
10	3	4	920.0	43°17.3'	124°30.0'	89	172	86°	15°
10	3	4	931.5	43°17.3'	124°31.7'	39	136	86°	4°
10	3	4	936.0	43°17.2'	124°32.4'	41	138	266°	3°
10	4	5	941.0	43°17.2'	124°33.2'	60	159	270°	0°
10	4	5	946.8	43°17.2'	124°34.1'	61	166	270°	2°
10	6	7	1001.8	43°17.3'	124°36.7'	239	359	273°	4°
10	7	8	1021.0	43°17.3'	124°39.6'	35	193	261°	2°
10	7	8	1017.8	43°17.3'	124°39.2'	79	229	81°	2°
10	7	8	1021.8	43°17.3'	124°39.6'	99	255	261°	8°
10	7	8	1024.5	43°17.3'	124°40.0'	33	197	261°	2°
10	7	8	1024.5	43°17.3'	124°40.0'	65	229	261°	1°
10	8	8A	1039.0			51	265	274°	1°
10	8	8A	1039.0			93	307	274°	0°

Sparker Line No.	Between Fixes		Average Time	Latitude (North)	Longitude (West)	Ave. Depth Below Ocean Bottom (Meters)	Ave. Depth Below Sea Level (Meters)	Heading (Degrees)	Dip Angle (Degrees)
11	8A	8B	1117.5			43	379	12°	1°
11	8A	8B	1121.5			46	371	12°	0°
11	8A	8B	1121.5			163	489	192°	1°
11	8A	8B	1127.8			52	364	12°	1°
11	8A	8B	1127.8			128	440	12°	4°
11	8A	8B	1132.5			76	380	192°	5°
11	8A	8B	1132.5			154	458	192°	7°
11	8A	8B	1141.0			82	377	192°	0°
11	8A	8B	1141.0			172	466	12°	1°
11	8A	8B	1141.0			296	591	12°	1°
11	8A	8B	1148.0			68	359	12°	2°
11	8A	8B	1148.0			128	419	12°	2°
11	8A	8B	1148.0			249	540	12°	3°
12	9	10	1202.8	43°12.2'	124°43.4'	33	285	277°	2°
12	9	10	1202.8	43°12.2'	124°43.4'	145	396	277°	4°
12	9	10	1213.0	43°12.1'	124°41.7'	102	295	277°	5°
12	9	10	1212.5	43°12.1'	124°41.8'	485	679	277°	11°
12	10	11	1226.0	43°11.6'	124°39.2'	56	219	286°	3°
12	11	12	1237.5	43°11.4'	124°37.7'	41	180	99°	2°
12	12	13	1256.0	43°11.4'	124°35.9'	38	134	85°	3°
12	12	13	1256.0	43°11.4'	124°35.9'	96	192	85°	5°
12	12	13	1300.5	43°11.4'	124°35.4'	45	138	265°	1°
12	12	13	1300.5	43°11.4'	124°35.4'	95	189	265°	4°
12	12	13	1300.5	43°11.4'	124°35.4'	178	271	265°	4°
12	13	14	1308.5	43°11.6'	124°34.5'	79	184	69°	7°
12	13	14	1317.0	43°11.9'	124°33.4'	72	165	69°	4°
12	13	14	1318.0	43°12.0'	124°33.3'	211	303	69°	2°
12	14	15	1325.5	43°12.1'	124°32.3'	33	105	84°	2°
12	14	15	1329.5	43°12.2'	124°31.8'	45.	114	264°	1°
12	15	16	1335.5	43°12.2'	124°31.1'	39	105	264°	2°
12	15	16	1335.5	43°12.2'	124°31.1'	150	216	264°	2°
12	15	16	1339.5	43°12.3'	124°30.8'	118	179	264°	6°
12	15	16	1343.0	43°12.3'	124°30.4'	77	137	84°	6°
12	16	17	1354.5	43°12.6'	124°29.2'	36	98	70°	2°
12	16	17	1354.5	43°12.6'	124°29.2'	75	137	73°	1°
12	17	18	1403.0	43°12.8'	124°28.1'	29	84	74°	2°
12	17	18	1403.0	43°12.8'	124°28.1'	63	118	74°	1°
12	17	18	1403.0	43°12.8'	124°28.1'	107	161	74°	0°
12	17	18	1406.0	43°12.9'	124°27.7'	52	105	74°	1°
12	17	18	1406.0	43°12.9'	124°27.7'	78	131	74°	1°
12	17	18	1406.0	43°12.9'	124°27.7'	111	164	74°	0°
13	20	21	1528.3	43°10.4'	124°26.3'	108	140	270°	0°
13	20	21	1529.8	43°10.4'	124°26.5'	72	106	90°	2°
13	20	21	1548.3	43°10.4'	124°29.2'	26	84	270°	1°
13	20	21	1548.3	43°10.4'	124°29.2'	48	106	270°	4°

Sparker Line No.	Between Fixes		Average Time	Latitude (North)	Longitude (West)	Ave. Depth Below Ocean Bottom (Meters)	Ave. Depth Below Sea Level (Meters)	Heading (Degrees)	Dip Angle (Degrees)
14	2	3	1050.8	43°12.8'	124°27.7'	53	106	7°	1°
14	2	3	1050.8	43°12.8'	124°27.7'	105	159	187°	0°
14	2	3	1051.0	43°12.8'	124°27.7'	78	131	7°	0°
14	3	4	1106.3	43°11.2'	124°28.1'	102	154	14°	4°
14	3	4	1107.0	43°11.1'	124°28.1'	13	64	14°	1°
14	4	5	1120.0	43° 9.6'	124°28.5'	50	93	185°	9°
14	5	6	1130.8	43° 8.2'	124°28.7'	18	63	199°	3°
14	6	7	1148.3	43° 6.4'	124°29.6'	37	92	203°	5°
14	6	7	1158.5	43° 5.4'	124°30.1'	43	105	203°	0°
14	6	7	1158.5	43° 5.4'	124°30.1'	64	127	203°	0°
15	8	9	1249.0	43° 5.5'	124°28.6'	32	79	274°	3°
15	8	9	1249.3	43° 5.5'	124°28.7'	20	68	274°	2°
15	8	9	1250.5	43° 5.5'	124°28.8'	127	177°	274°	10°
15	9	10	1300.0	43° 5.6'	124°30.1'	41	104	105°	0°
15	9	10	1300.0	43° 5.6'	124°30.1'	62	125	285°	0°
15	9	10	1309.0	43° 5.9'	124°31.3'	21	96	105°	0°
15	10	11	1320.5	43° 6.0'	124°32.9'	26	118	86°	1°
15	10	11	1327.3	43° 5.9'	124°33.8'	309	407	266°	8°
15	11	12	1331.8	43° 5.9'	124°34.5'	20	124	267°	4°
15	12	13	1346.3	43° 5.8'	124°36.8'	224	346	97°	10°
15	12	13	1354.5	43° 5.9'	124°37.9'	22	160	277°	2°
15	13	14	1410.5	43° 6.2'	124°40.5'	30	194	279°	1°
15	14	15	1426.5	43° 6.2'	124°42.8'	39	237	266°	1°
15	15	16	1434.0	43° 6.2'	124°43.9'	56	263	266°	0°
15	15	16	1441.5	43° 6.1'	124°44.9'	138	367	86°	2°
15	16	17	1452.5	43° 5.9'	124°46.5'	93	329	72°	2°
15	16	17	1452.5	43° 5.9'	124°46.5'	191	420	72°	3°
15	17	18	1503.5	43° 5.5'	124°48.1'	30	251	78°	2°
15	17	18	1503.5	43° 5.5'	124°48.1'	122	343	78°	2°
16	19	20	1518.5	43° 4.8'	124°48.9'	17	195	11°	2°
16	19	20	1518.5	43° 4.8'	124°48.9'	124	303	11°	2°
16	19	20	1533.8	43° 2.8'	124°49.5'	332	459	11°	5°
16	19	20	1540.0	43° 2.0'	124°49.7'	14	133	11°	1°
16	19	20	1540.0	43° 2.0'	124°49.7'	30	149	11°	1°
16	19	20	1541.0	43° 1.9'	124°49.7'	39	158	11°	1°
16	19	20	1541.0	43° 1.9'	124°49.7'	59	177	11°	1°
16	20	21	1547.0	43° 1.1'	124°49.9'	28	141	9°	2°
16	20	21	1553.0	43° .5'	124°50.1'	34	153	189°	0°
16	20	21	1608.0	42°58.8'	124°50.4'	32	158	189°	3°
16	20	21	1619.0	42°57.5'	124°50.7'	61	192	189°	1°
16	21	22	1640.0	42°55.0'	124°51.2'	56	250	187°	2°
16	21	22	1640.0	42°55.0'	124°51.2'	137	331	187°	2°
16	21	22	1641.5	42°54.8'	124°51.2'	29	230	187°	2°
16	22	23	1655.5	42°53.1'	124°51.8'	25	302	194°	1°
16	22	23	1655.5	42°53.1'	124°51.8'	67	344	194°	1°
16	23	24	1703.0	42°52.3'	124°51.9'	21	323	183°	1°

Sparker Line No.	Between Fixes		Average Time	Latitude (North)	Longitude (West)	Ave. Depth Below Ocean Bottom (Meters)	Ave. Depth Below Sea Level (Meters)	Heading (Degrees)	Dip Angle (Degrees)
16	23	24	1712.5	42°51.4'	124°52.0'	20	338	183°	0°
16	23	24	1712.5	42°51.4'	124°52.0'	71	389	183°	0°
17	25	26	1730.5	42°50.7'	124°53.0'	93	438	312°	0°
17	25	26	1734.5	42°51.0'	124°53.4'	30	396	312°	1°
17	25	26	1742.0	42°51.6'	124°54.3'	24	451	312°	2°
17	25	26	1742.0	42°51.6'	124°54.3'	120	547	312°	2°
18	29	30	1843.3	42°54.2'	124°56.2'	24	580	290°	6°
18	30	31	1849.0	42°54.2'	124°55.5'	34	515	266°	4°
18	30	31	1859.3	42°54.3'	124°54.1'	30	300	266°	6°
18	32	33	1924.5	42°54.9'	124°51.2'	62	248	75°	2°
18	32	33	1925.5	42°54.9'	124°51.1'	38	224	75°	1°
18	32	33	1925.5	42°54.9'	124°51.1'	143	330	75°	2°
18	33	34	1932.5	42°55.1'	124°50.2'	29	211	77°	1°
18	33	34	1932.5	42°55.1'	124°50.2'	63	245	77°	2°
18	33	34	1932.5	42°55.1'	124°50.2'	163	345	77°	3°
18	33	34	1946.5	42°55.4'	124°48.4'	47	217	257°	1°
18	33	34	1944.3	42°55.3'	124°48.7'	84	255	257°	1°
18	33	34	1949.0	42°55.4'	124°48.1'	113	280	257°	1°
18	34	35	1957.5	42°55.4'	124°46.8'	20	180	96°	0°
18	34	35	1957.5	42°55.4'	124°46.8'	66	226	276°	0°
18	35	36	2002.5	42°55.4'	124°46.0'	64	218	270°	1°
18	35	36	2002.5	42°55.4'	124°46.0'	89	244	270°	1°
18	35	36	2002.5	42°55.4'	124°46.0'	142	297	270°	1°
18	35	36	2010.5	42°55.4'	124°44.6'	48	193	270°	1°
18	35	36	2010.5	42°55.4'	124°44.6'	130	276	270°	2°
18	36	37	2022.0	42°55.4'	124°42.7'	36	167	267°	2°
18	36	37	2022.0	42°55.4'	124°42.7'	137	268	267°	3°
18	36	37	2027.8	42°55.5'	124°41.8'	64	186	267°	6°
18	37	38	2039.0	42°55.4'	124°40.0'	39	142	95°	4°
19	43	44	2209.0	42°56.0'	124°31.5'	107	144	26°	5°
19	44	45	2214.5	42°56.4'	124°31.3'	12	48	25°	0°
19	44	45	2214.5	42°56.4'	124°31.3'	32	68	25°	0°
19	44	45	2224.0	42°57.4'	124°30.6'	14	51	25°	0°
19	44	45	2224.0	42°57.4'	124°30.6'	30	67	205°	0°
19	45	46	2237.5	42°58.9'	124°30.0'	38	80	12°	1°
19	45	46	2243.3	42°59.5'	124°29.8'	44	87	12°	0°
20	48	49	2302.0	42°59.8'	124°32.2'	25	98	270°	1°
20	48	49	2302.0	42°59.8'	124°32.2'	45	119	270°	2°
20	48	49	2310.0	42°59.8'	124°33.3'	52	135	270°	0°
20	48	49	2310.0	42°59.8'	124°33.3'	78	161	270°	1°
20	48	49	2314.5	42°59.8'	124°34.0'	43	131	90°	1°
20	48	49	2314.5	42°59.8'	124°34.0'	73	160	90°	1°
20	48	49	2314.5	42°59.8'	124°34.0'	103	191	90°	3°
20	49	50	2330.3	42°59.6'	124°36.5'	62	166	264°	4°
20	50	51	2335.0	42°59.6'	124°37.3'	69	179	274°	4°
20	50	51	2341.5	42°59.7'	124°38.4'	40	157	274°	2°

Sparker Line No.	Between Fixes		Average Time	Latitude (North)	Longitude (West)	Ave. Depth Below Ocean Bottom (Meters)	Ave. Depth Below Sea Level (Meters)	Heading (Degrees)	Dip Angle (Degrees)
20	50	51	2341.5	42°59.7'	124°38.4'	83	200	274°	3°
20	51	52	2348.0	42°59.7'	124°39.5'	50	175	267°	1°
20	51	52	2348.0	42°59.7'	124°39.5'	111	237	267°	2°
20	52	53	2403.0	42°59.6'	124°41.3'	43	186	284°	0°
20	53	54	015.0	43° .1'	124°44.0'	62	227	126°	1°
20	53	54	015.0	43° .1'	124°44.0'	86	252	126°	2°
20	53	54	015.0	43° .1'	124°44.0'	150	315	126°	2°
20	54	55	036.5	43° 1.3'	124°46.3'	20	186	126°	1°
20	55	56	050.5	43° 1.9'	124°47.4'	42	196	127°	5°
20	55	56	050.5	43° 1.9'	124°47.4'	79	233	127°	6°
20	55	56	050.5	43° 1.9'	124°47.4'	125	278	127°	7°
20	56	57	105.0			36	153	105°	6°
20	56	57	105.0			53	170	105°	6°
20	56	57	105.0			73	190	105°	6°
22	62	63	353.5	42°49.5'	124°52.9'	23	355	274°	0°
22	62	63	359.0	42°49.4'	124°52.2'	39	356	94°	1°
22	63	64	411.5	42°49.4'	124°50.3'	30	341	90°	1°
22	63	64	411.5	42°49.4'	124°50.3'	129	440	90°	1°
22	64	65	417.0	42°49.4'	124°49.5'	84	396	270°	0°
22	65	66	435.0	42°49.4'	124°46.5'	22	248	272°	2°
22	66	67	452.0	42°49.5'	124°43.8'	53	211	257°	3°
22	66	67	455.8	42°49.5'	124°43.3'	27	173	77°	1°
22	66	67	457.0	42°49.6'	124°43.1'	91	233	77°	6°
22	67	68	502.8	42°49.6'	124°42.1'	21	146	273°	1°
22	67	68	506.3	42°49.5'	124°41.4'	49	161	273°	6°
22	67	68	508.5	42°49.5'	124°41.0'	32	134	273°	1°
22	68	69	515.0	42°49.7'	124°39.7'	23	106	248°	1°
23	70	71	530.3	42°48.7'	124°39.2'	16	81	28°	0°
24	75	76	618.5	42°44.9'	124°41.8'	28	198	281°	3°
24	75	76	618.5	42°44.9'	124°41.8'	65	236	281°	10°
24	76	77	628.8	42°45.2'	124°43.4'	18	276	296°	6°
50	2	3	406.3	42°52.3'	124°51.7'	20	322	100°	2°
50	3	4	416.3	42°52.2'	124°50.6'	39	326	86°	1°
50	3	4	419.8	42°52.2'	124°50.1'	17	302	86°	0°
50	3	4	428.0	42°52.3'	124°49.0'	44	306	266°	2°
50	4	5	435.0	42°52.4'	124°47.8'	45	258	264°	2°
50	5	6	452.5	42°52.4'	124°44.9'	57	224	275°	3°
50	6	7	458.0	42°52.4'	124°44.1'	75	220	270°	3°
50	6	7	502.5	42°52.4'	124°43.6'	37	175	270°	2°
50	7	8	520.8	42°52.5'	124°41.1'	98	198	84°	9°
51	11	12	617.8	42°54.5'	124°37.0'	47	116	6°	6°
51	12	13	634.0	42°53.0'	124°37.3'	19	81	10°	2°
51	12	13	638.3	42°52.6'	124°37.4'	17	77	190°	2°
51	13	14	648.5	42°51.7'	124°37.5'	29	89	0°	8°
51	14	15	656.5	42°51.8'	124°36.9'	52	108	70°	4°
51	14	15	700.0	42°51.9'	124°36.6'	25	75	70°	4°

Sparker Line No.	Between Fixes		Average Time	Latitude (North)	Longitude (West)	Ave. Depth Below Ocean Bottom (Meters)	Ave. Depth Below Sea Level (Meters)	Heading (Degrees)	Dip Angle (Degrees)
51	16	17	722.5	42°52.4'	124°34.6'	26	59	259°	0°
51	17	18	726.0	42°52.3'	124°34.4'	16	47	14°	6°
52	1	2	236.5	42°52.9'	124°45.0'	65	230	195°	0°
52	1	2	236.5	42°52.9'	124°45.0'	83	249	195°	1°
52	2	3	252.0	42°54.2'	124°44.6'	41	203	8°	0°
52	2	3	252.0	42°54.2'	124°44.6'	63	225	188°	1°
52	2	3	258.5	42°54.6'	124°44.5'	182	343	8°	0°
52	3	4	305.0	42°55.0'	124°44.6'	54	215	165°	1°
52	3	4	305.0	42°55.0'	124°44.6'	189	350	345°	1°
52	3	4	312.5	42°55.6'	124°44.8'	154	313	345°	1°
52	4	5	327.5	42°56.5'	124°45.6'	64	222	324°	0°
52	4	5	327.5	42°56.5'	124°45.6'	91	248	324°	0°
52	5	6	340.0	42°57.2'	124°46.1'	98	252	343°	1°
52	5	6	340.0	42°57.2'	124°46.1'	117	271	343°	1°
52	6	7	351.5	42°57.9'	124°46.3'	149	302	0°	1°
52	6	7	356.5	42°58.2'	124°46.3'	79	233	0°	2°
52	7	8	404.0	42°58.8'	124°46.1'	64	218	24°	1°
52	7	8	412.5	42°59.4'	124°45.7'	31	186	24°	1°
52	8	9	422.5	43° .2'	124°45.4'	83	242	4°	1°
52	9	10	438.0	43° 1.4'	124°45.4'	68	232	0°	0°
52	9	10	438.0	43° 1.4'	124°45.4'	95	259	0°	0°
52	9	10	439.5	43° 1.5'	124°45.4'	98	262	0°	0°
52	9	10	439.5	43° 1.5'	124°45.4'	148	313	0°	0°
52	10	11	450.0	43° 2.0'	124°45.9'	40	214	100°	2°
52	10	11	450.0	43° 2.0'	124°45.9'	135	309	280°	3°
52	11	12	507.5	43° 2.1'	124°47.9'	44	195	85°	3°
52	11	12	507.5	43° 2.1'	124°47.9'	86	237	85°	4°
52	11	12	508.0	43° 2.0'	124°47.9'	125	273	85°	4°
52	12	13	524.5	43° 2.1'	124°49.8'	45	162	94°	3°
52	12	13	524.5	43° 2.1'	124°49.8'	73	190	94°	3°
52	13	14	533.8	43° 2.1'	124°50.9'	201	358	275°	15°
52	13	14	539.0	43° 2.2'	124°51.5'	47	241	275°	2°
52	16	17	606.8	43° 1.0'	124°53.2'	52	393	297°	0°
52	17	18	616.5	43° 0.1'	124°53.1'	35	372	3°	2°
52	17	18	621.5	42°59.6'	124°53.1'	33	361	3°	0°
52	20	21	653.0	42°58.0'	124°51.5'	43	160	257°	8°
52	21	22	658.3	42°57.9'	124°51.0'	55	181	123°	5°
52	21	22	704.0	42°57.7'	124°50.6'	53	181	123°	3°
52	21	22	714.0	42°57.3'	124°49.8'	40	166	123°	2°
52	22	23	722.5	42°57.3'	124°48.8'	63	207	81°	2°
52	23	24	744.5	42°57.1'	124°46.5'	98	251	285°	1°
52	23	24	744.5	42°57.1'	124°46.5'	120	273	285°	2°
52	24	25	755.5	42°57.0'	124°45.2'	34	180	95°	0°
52	24	25	755.5	42°57.0'	124°45.2'	101	248	275°	0°
52	25	26	810.0	42°57.1'	124°43.2'	31	164	263°	2°
52	25	26	810.0	42°57.1'	124°43.2'	76	208	263°	2°

Sparker Line No.	Between Fixes		Average Time	Latitude (North)	Longitude (West)	Ave. Depth Below Ocean Bottom (Meters)	Ave. Depth Below Sea Level (Meters)	Heading (Degrees)	Dip Angle (Degrees)
52	26	27	817.8	42°57.1'	124°42.1'	33	158	280°	1°
52	26	27	817.8	42°57.1'	124°42.1'	104	229	280°	3°
52	26	27	817.8	42°57.1'	124°42.1'	185	310	280°	4°
52	26	27	824.5	42°57.0'	124°41.0'	40	159	100°	1°
52	26	27	824.5	42°57.0'	124°41.0'	186	305	100°	3°
52	27	28	833.0	42°57.0'	124°39.6'	49	159	258°	1°
52	27	28	833.0	42°57.0'	124°39.6'	81	191	258°	1°
52	27	28	838.5	42°57.1'	124°38.8'	34	137	258°	1°
52	27	28	838.5	42°57.1'	124°38.8'	70	174	258°	0°
52	28	29	851.5	42°57.1'	124°37.4'	57	150	282°	2°
52	28	29	901.5	42°57.0'	124°36.6'	40	125	282°	3°
52	28	29	901.5	42°57.0'	124°36.6'	73	158	282°	4°
52	29	30	909.0	42°56.9'	124°35.9'	39	120	83°	2°
52	29	30	912.0	42°56.9'	124°35.7'	67	145	83°	2°
52	29	30	919.0	42°57.0'	124°35.1'	50	123	263°	1°
52	30	31	923.0	42°57.1'	124°34.7'	41	113	254°	4°
52	30	31	927.0	42°57.2'	124°34.2'	57	125	74°	6°
52	30	31	932.0	42°57.3'	124°33.7'	30	95	74°	1°
52	30	31	932.0	42°57.3'	124°33.7'	43	108	74°	2°
52	31	32	943.5	42°57.3'	124°32.5'	47	103	90°	0°
52	32	33	946.5	42°57.3'	124°32.2'	48	102	247°	1°
52	32	33	957.5	42°57.6'	124°31.2'	29	72	247°	1°
52	33	34	1001.8	42°57.6'	124°30.8'	14	52	124°	0°
52	33	34	1001.3	42°57.6'	124°30.9'	26	64	304°	1°
52	33	34	1005.0	42°57.4'	124°30.4'	26	60	304°	0°
53	1	2	237.5	42°49.1'	124°42.0'	27	148	204°	0°
53	1	2	243.5	42°49.7'	124°41.7'	28	138	204°	2°
53	2	3	246.0	42°49.9'	124°41.5'	64	171	40°	6°
53	2	3	259.0	42°50.5'	124°40.8'	55	149	220°	2°
53	3	4	303.3	42°50.8'	124°40.7'	35	128	184°	4°
53	3	4	308.5	42°51.2'	124°40.6'	38	131	4°	3°
53	4	5	328.0	42°52.7'	124°40.3'	50	148	11°	7°
53	5	6	332.8	42°53.0'	124°40.2'	102	201	16°	5°
53	5	6	341.5	42°53.6'	124°40.0'	82	184	196°	4°
53	7	8	402.3	42°55.0'	124°39.6'	99	205	22°	5°
53	7	8	406.8	42°55.3'	124°39.4'	77	183	202°	10°
53	8	9	419.8	42°56.2'	124°39.0'	99	205	12°	15°
53	9	10	432.5	42°57.1'	124°38.8'	107	216	4°	6°
53	9	10	436.0	42°57.3'	124°38.8'	75	186	4°	3°
53	9	10	443.0	42°57.8'	124°38.7'	39	152	4°	1°
53	10	11	452.5	42°58.4'	124°38.5'	30	146	18°	1°
53	10	11	452.5	42°58.4'	124°38.5'	181	298	18°	1°
53	11	12	510.0	42°59.3'	124°38.4'	51	173	355°	1°
53	11	12	510.0	42°59.3'	124°38.4'	105	228	355°	1°
53	12	13	525.0	43° .0'	124°38.6'	56	181	160°	0°
53	12	13	525.0	43° .0'	124°38.6'	231	355	160°	6°

Sparker Line No.	Between Fixes		Average Time	Latitude (North)	Longitude (West)	Ave. Depth Below Ocean Bottom (Meters)	Ave. Depth Below Sea Level (Meters)	Heading (Degrees)	Dip Angle (Degrees)
53	13	14	542.5	43° .9'	124°38.9'	24	149	175°	1°
53	13	14	542.5	43° .9'	124°38.9'	88	213	175°	10°
53	13	14	547.0	43° 1.1'	124°38.9'	220	390	355°	16°
53	14	15	555.5	43° 1.7'	124°38.5'	30	153	27°	0°
53	15	16	605.0	43° 2.4'	124°38.0'	29	151	219°	1°
53	15	16	609.5	43° 2.7'	124°37.6'	38	158	219°	1°
53	15	16	609.5	43° 2.7'	124°37.6'	77	197	39°	5°
53	16	17	632.3	43° 3.9'	124°35.5'	48	159	241°	0°
53	16	17	632.3	43° 3.9'	124°35.5'	78	190	241°	3°
53	17	18	639.5	43° 4.3'	124°35.7'	37	145	171°	2°
53	17	18	644.0	43° 4.6'	124°35.8'	55	163	171°	8°
53	18	19	649.0	43° 4.9'	124°35.7'	28	135	14°	2°
53	18	19	658.5	43° 5.5'	124°35.5'	49	153	194°	1°
53	19	20	703.0	43° 5.8'	124°35.3'	44	146	216°	0°
53	20	21	716.0	43° 6.7'	124°34.5'	20	117	11°	3°
53	20	21	727.5	43° 7.5'	124°34.3'	37	129	191°	5°
53	20	21	727.3	43° 7.5'	124°34.3'	74	165	191°	20°
53	21	22	733.8	43° 8.1'	124°34.1'	43	135	186°	10°
53	22	23	757.0	43°10.1'	124°34.2'	18	112	174°	1°
53	23	24	806.3	43°11.0'	124°34.2'	46	137	180°	6°
53	23	24	812.5	43°11.6'	124°34.2'	26	110	180°	7°
53	24	25	819.0	43°12.3'	124°34.1'	73	153	188°	6°
53	25	26	831.5	43°13.7'	124°33.9'	84	175	185°	8°
53	26	27	849.5	43°15.5'	124°33.7'	38	141	3°	2°
53	27	28	904.0	43°16.9'	124°33.7'	52	168	349°	4°
53	27	28	913.0	43°17.7'	124°33.9'	56	168	349°	1°
53	28	29	922.5	43°18.6'	124°33.8'	31	143	14°	3°
53	29	30	935.5	43°19.6'	124°33.5'	83	192	11°	4°
53	30	31	950.5	43°20.6'	124°33.1'	44	155	22°	2°
53	30	31	959.0	43°21.1'	124°32.9'	33	144	202°	1°
53	31	32	1005.5	43°21.5'	124°32.6'	24	137	20°	1°
53	31	32	1005.5	43°21.5'	124°32.6'	90	203	200°	1°
53	31	32	1012.0	43°21.9'	124°32.4'	35	148	20°	1°
53	31	32	1012.0	43°21.9'	124°32.4'	90	204	20°	3°

APPENDIX III

TRUE DIPS AND STRIKES

Sparker Line No.	Between Fixes		Heading (Degrees)	Apparent Dip (Degrees)	Depth of Reflector (Meters)	Intersection of Lines	Strike	Dip (Degrees)	Aver. Depth Below Sea Level (Meters)
1	4	5	270	6	52				
						1 & 6	N 6°W	6°W	59
6	18	19	194	2	67				
1	8	9	255	2	36				
						1 & 53	N 48°E	4°N	40
53	30	31	22	2	44				
1	13	14	257	2	48				
						1 & 2	N 24°E	3°W	46
2	14	15	0	1	44				
1	13	14	77	8	181				
						1 & 2	N 44°E	14°S	166
2	14	15	180	10	150				
10	4	5	270	2	61				
						10 & 53	N 61°E	5°N	56
53	27	28	349	4	52				
10	7	8	261	2	33				
						10 & 2	N 23°E	3°W	35
2	15	16	0	1	38				
10	7	8	261	1	65				
						10 & 2	N 56°E	2°N	69
2	15	16	0	2	73				
12	17	18	74	2	29				
						12 & 6	N 18°E	2°E	31
6	12	13	18	0	32				
12	17	18	74	1	63				
						12 & 6	N 18°E	1°E	64
6	12	13	18	0	66				
12	17	18	74	0	107				
						12 & 6	N 74°E	1°S	109
6	12	13	198	1	114				
12	17	18	74	1	52				
						12 & 14	N 40°W	1°E	52
14	2	3	7	1	53				

Sparker Line No.	Between Fixes		Heading (Degrees)	Apparent Dip (Degrees)	Depth of Reflector (Meters)	Intersection of Lines	Strike	Dip (Degrees)	Aver. Depth Below Sea Level (Meters)
12	17	18	74	1	78	12 & 14	N 7°E	1°E	78
14	2	3	7	0	78				
12	17	18	74	0	111	12 & 14	---	0°	109
14	2	3	187	0	105				
5	8	9	270	9	46	5 & 9	N 10°W	9°W	45
9	18	19	197	4	43				
15	8	9	274	3	32	15 & 7	N 30°W	3°W	35
7	2	3	188	2	41				
15	8	9	274	10	127	15 & 14	N 40°W	14°W	93
7	2	3	188	10	58				
15	9	10	105	0	41	15 & 14	---	0°	42
14	6	7	203	0	43				
15	9	10	285	0	62	15 & 14	0°	0°	63
14	6	7	203	0	64				
15	9	10	105	0	21	15 & 9	N 80°W	1°S	25
9	17	18	190	1	28				
15	17	18	78	2	30	15 & 16	N 30°W	2°E	38
16	19	20	11	2	17				
15	17	18	78	2	122	15 & 16	N 30°W	2°E	123
16	19	20	11	2	124				
20	48	49	270	0	52	20 & 9	N 76°W	1°S	54
9	12	13	195	1	55				
20	48	49	270	1	78	20 & 9	N 33°W	1°W	77
9	12	13	195	1	77				

Sparker Line No.	Between Fixes		Heading (Degrees)	Apparent Dip (Degrees)	Depth of Reflector (Meters)	Inter-section of Lines	Strike	Dip (Degrees)	Aver. Depth Below Sea Level (Meters)
20	51	52	267	1	50				
						20 & 53	N 42°E	2°W	50
53	11	12	355	1	51				
20	51	52	267	2	111				
						20 & 53	N 25°E	2°W	109
53	11	12	355	1	105				
20	53	54	203	1	62				
						20 & 52A	N 36°E	1°E	65
52A	9	10	0	0	68				
20	53	54	126	2	86				
						20 & 52A	N 36°E	2°E	87
52A	9	10	0	0	95				
20	55	56	127	5	42				
						20 & 52B	N 50°E	5°S	43
52B	11	12	85	3	44				
20	55	56	127	6	79				
						20 & 52B	N 43°E	6°S	83
52B	11	12	85	4	86				
20	55	56	127	7	125				
						20 & 52B	N 50°E	7°S	125
52B	11	12	85	4	125				
52D	33	34	304	0	26				
						52D & 7	---	0°	28
7	6	7	16	0	30				
52D	33	34	124	0	14				
						52D & 19	---	0°	14
19	44	45	25	0	14				
52D	33	34	304	1	26				
						52D & 19	N 34°E	1°W	28
19	44	45	205	0	30				
52D	30	31	74	1	30				
						52D & 9	N 83°W	3°N	31
9	10	11	10	3	30				
52D	30	31	74	2	43				
						52D & 9	N 64°W	3°N	42
9	10	11	10	3	40				

Sparker Line No.	Between Fixes		Heading (Degrees)	Apparent Dip (Degrees)	Depth of Reflector (Meters)	Intersection of Lines	Strike	Dip (Degrees)	Aver. Depth Below Sea Level (Meters)
52D	27	28	258	1	81				
						52D & 53	N 60°E	4°N	78
53	9	10	4	3	75				
52D	23	24	285	1	98				
						52D & 52A	N 44°E	1°N	98
52A	5	6	343	1	98				
52D	23	24	285	2	120				
						52D & 52A	N 27°E	2°W	119
52A	5	6	343	1	117				
52D	21	22	123	3	53				
						52D & 16	N 30°E	3°E	57
16	20	21	189	1	61				
18	35	36	270	1	64				
						18 & 52A	N 18°W	1°W	64
52A	4	5	324	0	64				
18	35	36	270	1	89				
						18 & 52A	N 18°W	1°W	90
52A	4	5	324	0	91				
18	32	33	75	1	38				
						18 & 16	N 60°E	3°S	33
16	21	22	187	2	29				
18	32	33	75	2	62				
						18 & 16	N 41°E	4°W	59
16	21	22	187	2	56				
18	32	33	75	2	143				
						18 & 16	N 41°E	4°W	140
16	21	22	187	2	137				
50	7	8	84	9	98				
						50 & 53	N 52°W	12°N	74
53	4	5	11	7	50				
50	5	6	275	3	57				
						50 & 52A	N 6°E	3°W	61
52A	1	2	195	0	65		186		
50	2	3	100	2	20				
						50 & 16	N 32°E	2°S	20
16	23	24	183	1	21				

Sparker Line No.	Between Fixes		Heading (Degrees)	Apparent Dip (Degrees)	Depth of Reflector (Meters)	Intersection of Lines	Strike	Dip (Degrees)	Aver. Depth Below Sea Level (Meters)
51	13	14	0	8	29				
						51 & 51	N 80°W	8°N	41
51	14	15	70	4	52				
51	16	17	259	0	26				
						51 & 51	N 76°W	6°N	21
51	17	18	14	6	16				
52B	12	13	94	3	45				
						52B & 16	N 4°W	3°E	42
16	19	20	11	1	39				
52B	12	13	94	3	73				
						52B & 16	N 4°W	3°E	66
16	19	20	11	1	59				
12	13	14	69	4	72				
						12 & 53	N 43°E	8°E	58
53	23	24	180	6	46				
15	8	9	274	2	20				
						15 & 7	N 40°W	2°W	24
7	2	3	188	2	27				

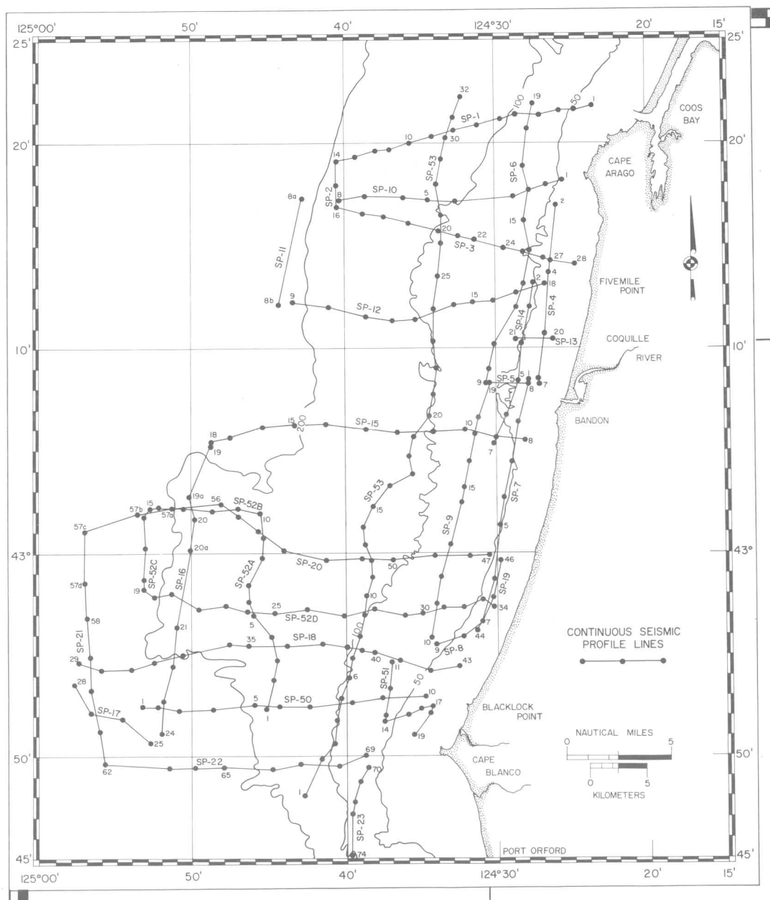

PLATE I. STRUCTURE MAP OF THE CONTINENTAL SHELF OFF SOUTHERN OREGON. SEE TEXT FOR COMPLETE DISCUSSION OF SEISMIC UNITS AND SUB-UNITS.